HAL open science

Tangent spaces for self-similair shapes

Sergey Podkorytov

▶ To cite this version:

Sergey Podkorytov. Tangent spaces for self-similair shapes. General Mathematics [math.GM]. Université de Bourgogne, 2013. English. NNT : 2013DIJOS062 . tel-01005330

HAL Id: tel-01005330

https://theses.hal.science/tel-01005330v1

Submitted on 12 Jun 2014

HAL is a multi-disciplinary open access archive for the deposit and dissemination of scientific research documents, whether they are published or not. The documents may come from teaching and research institutions in France or abroad, or from public or private research centers.

L'archive ouverte pluridisciplinaire **HAL**, est destinée au dépôt et à la diffusion de documents scientifiques de niveau recherche, publiés ou non, émanant des établissements d'enseignement et de recherche français ou étrangers, des laboratoires publics ou privés.

SPIM

Thèse de Doctorat

école doctorale **sciences pour l'ingénieur et microtechniques**

UNIVERSITÉ DE BOURGOGNE

Espaces tangents pour les formes auto-similaires

Sergey PODKORYTOV

SPIM

Thèse de Doctorat

école doctorale **sciences pour l'ingénieur et microtechniques**

UNIVERSITÉ DE BOURGOGNE

THÈSE présentée par

Sergey PODKORYTOV

pour obtenir le

Grade de Docteur de
l'Université de Bourgogne

Spécialité : **Informatique**

Espaces tangents pour les formes auto-similaires

Soutenue le 20 décembre 2013 devant le Jury :

Loic BARTHE	Rapporteur	HDR, Maître de conférences de l'Université de Toulouse
Raphaëlle CHAINE	Examinateur	Professeur de l'Université de Lyon
Christian GENTIL	Directeur de thèse	HDR, Maître de conférences de l'Université de Bourgogne
Ronald GOLDMAN	Examinateur	Professeur de l'Université Rice
Pascal SCHRECK	Rapporteur	Professeur de l'Université de Strasbourg
Dmitry SOKOLOV	Coencadrant	Maître de conférences de l'Université de Lorraine

Contents

1 Introduction **1**
1.1 Organisation and contributions . . . 2

2 State of the art **5**
2.1 Subdivision curves and surfaces . . . 5
2.1.1 Joining subdivision schemes . . . 8
2.2 FIF development and differentiability analysis . . . 8
2.3 Previous results for IFS on $\mathbb{R}^2$ . . . 10

3 Background on IFS, CIFS and BCIFS **13**
3.1 Iterated Function Systems . . . 13
3.1.1 Hutchinson operator . . . 14
3.1.2 Algorithm for IFS attractor approximation . . . 14
3.2 Address function . . . 16
3.3 Projective Iterated Function Systems . . . 16
3.4 Controlled Iterated Function System . . . 16
3.4.1 Projected IFS as CIFS . . . 17
3.5 Boundary Controlled IFS . . . 18
3.5.1 Boundary Representation (B-rep) . . . 18
3.5.2 Definitions . . . 18
3.5.3 Topological constraints . . . 20
3.6 Subdivision schemes as BCIFS . . . 22
3.6.1 Regular patch . . . 23
3.6.2 Irregular patch . . . 26
3.7 Generalised eigenvectors . . . 27
3.7.1 Eigenvalues and multiplicities . . . 27
3.7.2 Chains of generalised eigenvectors . . . 28
3.8 Eigenvalues, eigenvectors and barycentric spaces . . . 28
3.9 Conclusion . . . 29

4 Tangent space **31**
4.1 Tangent definition . . . 31
4.2 Rings . . . 33
4.2.1 Points and addresses . . . 33

4.2.2 Sequence of rings definition . . . 35
4.2.3 Tangents, sequences of secants and rings . . . 36
4.3 Tangents and eigenvectors . . . 36
4.4 Angular deviation . . . 37
4.5 Complete set of eigenvectors . . . 39
4.5.1 Complex eigenvalue . . . 40
4.5.2 Double sub-dominant eigenvalues . . . 42
4.5.3 Null component problem . . . 43
4.5.4 Mixed eigenvalues from $\mathbb{R}$ and $\mathbb{C}$ . . . 43
4.5.5 Summary . . . 45
4.6 Incomplete set of eigenvectors . . . 45
4.7 Convergence of the angular deviation. . . . 48
4.8 Summary and points with non-uniform addresses . . . 50
4.9 Examples and applications . . . 51
4.9.1 Curves . . . 51
4.9.2 Surfaces . . . 60
4.9.3 Surfaces as tensor product of curves . . . 64
4.10 Conclusion . . . 66

5 Joining shapes 67
5.1 Joining curves . . . 68
5.1.1 Constructing the intermediate curve . . . 68
5.1.2 Differential properties of the intermediate curve . . . 72
5.1.3 Refinement of the BCIFS . . . 76
5.1.4 Examples . . . 80
5.2 Joining surfaces . . . 81
5.2.1 Continuity constraints . . . 81
5.2.2 Approximation of the limit surface . . . 85
5.2.3 Differential properties of the intermediate surface . . . 86
5.2.4 Refinement of the BCIFS . . . 86
5.2.5 Example . . . 88
5.3 Conclusion . . . 94

6 Conclusion and perspectives 97
6.1 Conclusion . . . 97
6.2 Perspectives and future work . . . 98

A Appendix 99
A.1 Regular patches subdivision . . . 99
A.2 Intermediate patches subdivision . . . 100

Abstract

The fractal geometry is a relatively new branch of mathematics that studies complex objects of non-integer dimensions. It finds applications in many branches of science as objects of such complex structure often poses interesting properties. In [Bar88] Barnsley presented the Iterative Function System (IFS) model that allows modelling complex fractal shapes with only a limited set of contractive transformations. Later many other models were based on the IFS model such as Language-Restricted IFS, Projective IFS, Controlled IFS and Boundary Controlled IFS. The last to allow modelling complex shapes with control points and specific topology. These models cover classical geometric models such as B-splines and subdivision surfaces as well as fractal shapes.

This thesis focuses on the analysis of the differential behaviour of the shapes described with Controlled IFS and Boundary Controlled IFS. We derive the necessary and sufficient conditions for differentiability for everywhere dense set of points. Our study is based on the study of the eigenvalues and eigenvectors of the transformations composing the IFS.

We apply the obtained conditions to modelling curves in surfaces. We describe different examples of differential behaviour presented in shapes modelled with Controlled IFS and Boundary Controlled IFS. We also use the Boundary Controlled IFS to solve the problem of connecting different subdivision schemes. We construct a junction between Doo-Sabin and Catmull-Clark subdivision surfaces and analyse the differential behaviour of the intermediate surface.

Keywords: fractal curve, fractal surface, IFS, tangent, subdivision

Chapter 1

Introduction

Iterative ways of modelling shapes are widely spread in modern Computer Aided Design (CAD) systems. They allow us to model complex shapes as algorithms that are iteratively applied to an initial small set of data points. Many subdivision techniques are well known such as Doo-Sabin [DS78], Catmull-Clark [CC78] and Loop [Loo87].

Most iterative models used in CAD can only describe smooth shapes such as piecewise-polynomial curves or surfaces. However, nature is full of objects that are not smooth and are thus difficult to model with modern CAD systems. Most natural forms tend to have irregular and chaotic patterns. Over the years, different mathematical objects that possess such properties have been studied.

B. Mandelbrot introduced the notion of fractal geometry, a new theory about complex objects that possess features on any level of detail [Man82]. While studying coastal lines he observed that they possess the same irregular structure at all levels of scale and that their length increases with more precise measurements. The same properties are shared by fractal curves — objects of non-integer dimensions, that is called the fractal dimension. Fractal geometry is a relatively new branch of mathematics that provides a way of modelling natural phenomena while respecting their irregular structure.

The global objective of our work is to develop a geometric modeller based on the paradigm of fractal geometry. More precisely, we aim to model shapes by means of iterative processes. Our formalism covers traditional models like NURBS[1] and subdivision surfaces and also a new world of shapes, not accessible by the polynomial models and having a particular aesthetic. Our study is based on the Iterated Function System model introduced by M. Barnsley in [Bar88]. This model provides a way to model complex irregular objects by iterative modelling, utilising the properties of self-similarity.

Self-similar shapes possess not only a particular aesthetic, but a variety of physical qualities. They may exhibit extreme surface-to-volume ratios, which is an important property in many physical and chemical processes. Fractal-shaped antennae have long been used in electronics because of their ability to receive signals at different frequencies. Integrating tools to model fractal shapes into wide-spread CAD systems will allow for the easy design and manufacturing of such shapes.

[1] Non-Uniform Rational B-Splines

There are many models based on the concept of Iterative Function System (or IFS for short) that add various features to the model. Among them is Projective IFS that allows for the modelling of fractal shapes with control points. Projective Iterative Function Systems were introduced by C.E. Zair and E. Tosan [ZT96]. In [ZT97] they also show that this model can be used to describe both smooth and rugged shapes. S. Schaefer, D. Levin, and R. Goldman in [SLG05] showed that subdivision curves and surfaces can be viewed as attractors of Iterative Function Systems. Thus the Projective IFS model incorporates the ability to model both classical polynomial and fractal shapes.

The classic differential analysis of subdivision surfaces is based on the notion of a characteristic map proposed by U. Reif and in [Rei95] and expanded by H. Prautzsch in [Pra98]. According to their work, a subdivision schemes with injective and regular characteristic maps produce tangent continuous surfaces at the extraordinary points. However, verifying whether the characteristic map is injective requires calculation for each type of extraordinary point. Later, D. Zorin showed that for a general class of subdivision schemes, regularity can be inferred from the properties of a sufficiently close linear approximation, and injectivity can be verified by computing the index of a curve in [Zor00].

Nevertheless, the injectivity and regularity conditions are too strict to be useful for modelling rough fractal shapes, since shapes without injective characteristic maps and tangents exist (see section 2.1). Also, the characteristic map is linked to the specific vertex of the control mesh, whereas control points of the Projective IFS are not necessarily a part of the mesh.

This thesis examines the differential properties of self-similar objects in the context of geometric modelling. The objective is to study, from the geometric point of view, different ways a self-similar set may behave and to derive the necessary and sufficient conditions for differentiability. We search for a way to establish the differential behaviour of shapes that does not involve their explicit parametrisation, because searching for a parametrisation that does not possess vanishing derivatives can be a arduous task and parametrisation is shape specific. Developing strict criteria will allow us to quickly analyse newly constructed objects. In particular, our method could be applied to the analysis of new subdivision schemes. Our approach also allows us to directly control the topological subdivision of the shapes. Hence it is not limited to subdivisions of the control meshes of a specific type.

1.1 Organisation and contributions

This thesis consists of 5 chapters, in addition the current one.

In chapter 2 we discuss previous studies of fractal shape differentiability. We also discuss various studies of subdivision scheme differentiability.

In chapter 3 we recall the definition of the IFS model as well as its more generalised counterparts such as Controlled Iterated Function Systems (CIFS) and Boundary Controlled Function Systems (BCIFS).

Chapter 4 is dedicated to the main findings of this work. In this chapter we define the notion of tangent subspace and study various cases of differential behaviour of the shapes designed with iterative modelling. We present the necessary and sufficient conditions for differentiability for the class of points that is everywhere dense within the modelled shape. We also provide numerous examples of calculation of the tangent subspaces for different

kinds of attractors.

In chapter 5 we discuss the problem of connecting different shapes within the BCIFS model. We propose a way to construct a junction between two curves or two surfaces. Using the BCIFS formalism, we describe the subdivision of the junction's topology and define it as the attractor of BCIFS. Then we use the results obtained in chapter 4 to analyse the differential properties of the junction. Results presented in this chapter have been published in two articles: [PGSL13a] covers the construction of the intermediate curve, while [PGSL13b] discusses junction between surfaces.

Finally, in chapter 6 we provide a summary of our work and discuss some open problems.

Chapter 2

State of the art

In this chapter we discuss developments in the differential analysis of self-similar and fractal shapes. First we discuss the use of the characteristic map in the analysis of subdivision surfaces. We also give an example of a subdivision with a non-injective characteristic map and a tangent. Then we discuss various studies of the differential properties of fractal and self-similar shapes.

2.1 Subdivision curves and surfaces

Since 1978 subdivision surfaces has become a major staple in geometric modelling. They allow a coarse mesh of control points to represent a refined and smooth surface of arbitrary topology with known degrees of continuity. Subdivision schemes started from simultaneous developments by Catmull and Clark [CC78] and by Doo and Sabin [DS78].

Differential properties of subdivision surfaces are the subject of many studies. In [Pra98] Prautzsch studies the differentiability of subdivision schemes at the extraordinary vertices. His study exploits the following idea: for every extraordinary vertex at every step of the subdivision, its neighbouring control points define a ring of m irregular patches, where m is the valence of that vertex. After one step of the subdivision, m irregular patches are subdivided into m smaller irregular patches and $3m$ regular patches. These $3m$ regular patches form a ring on a surface that can be parametrised over $[0,1]^2 \times \{1,2,\ldots,3m\}$. The next subdivision step produces a smaller ring that also consists of $3m$ regular patches. A certain parametrisation used by Prautzsch is derived from the notion of characteristic map introduced by Reif and Peters in [Rei95].

Each ring r_m, can be parametrized in terms of control points for each regular patch $B_m^3 \in \mathbb{R}^3$, and basis functions N^l:

$$r_m : (u,v,j) \in [0,1]^2 \times \{1,2,\ldots,3m\} \mapsto \sum_{l=0}^{L} N^l(u,v,j) B_m^l.$$

Let S be a row stochastic subdivision matrix such that control points for the next ring are obtained from the previous one:

$$B_{m+1} = SB_m, \quad B_m = S^m B_0.$$

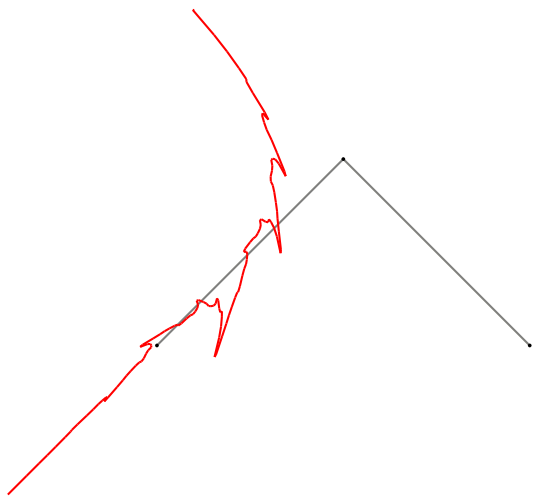

Figure 2.1: A curve with half-tangent at the endpoints and a non-injective characteristic map.

Definition 1 (Characteristic map)**.** *Let $\lambda_0, \ldots, \lambda_L$ be the eigenvalues of S ordered by their absolute value:*

$$|\lambda_0| \geq |\lambda_2| \geq \ldots \geq |\lambda_L|,$$

and $\vec{v}_0, \ldots, \vec{v}_L$ be the corresponding generalized real eigenvectors. If $|\lambda_0| > |\lambda_1| = |\lambda_2| > |\lambda_3|$ then the characteristic map of the subdivision is defined as

$$\psi : [0,1]^2 \times \{1, 2, \ldots, 3m\} \mapsto N[\vec{v}_1, \vec{v}_2],$$

where $[\vec{v}_1, \vec{v}_2]$ is the matrix whose columns are sub-dominant eigenvectors of S.

Here rows of $[\vec{v}_1, \vec{v}_2]$ serve as control points for the ring placed into $\mathbb{R}^2$. In [Rei95], Reif and Peters proved that if the characteristic map is regular and invertible then the resulting surface is C^1-continuous. Prautzsch showed that under certain conditions on eigenvalues and eigenvectors of the subdivision matrices the subdivision schemes with a regular and invertible characteristic map produce G^k-continuous surfaces at the extraordinary points.

However the characteristic map is often not injective for fractal shapes. As an example we consider the curve presented in figure 2.1. The end points of the curve are obtained with the following subdivision mask:

$$S = \begin{pmatrix} \frac{5}{4} & -\frac{1}{4} & 0 \\ \frac{1}{2} & \frac{1}{2} & 0 \\ 0 & \frac{5}{4} & -\frac{1}{4} \end{pmatrix}.$$

Like any other curve obtained with subdivision, such a curve is self-similar. The corresponding IFS is described in section 3.6. According to [Ben09] the half-tangents exist at the vertices; however, as we will show, the characteristic map is not injective.

If we calculate the eigenvectors of S and associated eigenvalues we obtain the following:

$$\lambda_0 = 1, \lambda_1 = 3/4, \lambda_2 = -1/4,$$

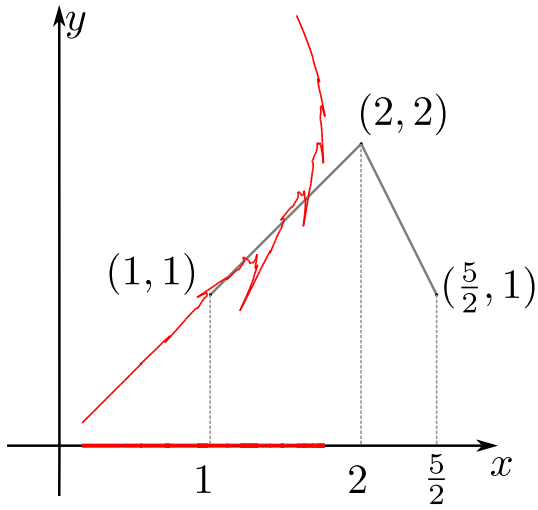

Figure 2.2: Graph of the characteristic map as a projection from $\mathbb{R}^2$.

$$\vec{v}_0 = \begin{pmatrix} 1 \\ 1 \\ 1 \end{pmatrix}, \ \vec{v}_1 = \begin{pmatrix} 1 \\ 2 \\ 5/2 \end{pmatrix}, \ \vec{v}_2 = \begin{pmatrix} 0 \\ 0 \\ 1 \end{pmatrix}.$$

The characteristic map is a natural parametrisation of such curve placed in $\mathbb{R}$ using components of $\vec{v}_1$ as control points. This parametrisation is not injective as we can demonstrate. Consider a vector $p = (p_1, p_2, p_3)$ of three control points from $\mathbb{R}^2$ such that their first coordinates are equal to the components of $\vec{v}_1$ (see figure 2.2). The following is a parametrisation of the curve with such control points:

$$f(x) = \sum_{i=1}^{3} N^i(x) p_i,$$

where N^i are basis function. If we denote the projection onto Ox as Pr the characteristic map $\phi(x)$ can be written as follows:

$$\phi(x) = \sum_{i=1}^{3} N^i(x) Pr(p_i) = Pr(f(x)).$$

Thus $\phi(x)$ is not injective since Pr does not map the graph of f to the graph of ϕ injectivly. Verifying the injectivity of the characteristic map is therefore not only difficult, but such a condition is too strict to be used for rough non-polynomial shapes.

In [MG01], Morin and Goldman study the convergence of discrete derivatives of arbitrary degree of Bézier curve approximations. Given a parametrisation, control polygons produced by subdivision algorithms can serve as approximations for the limit curve. A specific way to parametrize the control polygons is chosen to show that as the approximations converge to the limit curve, their respective derivatives converge to the continuous derivative of the original Bézier curve.

Boier-Martin and Zorin also study the differentiability of Catmull-Clark subdivision scheme. In [BMZ04] they present a parametrisation that possesses non vanishing derivatives at the extraordinary points.

2.1.1 Joining subdivision schemes

Different subdivision schemes operate on different types of meshes and the visual properties of the final surface depend on the subdivision scheme. So for modelling complex objects an amalgamation of different subdivision schemes is often necessary.

Quad-triangle schemes

Two of the most popular subdivision schemes operate on different type of meshes. Catmull and Clark [CC78] scheme operates on quads, while Loop [Loo87] scheme operates on triangles. The visual properties of a limit surfaces vary according the method used, so in modelling complex shapes there is often a need to use both quad and triangle schemes. A number of studies have been performed on schemes that combine two subdivision schemes to develop a way to work with quad-triangle meshes.

Different biregular subdivision schemes have been studied for primal schemes. Stam and Loop propose a generalization of the Catmull-Clark and Loop subdivisions that operates on quad/triangle meshes [SL03]. While mimicking Loop subdivision on triangle regions and Catmull-Clark on quadrilateral, the border between the two regions is subdivided with the averaging mask of Catmull-Clark and Loop. That generalisation produces a C^2 surface with the exception of extraordinary points and a quad-triangle border which is C^1.

Levin and Levin proposed a new set of rules along the quad-triangle border [LL03]. For schemes that are C^m-continuous at each side of the border, they derive a sufficient condition for C^m-continuity of the limit function. This condition requires that the value of the joint spectral radius of a certain pair of matrices is less than 2^{-m}.

Schaefer and Warren [SW05] modify the scheme proposed by Stam and Loop [SL03] by introducing an additional step called unzipping pass. This improves the smoothness along the regular quad-triangle border from C^1 to C^2. Using the approach developed in [LL03] they prove that their schemes is indeed C^2-continuous along the quad-triangle border.

Primal/dual schemes

While many studies have been performed to unify the quad/triangle subdivision scheme, to our knowledge, no biregular subdivision has been performed on primal/dual schemes. The problem lies in the fact that the subdivision process is based on mesh subdivision. The study [KSD12] which proposes a way to transform a primal scheme into a dual scheme may open up new perspectives on this problem.

2.2 FIF development and differentiability analysis

In the context of fractal geometry, many studies have developed the Iterated Function System model. In [Bar86], Barnsley introduced a model called Fractal Interpolation Function (FIF) that allows us to generate a function which interpolates a given set of points and

whose graph is an attractor of an IFS. Given a data set $\{(x_i, y_i) \in I \times \mathbb{R} | i = 0, 1, \ldots, N\}$ where $I = [x_0, x_N] \subset \mathbb{R}$, an Iterated Function System is defined in such a way that its attractor is a graph of the function $f : I \to \mathbb{R}$ such that $\forall i = 0, 1, \ldots N$ $f(x_i) = y_i$.

Let $x_0 < x_1 < \ldots < x_N$. Let L_j be affine maps satisfying

$$L_j(x_0) = x_{j-1},\ L_j(x_N) = x_j,\ j = 1, 2, \ldots, N. \tag{2.1}$$

Let $y_0, y_1, \ldots, y_N \in \mathbb{R}$. Let $-1 < \alpha_j < 1$, $j = 1, 2, \ldots, N$. Let $X = [x_0, x_N]$. Let $F_j : X \times \mathbb{R} \to \mathbb{R}$ such that it satisfies

$$|F_j(x, y_1) - F_j(x, y_2)| \leq |\alpha_j||y_1 - y_2|,\ x \in X,\ y_1, y_2 \in \mathbb{R}, \tag{2.2}$$

$$F_j(x_0, y_0) = y_{j-1},\ F_j(x_N, y_N) = y_j,\ y = 1, 2, \ldots, N. \tag{2.3}$$

The fractal interpolation function associated with $\{(L_j(x), F_j(x, y))\}_{j=1}^N$ is the unique function $f : X \to \mathbb{R}$ such that:

$$f(L_j(x)) = F_j(x, f(x)),\ y = 1, 2, \ldots, N,\ x \in X.$$

The continuity of the function f is guaranteed by conditions 2.3. The graph of the function f is the attractor of the iterated function system on $X \times \mathbb{R}$ composed of the following maps:

$$\{T_j | T_j(x, y) = (L_j(x), F_j(x, y))\}_{j=1}^N.$$

In [BH89], Barnsley and Harrington presented a method to construct FIF that are C^k differentiable. They show that derivatives of f are also fractal interpolation functions. The following theorem demonstrates that it is possible to define the fractal interpolation function that is C^k differentiable.

Theorem 1 (Barnsley and Harrington, [BH89])**.** *Let $x_0 < x_1 < \ldots < x_N$ and let the affine functions $L_j(x) = a_j x + b_j$ that verify 2.1, where $a_j = L_j'(x) = \frac{x_j - x_{j-1}}{x_N - x_0}$. Let $F_j(x, y) = \alpha_j y + q_j(x)$, $j = 1, 2, \ldots, N-1$ such that F_j verify 2.2 and 2.3. Suppose that for some integer $n \geq 0$, $|\alpha_n| < a_j^n$, $q_j \in C^n[x_0, x_N]$, $j = 1, 2, \ldots, N$. Let*

$$F_{j,k}(x, y) = \frac{\alpha_j y + q_j^{(k)}(x)}{a_j^k},$$

$$y_{0,k} = \frac{q_1^{(k)}(x_0)}{a_1^k - \alpha_1},\ y_{N,k} = \frac{q_N^{(k)}(x_N)}{a_N^k - \alpha_N},\ k = 1, 2, \ldots, n.$$

If $F_{j-1,k}(x_N, y_{N,k}) = F_{j,k}(x_0, y_{0,k})$, $j = 2, 3, \ldots, N$ and $k = 1, 2, \ldots, n$, then $\{(L_j(x), F_j(x, y))\}_{j=1}^N$ determines a fractal interpolation function $f \in C^n[x_0, x_N]$ and $f^{(k)}$ is the fractal interpolation function associated with $\{(L_j(x), F_{(j,k)}(x, y))\}_{j=1}^N$, $k - 1, 2, \ldots, n$.

Later, in [Mas91], Massopust expands the notion of the fractal interpolation function into a vector valued fractal interpolation function. This notion allow us to define the functions interpolating data points in $\mathbb{R}^n$.

Using on the FIF model, Cochran et al. [CLH01] discovered a class of fractal surfaces that are differentiable. They used the fact that an integral of a fractal interpolation function

remains a fractal interpolation function, and this new function is everywhere differentiable. The corresponding derivative f' is of course a solution of the differential equation:

$$f(x) = y_0 + \int_{x_0}^{x} f'(t)dt.$$

They study surfaces obtained as tensor product of fractal interpolation functions and show that such surfaces are both fractal and have well-defined surface normals. Given two differentiable fractal interpolation functions $f(x)$ and $g(y)$ a height map $h(x, y)$ is defined:

$$h(x, y) = f(x)g(y),\ x_0 \leq x \leq x_N,\ y_0 \leq y \leq y_M.$$

Then the partial derivatives are used to calculate the tangent plane and normal at (x, y):

$$h_x(x, y) = f'(x)g(y),$$

$$h_y(x, y) = f(x)g'(y).$$

So the tangent plane at (x, y) is spanned by vectors $\vec{v}_1 = (1, 0, h_x(x, y))$ and $\vec{v}_2 = (0, 1, h_y(x, y))$. The normal vector $N(x, y)$ can be computed as the cross product of $\vec{v}_1$ and $\vec{v}_2$:

$$N(x, y) = \vec{v}_1 \times \vec{v}_2 = (-h_x(x, y), -h_y(x, y), 1) = (-f'(x)g(y), -f(x)g'(y), 1).$$

2.3 Previous results for IFS on $\mathbb{R}^2$

Hicham Bensoudane [Ben09] focuses on applying IFS to geometric modelling. He developed a method of studying the differential properties of fractal curves in $\mathbb{R}^2$. Bensoudane used the notion of local fraction derivative and exploits the self-similar nature of shapes modelled with the Iterative Function System model.

For a curve modelled as an attractor of an IFS in $\mathbb{R}^2$ a general expression of the local fractional derivative is given in terms of operators composing the corresponding IFS. It is shown that under a certain condition on eigenvalues of the linear part of the affine operators composing the IFS, this expression is well defined and for an everywhere dense set of points: points with periodic addresses.

Definition 2 (Local fractional derivative)**.** *If for a function f the following limit exists:*

$$D^q f(y) = \lim_{x \to y} \frac{d^q(f(x) - f(y))}{[d(x - y)^q]}$$

and is bounded for some $q \in (0, 1)$ then it is called the local fractional derivative of order q.

Considering $x < y$ or $y < x$ gives the definition for left and right fractional derivatives at y. Left and right local fractional derivatives of the function f are denoted by $D^q_+ f$ and $D^q_- f$ respectively.

For a given self-similar curve $\mathcal{A}$ a parametrisation is defined in the form of a transport function denoted by H. A supplementary IFS has a parameter domain as an attractor (for example unit segment $[0, 1]$ for a curve). If this supplementary IFS has the same number of transformations, then the transport function H maps a point on the parameter domain

$t \in [0,1]$ with address σ to the corresponding point $\bar{t} \in \mathcal{A}$ that corresponds to the same address σ. Under certain conditions on the supplementary IFS function H is continuous.

Given an IFS and a transport function, necessary conditions for the existence of $D_+^q H$ and $D_-^q H$ are deduced for points t that have a periodic address without any finite prefix (addresses like i^ω). Then existence of local fractional derivative at points that have periodic addresses with some finite prefix (σi^ω) is studied. It is shown that its existence depends on the local fractional derivative at the point with address i^ω. A way to calculate the local fractional derivative for periodic points with a finite prefix (σi^ω) from the local fractional derivative of periodic point with an empty prefix(i^ω) is given. Finally, sufficient conditions for the existence of local fractional derivatives for IFS defined in $\mathbb{R}^2$ are given at the points with periodic addresses σi^ω.

The relation between the critical order of derivation, the local Hölder coefficient and the fractal dimension of curves is also studied. The author shows that the critical order of derivation and the local Hölder coefficient can be used as a measure of roughness as well as fractal dimension.

Chapter 3

Background on IFS, CIFS and BCIFS

In this chapter we recall the concepts of the Iterated Function Systems, Projective Iterated Function Systems, Controlled Iterated Function Systems and Boundary Controlled Function Systems. We also review some facts about eigenvectors and eigenvalues of the operators acting on barycentric spaces.

3.1 Iterated Function Systems

Iterated Function Systems (or IFS for short) were first introduced by Hutchinson in [Hut81]. The notion of Iterated Function Systems is based on the fact that a contractive operator acting on a space of compacts has a unique fixed point, and therefore each contractive operator corresponds to a compact set called an attractor of the IFS. Attractors are always self-similar, i.e. they consist of smaller copies of themselves.

Definition 3 (Contractive operator)**.** *An operator T acting on a metric space $(\mathcal{X}, d)$ is called contractive if:*

$$\exists 0 < s < 1, \quad \forall x, y \in X, d(T(x), T(y)) \leq sd(x, y).$$

The value s is called the contractive factor of the operator T.

Example 1 (Contractive operator)**.** The function $f(x) = \frac{1}{2}x$ acting on $\mathbb{R}$ is contractive in respect to the Euclidean distance. The corresponding contractive factor is $\frac{1}{2}$.

If T is a contractive operator on a complete metric space $(\mathcal{X}, d)$, then

$$\exists! p \in \mathcal{X} : T(p) = p.$$

The point p is called a fixed point of the operator T.

Example 2 (Fixed point)**.** For the contractive operator $f(x) = \frac{1}{2}x$ from example 1 the origin is a fixed point. However for the operator $f'(x) = \frac{1}{2}x + \frac{1}{2}$ acting on the same space 1 is the fixed point.

3.1.1 Hutchinson operator

Consider the complete metric space $(\mathcal{X}, d)$. We denote the set of non-empty compacts subsets of $(\mathcal{X}, d)$ as $H(\mathcal{X})$. $H(\mathcal{X})$ can be equipped with the Hausdorff distance.

Definition 4 (Hausdorff distance)**.** *Let $X, Y \in H(\mathcal{X})$. The following metric is thus called a Hausdorff distance:*

$$d_H(X, Y) = \max\{\max_{x \in X} \min_{y \in Y} d(x, y), \max_{y \in Y} \min_{x \in X} d(x, y)\}.$$

As shown in [Bar88] if $(\mathcal{X}, d)$ is a complete metric space then $(H(\mathcal{X}), d_H)$ is also complete. Given a set of operators on $\mathcal{X}$ we can define a so-called Hutchinson operator on $H(\mathcal{X})$.

Definition 5 (Hutchinson operator)**.** *Consider a set of operators on $\mathcal{X}$, $\{T_i\}_{i=0}^{N-1}$. We can define a new operator $\mathbb{T}$ as follows:*

$$\mathbb{T}(X) = \cup_{i=0}^{N-1} T_i(X).$$

If $\forall i$ T_i is a contractive operator on $(\mathcal{X}, d)$, then $\mathbb{T}$ is also contractive on $(H(\mathcal{X}), d_H)$ [Bar88].

Definition 6 (Iterated Function System)**.** *Given a complete metric space $(\mathcal{X}, d)$ an Iterated Function System is a finite set of contractive operators $\{T_i\}_{i=0}^{N-1}$ on $(\mathcal{X}, d)$.*

The set of contractive operators defines a Hutchinson operator on $(H(\mathcal{X}), d_H)$, which is also contractive and has a unique fixed point that we denote as A. The compact $\mathcal{A}$ is called an attractor of the IFS. Note that A is a self-similar set since

$$\mathcal{A} = \mathbb{T}(\mathcal{A}) = \bigcup_{i=0}^{N-1} T_i(\mathcal{A}).$$

Example 3 (Sierpiński Triangle)**.** The Sierpiński triangle is an attractor of an IFS composed of three transformations on $\mathbb{R}^2$

$$T_0 = \begin{pmatrix} 0.5 & 0 \\ 0 & 0.5 \end{pmatrix}, T_1 = \begin{pmatrix} 0.5 & 0 \\ 0 & 0.5 \end{pmatrix} + \begin{pmatrix} 0.5 \\ 0 \end{pmatrix}, T_2 = \begin{pmatrix} 0.5 & 0 \\ 0 & 0.5 \end{pmatrix} + \begin{pmatrix} 0.25 \\ 0.5 \end{pmatrix}$$

Its approximation is presented in figure 3.1

3.1.2 Algorithm for IFS attractor approximation

Two algorithms for computing an attractor of an Iterated Function System are presented by Barnsley [Bar88]. The algorithms are the Deterministic Algorithm and the Random Iteration Algorithms also known as Chaos Game.

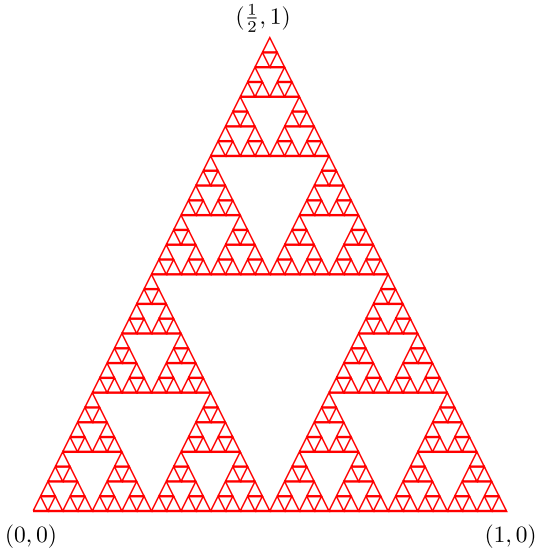

Figure 3.1: Sierpiński triangle.

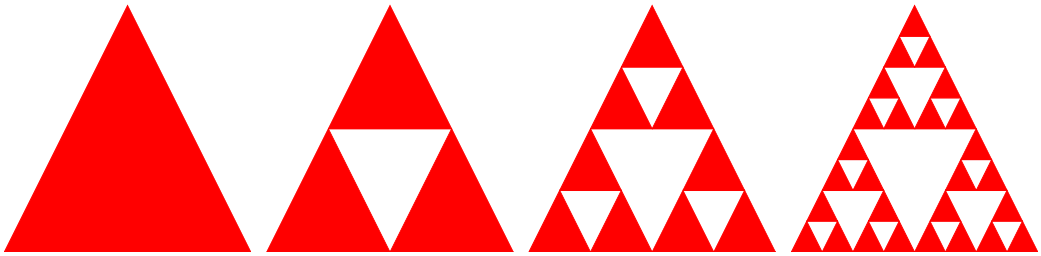

Figure 3.2: A sequence of compact sets approximating the Sierpiński triangle.

Deterministic Algorithm

The Deterministic Algorithm directly computes a sequence of approximation using the Hutchinson operator. For a given IFS $\{T_i\}_{i=0}^{N-1}$ acting on metric space $(\mathcal{X}, d)$ we start by choosing any compact set K_0 in $\mathcal{X}$ and computing $K_n = \mathbb{T}^n(K_0)$. Since $\mathbb{T}$ is a contractive map on $H(\mathcal{X})$ there exists a limit $\lim_{n\to\infty} \mathbb{T}^n(K) = \mathcal{A}$. Thus we have constructed a sequence of compact sets that converge to the attractor of the IFS. Note that the limit is independent of K. Therefore we can start computing the approximation with any non-empty compact set in $\mathcal{X}$. Four iterations of approximation of the Sierpiński triangle are presented in figure 3.2. This example uses a single triangle as a starting point.

Random walk

For a given IFS $\{T_i\}_{i=0}^{N-1}$ acting on metric space $(\mathcal{X}, d)$ assign a non-zero probability p_i for each $i = 0, \ldots, n-1$ such that $\sum_{i=0}^{n-1} p_i = 1$. Choose any $x_0 \in \mathcal{X}$ and then chose x_n from

$\{T_i(x_{n-1})\}_{i=0}^{n-1}$ with respective probabilities p_i. For any $n \in \mathbb{N}$ $x_n \in \mathcal{A}$. As n increases x_n fills out the shape of the attractor. For more details, refer to [Bar88].

3.2 Address function

The address function [Bar88] allows us to associate any point belonging to the attractor of an IFS with an infinite string of symbols from the finite alphabet. Each symbol corresponds to an operator of the IFS. Here is the underlying idea: when we apply one of the operators to the attractor we obtain its smaller part. We can repeat the process, obtaining a sequence of nested sets. These sets have only one common point. In this way we can set a correspondence between an infinite string (address) and a point of the attractor.

Definition 7 (Address function)**.** *Let us consider an IFS* $\mathbb{T} = \{T_0, \ldots, T_{N-1}\}$*. We can denote the alphabet associated with it as* $\Sigma = \{0, \ldots, N-1\}$*. We also denote the set of infinite length words on* Σ *as* Σ^ω*. The address function is defined as follows:*

$$\phi : \Sigma^\omega \to A$$

$$\sigma \to \phi(\sigma) = \lim_{i \to \infty} T_{\sigma_1} T_{\sigma_2} \cdots T_{\sigma_i} p,$$

for any point p*. The limit is independent of* p *as shown in [Bar88].*

3.3 Projective Iterated Function Systems

The idea of projective IFS was introduced by Zair and Tosan [ZT96]. By separating the iterative space from the modelling space, it is possible to construct fractal shapes with control points. Similar to splines determined by the basic functions defined in a barycentric space, attractors are also defined in a barycentric space whose dimensions correspond to the number of control points: $\mathcal{A} \subset BI^n = \{\lambda \in \mathbb{R}^n | \sum_{i=0}^{n-1} \lambda_i = 1\}$, where n is the number of control points. Then the attractor is projected into the modelling space with the transformation defined by control points $P\mathcal{A} = \{\sum_{i=0}^{n-1} P_i \lambda_i | \lambda_i \in \mathcal{A}\}$, where $P = [P_0 \ P_1 \cdots P_{n-1}]$ is the vector composed of control points.

The operators on the barycentric space can be written as linear operators on $\mathbb{R}^n$, with a specific constraint on its matrix representation: each column of the matrix must have the sum of its elements equal to 1. The fixed point of such operator, as well as an attractor of the IFS composed of such operators, always belong to the barycentric plane.

3.4 Controlled Iterated Function System

In this section we cover the notion of Controlled Iterated Function System. Attractors of the plain IFS can be viewed as a union of parts, where each part is similar to the whole. The CIFS model allows us to describe shapes where some of these parts are not the image of the attractor itself, but of something else (usually an attractor of another IFS).

Definition 8 (Controlled Iterated Function System)**.** *The set of the following items is called Controlled Iterated Function System:*

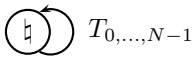

Figure 3.3: Simple IFS as a CIFS automaton.

- *an automaton* $(E,\ \Sigma, \delta, \natural)$*, where* E *is a set of states,* Σ *is an alphabet and* δ *is a transition function* $\delta : E \times \Sigma \to E$ *and* $\natural \in E$ *is a starting state.*
- *a set of metric spaces associated with each state* $\{\mathcal{X}^e | e \in E\}$
- *a set of transformations associated with each transition* $T_i^e : E^{\delta(e,i)} \to E^e$

We also denote as Σ_e the subset of Σ such that for all $i \in \Sigma_e$ there exist $\delta(e, i)$.

Definition 9 (Attractor of the CIFS state)**.** *Each CIFS state* $e \in E$ *is associated with an attractor that is denoted as* $\mathcal{A}^e$*:*

$$\mathcal{A}^e = \bigcup_{i \in \Sigma_e} T_i^e(\mathcal{A}^{\delta(e,i)}).$$

In other wordsm an attractor associated with the state e is composed of attractors associated with states e_i such that there exists a transition from e to e_i. If all outgoing transitions from the state lead to the same state, then the attractor associated with the state is an attractor of a normal IFS composed of the transformation corresponding to the transitions (see figure 3.3).

Definition 10 (Attractor of the CIFS)**.** *The attractor associated with the initial state of the CIFS is also considered the attractor of the CIFS as a whole.*

Iterative algorithm for CIFS attractor approximation

For each state $e \in E$ of the CIFS we can approximate the associated attractor $\mathcal{A}^e$ with a sequence of compact sets, that we denote $\{K_n^e\}_{n \in \mathbb{N}}$. For each state e we choose a non-empty compact set $K_0^e \in H(\mathcal{X}^e)$. Using K_0^e we can compute the next iteration as follows:

$$K_{i+1}^e = \bigcup_{i \in \Sigma_e} T_i^e K^{\delta(e,i)_n}.$$

3.4.1 Projected IFS as CIFS

Within the CIFS framework the principle of Projective IFS can be implemented. Let us consider a CIFS such that there is no incoming transition for the initial state $\natural$. Or in other words:

$$\forall e \in E, i \in \Sigma_e \quad \delta(e, i) \neq \natural.$$

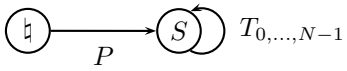

Figure 3.4: A projective IFS as a CIFS automaton.

As an example consider the automaton presented in figure 3.4. The metric space associated with the initial state $\mathcal{X}^\natural$ can be treated as a modelling space, while space associated with state S is the barycentric space of some dimension n. The operator associated with the transition from P to S can be viewed as a vector of n control points.

3.5 Boundary Controlled IFS

Both IFS and CIFS models allows us to model a variety of different forms. However, they provide little to no ability to control the topology of the objects. Since shapes are described via a set of transformations, small changes in description lead to changes on both local and global scales. The IFS and CIFS models cannot guarantee that the topology of the attractor is conserved for even small changes in the transformations, for example when the continuous curve will turn into a disconnected set of points. To remedy this issue the BCIFS model was developed. Here we give a brief overview of the model, for more details please refer to [Gou10].

3.5.1 Boundary Representation (B-rep)

In classical CAD-systems the B-rep model is used to control the topology of the geometric model. The model is stored as a set of topological cells such as face, edge or vertex, and their relations. There are two types of relations between the cells. First, there is incidence based on the notion of inclusion: each face is bordered by a number of edges; edges are in turn bordered by vertices. The second type of relation is adjacency. Two cells are said to be adjacent if there exists a common cell incident to both of them, such as a common edge between neighbouring faces, or a common vertex for two adjacent edges.

In classical B-rep, models edges are curves, while faces are surfaces. The BCIFS model allows us to use B-rep notion with fractal objects such as faces or curves. For example, neither Sierpiński triangle nor Mengers carpet has a topological dimension of a surfaces, but one can easily identify that they both have a set of edges. Such an object may also be a face of a higher dimensional shape. So the notion of the iterative cell is introduced instead that of the topological cell. The iterative cell is an attractor of an IFS or a CIFS and is not necessarily homeomorphic to a curve or a surface.

3.5.2 Definitions

The simplest topological cell is a vertex. In the BCIFS model, a vertex is represented as a state with a single transition, which is associated with a transformation called vertex

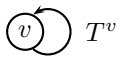

Figure 3.5: A BCIFS representation of a vertex.

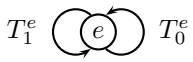

Figure 3.6: A BCIFS representation of an edge with two subdivision operators.

subdivision (see figure 3.5).

The second type of topological cell is an edge. An edge is represented as a state with two or more transitions, which are associated with a set of transformations called edge subdivisions (see figure 3.6).

To describe the incidence relation between the vertex and an edge, a special transition is introduced. The associated operator is called a boundary operator and is denoted as ∂. The boundary operator projects the vertex from its iterative space into the iterative space of the edge (see figure 3.6).

BCIFS and barycentric spaces

Iterative spaces and boundary operators can be chosen at whim, but it is convenient to use barycentric spaces of the appropriate dimensions. Such choice also allows us to identify the relation between control the points of topological cells.

For example, consider a curve with three control points. If the first vertex depends on the first two control points and the second one depends on the last two, then their respective boundary operators can be chosen as follows:

$$\partial_0 = \begin{pmatrix} 1 & 0 \\ 0 & 1 \\ 0 & 0 \end{pmatrix}, \partial_1 = \begin{pmatrix} 0 & 0 \\ 1 & 0 \\ 0 & 1 \end{pmatrix}.$$

The operators ∂_0 and ∂_1 describe the embedding/nesting of the barycentric spaces of the vertices in the barycentric space of the curve. The first operator maps the first dimension of the vertex barycentric space is to the first dimension of the curve barycentric space. Second dimension of the vertex space is mapped to the second dimension of the curve space. Likewise, the second operator maps two dimensions of the vertex space to the second and third dimensions of the curve space. For reference see figure 3.8.

The complete automaton for a simple edge is presented in figure 3.7. Note that this automaton distinguishes between two vertices labelled as v^l for the left vertex, and v^r for the right vertex.

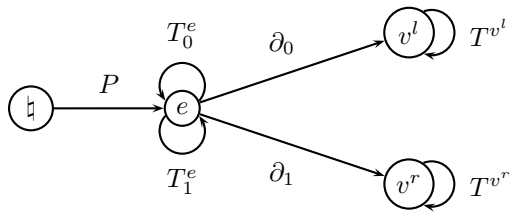

Figure 3.7: An automaton representing a curve with two edge subdivisions $T^e_{0,1}$ and two different vertex subdivisions T^{v^l}, T^{v^r}.

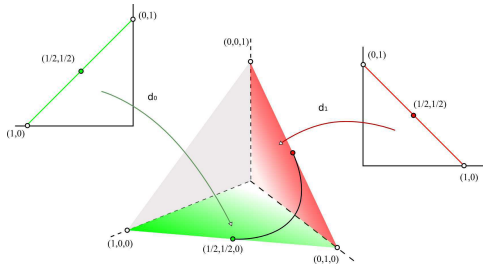

Figure 3.8: Vertex spaces are embedded into the higher dimension curve space.

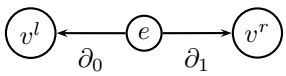

Figure 3.9: The first level of the edge subdivision.

3.5.3 Topological constraints

Let us consider the B-rep structure during the iterative process. At the beginning we have an edge state and two vertex states (see figure 3.9).

When we apply the respective subdivision operators we obtain the next iteration (see figure 3.10).

Adjacency constraints

The edge is subdivided into two parts, so the "left" part has to be connected to the "right" one through the intermediate vertices (see figure 3.11). First of all the states v^l and v^r have to be identical, or in other words, the "left" and the "right" vertices need be of the same "nature" and be subdivided by the same operator, otherwise continuity is not ensured. The

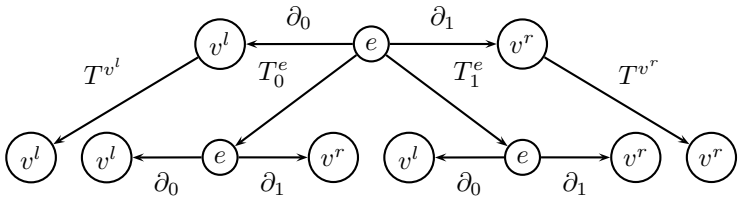

Figure 3.10: The first and second levels of subdivision.

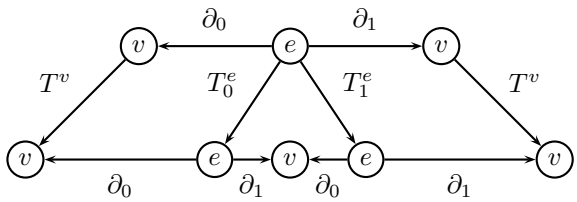

Figure 3.11: Unfolding of the automaton after applying the adjacency and incidence constraints.

condition $T^{v^l} = T^{v^r} = T^v$ is therefore necessary.

Another condition is deduced by writing the equivalence of paths in the graph: the left vertex of the right subdivision has to correspond to the right vertex of the left subdivision:

$$T_0 \partial_1 = T_1 \partial_0.$$

Incidence constraints

In the same manner, incidence constraints express the fact that vertices must remain at the ends of the edges during the subdivision process: subdivision of the left vertex of the edge has to correspond to the left vertex of the left subdivision of the edge (see figure 3.11). Writing down equivalences between paths gives the following equations:

$$\partial_0 T^v = T_0 \partial_0,$$

$$\partial_1 T^v = T_1 \partial_1.$$

Resolving the constraints, adjacency and incidence determine the structures in the subdivision matrices in the form of equalities between columns and sub-matrices (see figure 3.12). Two examples of curves that can be described by a BCIFS are presented in figure 3.13.

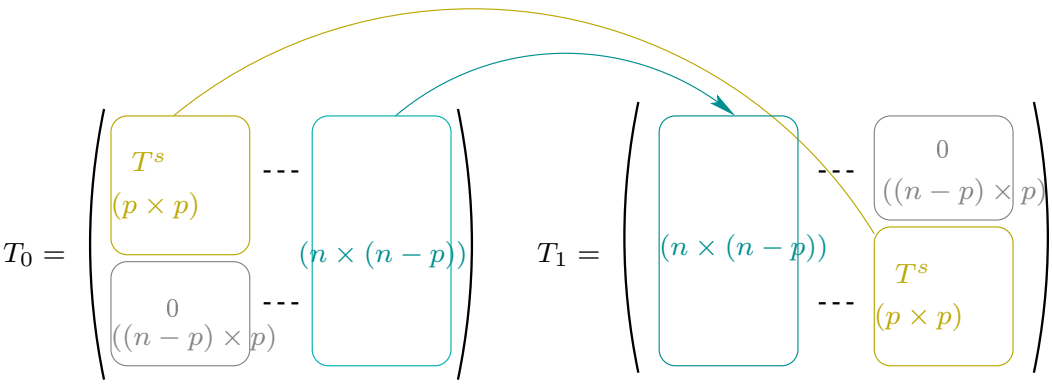

Figure 3.12: General structure of the subdivision matrices for a curve with n control points, whose vertices are controlled by p control points.

Figure 3.13: Left: a cubic spline with 4 control points. Right: a fractal curve with 3 control points.

3.6 Subdivision schemes as BCIFS

It was shown in [SLG05] that subdivision surfaces as well as B-splines are self-similar (also see [CE98] and [ZT96]). Thus they can be modelled as attractors of BCIFS. In this section we present some examples. First, we start with a simple B-spline of degree n. We know that a B-spline of degree n has $n+1$ control points. A single step of subdivision produces $n+2$ points. These points can be viewed as two B-splines of degree n with $n-1$ common control points. The operators that map the initial $n+1$ control points into the first and last $n+1$ control points are the IFS operators that we are looking for.

So we have established that our curve is subdivided into two parts. Thus our edge-state has two transformations associated with it. Let us denote them as T_0 and T_1.

We also recall that each vertex is controlled by n control points. With this knowledge, we can write the boundary operators for each vertex. In matrix form, they can be written as two matrices $\partial_{0,1} \in \mathbb{R}^{(n \times n-1)}$ such that any element $a_{i,j} = 1$ if $i = j$ and $a_{i,j} = 1$ otherwise. For example, for a B-spline of degree two we obtain:

$$\partial_0 = \begin{pmatrix} 1 & 0 \\ 0 & 1 \\ 0 & 0 \end{pmatrix}, \partial_1 = \begin{pmatrix} 0 & 0 \\ 1 & 0 \\ 0 & 1 \end{pmatrix}.$$

Using them and the continuity conditions derived earlier we can derive the structure of the operators. Using the example of $n = 2$ we obtain the following transformations:

$$T_0 = \begin{pmatrix} 1-a & b & 0 \\ a & 1-b & 1-a \\ 0 & 0 & a \end{pmatrix}, T_1 = \begin{pmatrix} b & 0 & 0 \\ 1-b & 1-a & b \\ 0 & a & 1-b \end{pmatrix}.$$

The differential behaviour of the curves obtained by means with such transformations was studied in [SGB12].

Using the values $a = 0.25, b = 0.25$ we obtain the two subdivision operators for the B-spline of degree 2:

$$T_0 = \begin{pmatrix} 0.75 & 0.25 & 0 \\ 0.25 & 0.75 & 0.75 \\ 0 & 0 & 0.25 \end{pmatrix}, T_1 = \begin{pmatrix} 0.25 & 0 & 0 \\ 0.75 & 0.75 & 0.25 \\ 0 & 0.25 & 0.75 \end{pmatrix}.$$

3.6.1 Regular patch

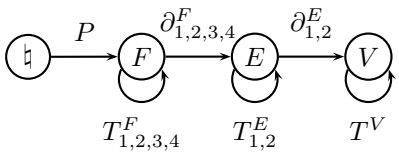

Figure 3.14: An automaton for the surface with four edges.

Next we present an example of a surface that is bi-cubic spline. The same principle can be used to describe the subdivision process for any quadrangular surface. An automaton for such a surface has three states: F for the face, E for the edges that border the face (in this case all the edges have the same nature, i.e., are defined by the same iterative procedure) and V for the vertices (see figure 3.14).

In general, a larger number of the incidence and adjacency constraints is required for surfaces than for curves, but the underlying principle is the same. Subdividing an edge should be equal to an edge of the patch subdivision, while neighbouring patches should share common edges. All the constraints are illustrated in the figure 3.15. Here is the full list of constraints for quadrangular subdivision:

Adjacency constraints:

$$\begin{aligned}
\partial^F_1 T^E_1 &= T^F_1 \partial^F_1\,, & \partial^F_1 T^E_2 &= T^F_2 \partial^F_1\,,\\
\partial^F_2 T^E_1 &= T^F_2 \partial^F_2\,, & \partial^F_2 T^E_2 &= T^F_4 \partial^F_2\,,\\
\partial^F_3 T^E_1 &= T^F_3 \partial^F_3\,, & \partial^F_3 T^E_2 &= T^F_4 \partial^F_3\,,\\
\partial^F_4 T^E_2 &= T^F_1 \partial^F_4\,, & \partial^F_4 T^E_1 &= T^F_3 \partial^F_4\,.
\end{aligned}$$

Incidence constraints:

$$\begin{aligned}
T^F_1 \partial^F_2 &= T^F_2 \partial^F_4\,, & T^F_4 \partial^F_4 &= T^F_3 \partial^F_2\,,\\
T^F_2 \partial^F_3 &= T^F_4 \partial^F_1\,, & T^F_3 \partial^F_1 &= T^F_1 \partial^F_3\,.
\end{aligned}$$

To be able to derive the subdivision matrices we need to choose our boundary operators. The cubic B-spline patch has 16 control points and each edge depends on 12 of them (see figure 3.16).

With this knowledge, we can write down our boundary operators:

$$\partial^F_1 = \begin{pmatrix}
0&0&0&0&0&0&0&0&0&0&0&0\\
0&0&0&0&0&0&0&0&0&0&0&0\\
0&0&0&0&0&0&0&0&0&0&0&0\\
0&0&0&0&0&0&0&0&0&0&0&0\\
1&0&0&0&0&0&0&0&0&0&0&0\\
0&1&0&0&0&0&0&0&0&0&0&0\\
0&0&1&0&0&0&0&0&0&0&0&0\\
0&0&0&1&0&0&0&0&0&0&0&0\\
0&0&0&0&1&0&0&0&0&0&0&0\\
0&0&0&0&0&1&0&0&0&0&0&0\\
0&0&0&0&0&0&1&0&0&0&0&0\\
0&0&0&0&0&0&0&1&0&0&0&0\\
0&0&0&0&0&0&0&0&1&0&0&0\\
0&0&0&0&0&0&0&0&0&1&0&0\\
0&0&0&0&0&0&0&0&0&0&1&0\\
0&0&0&0&0&0&0&0&0&0&0&1
\end{pmatrix}, \quad
\partial^F_2 = \begin{pmatrix}
0&0&0&0&0&0&0&0&0&0&0&0\\
1&0&0&0&0&0&0&0&0&0&0&0\\
0&1&0&0&0&0&0&0&0&0&0&0\\
0&0&1&0&0&0&0&0&0&0&0&0\\
0&0&0&0&0&0&0&0&0&0&0&0\\
0&0&0&1&0&0&0&0&0&0&0&0\\
0&0&0&0&1&0&0&0&0&0&0&0\\
0&0&0&0&0&1&0&0&0&0&0&0\\
0&0&0&0&0&0&0&0&0&0&0&0\\
0&0&0&0&0&0&1&0&0&0&0&0\\
0&0&0&0&0&0&0&1&0&0&0&0\\
0&0&0&0&0&0&0&0&1&0&0&0\\
0&0&0&0&0&0&0&0&0&0&0&0\\
0&0&0&0&0&0&0&0&0&1&0&0\\
0&0&0&0&0&0&0&0&0&0&1&0\\
0&0&0&0&0&0&0&0&0&0&0&1
\end{pmatrix},$$

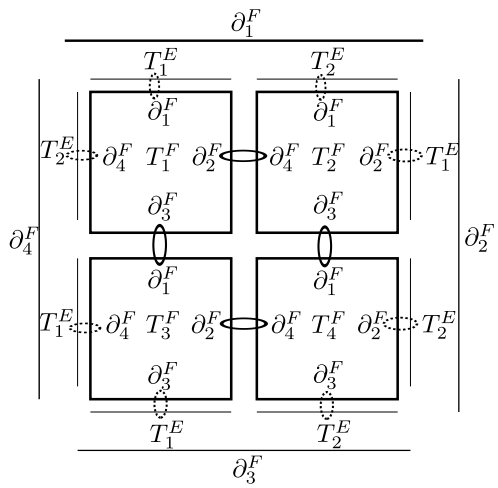

Figure 3.15: Incidence and adjacency constraints for quadrangular surface subdivision. Each subdivided face has to be connected with neighbouring faces by sharing respective edges (represented by solid-line ellipses), while edge subdivision must be an edge for one of the subdivided faces (dotted-line ellipses).

$$\partial_3^F = \begin{pmatrix}
1&0&0&0&0&0&0&0&0&0&0&0\\
0&1&0&0&0&0&0&0&0&0&0&0\\
0&0&1&0&0&0&0&0&0&0&0&0\\
0&0&0&1&0&0&0&0&0&0&0&0\\
0&0&0&0&1&0&0&0&0&0&0&0\\
0&0&0&0&0&1&0&0&0&0&0&0\\
0&0&0&0&0&0&1&0&0&0&0&0\\
0&0&0&0&0&0&0&1&0&0&0&0\\
0&0&0&0&0&0&0&0&1&0&0&0\\
0&0&0&0&0&0&0&0&0&1&0&0\\
0&0&0&0&0&0&0&0&0&0&1&0\\
0&0&0&0&0&0&0&0&0&0&0&1\\
0&0&0&0&0&0&0&0&0&0&0&0\\
0&0&0&0&0&0&0&0&0&0&0&0\\
0&0&0&0&0&0&0&0&0&0&0&0\\
0&0&0&0&0&0&0&0&0&0&0&0
\end{pmatrix}, \partial_4^F = \begin{pmatrix}
1&0&0&0&0&0&0&0&0&0&0&0\\
0&1&0&0&0&0&0&0&0&0&0&0\\
0&0&1&0&0&0&0&0&0&0&0&0\\
0&0&0&0&0&0&0&0&0&0&0&0\\
0&0&0&1&0&0&0&0&0&0&0&0\\
0&0&0&0&1&0&0&0&0&0&0&0\\
0&0&0&0&0&1&0&0&0&0&0&0\\
0&0&0&0&0&0&0&0&0&0&0&0\\
0&0&0&0&0&0&1&0&0&0&0&0\\
0&0&0&0&0&0&0&1&0&0&0&0\\
0&0&0&0&0&0&0&0&1&0&0&0\\
0&0&0&0&0&0&0&0&0&0&0&0\\
0&0&0&0&0&0&0&0&0&0&0&0\\
0&0&0&0&0&0&0&0&0&0&1&0\\
0&0&0&0&0&0&0&0&0&0&0&1\\
0&0&0&0&0&0&0&0&0&0&0&0
\end{pmatrix}.$$

Using the boundary operators $\partial_1^F, \partial_2^F, \partial_3^F, \partial_4^F$ and the constraints derived above we can deduce the matrix form of the operators $T_{1,2,3,4}^F$:

$$T_1^F = \begin{pmatrix}
a_0&b_0&0&0&b_2&f_0&0&0&0&0&0&0&0&0&0&0\\
a_0&b_1&a_0&b_0&b_0&f_1&b_2&f_0&0&0&0&0&0&0&0&0\\
0&b_2&a_0&b_1&0&f_0&b_0&f_1&0&0&0&0&0&0&0&0\\
0&0&0&b_2&0&0&0&f_0&0&0&0&0&0&0&0&0\\
a_0&b_2&0&0&b_1&f_1&0&0&a_0&b_0&0&0&b_2&f_0&0&0\\
a_0&b_1&a_0&b_2&b_1&f_5&b_1&f_1&a_0&b_1&a_0&b_0&b_0&f_1&b_2&f_0\\
0&b_0&a_0&b_1&0&f_1&b_1&f_5&0&b_2&a_0&b_1&0&f_0&b_0&f_1\\
0&0&0&b_0&0&0&0&f_1&0&0&0&b_2&0&0&0&f_0\\
0&0&0&0&b_0&f_0&0&0&a_0&b_2&0&0&b_1&f_1&0&0\\
0&0&0&0&b_2&f_1&b_0&f_0&a_0&b_1&a_0&b_2&b_1&f_5&b_1&f_1\\
0&0&0&0&0&f_0&b_2&f_1&0&b_0&a_0&b_1&0&f_1&b_1&f_5\\
0&0&0&0&0&0&0&f_0&0&0&0&b_0&0&0&0&f_1\\
0&0&0&0&0&0&0&0&0&0&0&0&b_0&f_0&0&0\\
0&0&0&0&0&0&0&0&0&0&0&0&b_2&f_1&b_0&f_0\\
0&0&0&0&0&0&0&0&0&0&0&0&0&f_0&b_2&f_1\\
0&0&0&0&0&0&0&0&0&0&0&0&0&0&0&f_0
\end{pmatrix},$$

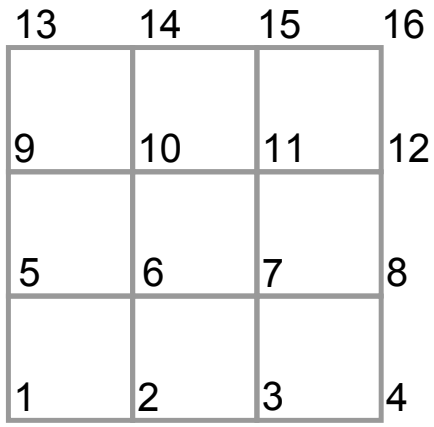

Figure 3.16: Control mesh for a cubic B-spline patch.

$$T_2^F = \begin{pmatrix}
b_2 & f_0 & 0 & 0 & 0 & 0 & 0 & 0 & 0 & 0 & 0 & 0 & 0 & 0 & 0 & 0 \\
b_0 & f_1 & b_2 & f_0 & 0 & 0 & 0 & 0 & 0 & 0 & 0 & 0 & 0 & 0 & 0 & 0 \\
0 & f_0 & b_0 & f_1 & 0 & 0 & 0 & 0 & 0 & 0 & 0 & 0 & 0 & 0 & 0 & 0 \\
0 & 0 & 0 & f_0 & 0 & 0 & 0 & 0 & 0 & 0 & 0 & 0 & 0 & 0 & 0 & 0 \\
b_1 & f_1 & 0 & 0 & a_0 & b_0 & 0 & 0 & b_2 & f_0 & 0 & 0 & 0 & 0 & 0 & 0 \\
b_1 & f_5 & b_1 & f_1 & a_0 & b_1 & a_0 & b_0 & b_0 & f_1 & b_2 & f_0 & 0 & 0 & 0 & 0 \\
0 & f_1 & b_1 & f_5 & 0 & b_2 & a_0 & b_1 & 0 & f_0 & b_0 & f_1 & 0 & 0 & 0 & 0 \\
0 & 0 & 0 & f_1 & 0 & 0 & 0 & b_2 & 0 & 0 & 0 & f_0 & 0 & 0 & 0 & 0 \\
b_0 & f_0 & 0 & 0 & a_0 & b_2 & 0 & 0 & b_1 & f_1 & 0 & 0 & a_0 & b_0 & 0 & 0 \\
b_2 & f_1 & b_0 & f_0 & a_0 & b_1 & a_0 & b_2 & b_1 & f_5 & b_1 & f_1 & a_0 & b_1 & a_0 & b_0 \\
0 & f_0 & b_2 & f_1 & 0 & b_0 & a_0 & b_1 & 0 & f_1 & b_1 & f_5 & 0 & b_2 & a_0 & b_1 \\
0 & 0 & 0 & f_0 & 0 & 0 & 0 & b_0 & 0 & 0 & 0 & f_1 & 0 & 0 & 0 & b_2 \\
0 & 0 & 0 & 0 & 0 & 0 & 0 & 0 & b_0 & f_0 & 0 & 0 & a_0 & b_2 & 0 & 0 \\
0 & 0 & 0 & 0 & 0 & 0 & 0 & 0 & b_2 & f_1 & b_0 & f_0 & a_0 & b_1 & a_0 & b_2 \\
0 & 0 & 0 & 0 & 0 & 0 & 0 & 0 & 0 & f_0 & b_2 & f_1 & 0 & b_0 & a_0 & b_1 \\
0 & 0 & 0 & 0 & 0 & 0 & 0 & 0 & 0 & 0 & 0 & f_0 & 0 & 0 & 0 & b_0
\end{pmatrix},$$

$$T_3^F = \begin{pmatrix}
f_0 & 0 & 0 & 0 & 0 & 0 & 0 & 0 & 0 & 0 & 0 & 0 & 0 & 0 & 0 & 0 \\
f_1 & b_2 & f_0 & 0 & 0 & 0 & 0 & 0 & 0 & 0 & 0 & 0 & 0 & 0 & 0 & 0 \\
f_0 & b_0 & f_1 & b_2 & 0 & 0 & 0 & 0 & 0 & 0 & 0 & 0 & 0 & 0 & 0 & 0 \\
0 & 0 & f_0 & b_0 & 0 & 0 & 0 & 0 & 0 & 0 & 0 & 0 & 0 & 0 & 0 & 0 \\
f_1 & 0 & 0 & 0 & b_0 & 0 & 0 & 0 & f_0 & 0 & 0 & 0 & 0 & 0 & 0 & 0 \\
f_5 & b_1 & f_1 & 0 & b_1 & a_0 & b_0 & 0 & f_1 & b_2 & f_0 & 0 & 0 & 0 & 0 & 0 \\
f_1 & b_1 & f_5 & b_1 & b_2 & a_0 & b_1 & a_0 & f_0 & b_0 & f_1 & b_2 & 0 & 0 & 0 & 0 \\
0 & 0 & f_1 & b_1 & 0 & 0 & b_2 & a_0 & 0 & 0 & f_0 & b_0 & 0 & 0 & 0 & 0 \\
f_0 & 0 & 0 & 0 & b_2 & 0 & 0 & 0 & f_1 & 0 & 0 & 0 & b_0 & 0 & 0 & 0 \\
f_1 & b_0 & f_0 & 0 & b_1 & a_0 & b_2 & 0 & f_5 & b_1 & f_1 & 0 & b_1 & a_0 & b_0 & 0 \\
f_0 & b_2 & f_1 & b_0 & b_0 & a_0 & b_1 & a_0 & f_1 & b_1 & f_5 & b_1 & b_2 & a_0 & b_1 & a_0 \\
0 & 0 & f_0 & b_2 & 0 & 0 & b_0 & a_0 & 0 & 0 & f_1 & b_1 & 0 & 0 & b_2 & a_0 \\
0 & 0 & 0 & 0 & 0 & 0 & 0 & 0 & f_0 & 0 & 0 & 0 & b_2 & 0 & 0 & 0 \\
0 & 0 & 0 & 0 & 0 & 0 & 0 & 0 & f_1 & b_0 & f_0 & 0 & b_1 & a_0 & b_2 & 0 \\
0 & 0 & 0 & 0 & 0 & 0 & 0 & 0 & f_0 & b_2 & f_1 & b_0 & b_0 & a_0 & b_1 & a_0 \\
0 & 0 & 0 & 0 & 0 & 0 & 0 & 0 & 0 & 0 & f_0 & b_2 & 0 & 0 & b_0 & a_0
\end{pmatrix},$$

$$T_4^F = \begin{pmatrix}
b_0 & 0 & 0 & 0 & f_0 & 0 & 0 & 0 & 0 & 0 & 0 & 0 & 0 & 0 & 0 & 0 \\
b_1 & a_0 & b_0 & 0 & f_1 & b_2 & f_0 & 0 & 0 & 0 & 0 & 0 & 0 & 0 & 0 & 0 \\
b_2 & a_0 & b_1 & a_0 & f_0 & b_0 & f_1 & b_2 & 0 & 0 & 0 & 0 & 0 & 0 & 0 & 0 \\
0 & 0 & b_2 & a_0 & 0 & 0 & f_0 & b_0 & 0 & 0 & 0 & 0 & 0 & 0 & 0 & 0 \\
b_2 & 0 & 0 & 0 & f_1 & 0 & 0 & 0 & b_0 & 0 & 0 & 0 & f_0 & 0 & 0 & 0 \\
b_1 & a_0 & b_2 & 0 & f_5 & b_1 & f_1 & 0 & b_1 & a_0 & b_0 & 0 & f_1 & b_2 & f_0 & 0 \\
b_0 & a_0 & b_1 & a_0 & f_1 & b_1 & f_5 & b_1 & b_2 & a_0 & b_1 & a_0 & f_0 & b_0 & f_1 & b_2 \\
0 & 0 & b_0 & a_0 & 0 & 0 & f_1 & b_1 & 0 & 0 & b_2 & a_0 & 0 & 0 & f_0 & b_0 \\
0 & 0 & 0 & 0 & f_0 & 0 & 0 & 0 & b_2 & 0 & 0 & 0 & f_1 & 0 & 0 & 0 \\
0 & 0 & 0 & 0 & f_1 & b_0 & f_0 & 0 & b_1 & a_0 & b_2 & 0 & f_5 & b_1 & f_1 & 0 \\
0 & 0 & 0 & 0 & f_0 & b_2 & f_1 & b_0 & b_0 & a_0 & b_1 & a_0 & f_1 & b_1 & f_5 & b_1 \\
0 & 0 & 0 & 0 & 0 & 0 & f_0 & b_2 & 0 & 0 & b_0 & a_0 & 0 & 0 & f_1 & b_1 \\
0 & 0 & 0 & 0 & 0 & 0 & 0 & 0 & 0 & 0 & 0 & 0 & f_0 & 0 & 0 & 0 \\
0 & 0 & 0 & 0 & 0 & 0 & 0 & 0 & 0 & 0 & 0 & 0 & f_1 & b_0 & f_0 & 0 \\
0 & 0 & 0 & 0 & 0 & 0 & 0 & 0 & 0 & 0 & 0 & 0 & f_0 & b_2 & f_1 & b_0 \\
0 & 0 & 0 & 0 & 0 & 0 & 0 & 0 & 0 & 0 & 0 & 0 & 0 & 0 & f_0 & b_2
\end{pmatrix}.$$

Substituting $a0 = 1/4$, $b_0 = 1/16$, $b_1 = 3/8$, $b_2 = 1/16$, $f0 = 1/64$, $f1 = 3/32$, $f5 = 9/16$ we obtain the subdivision for a bi-cubic spline surface.

3.6.2 Irregular patch

Here we show how to modify the automaton to change the regular patch into a patch with one irregular vertex. Consider a quadrangular patch with one irregular vertex. Such a patch is subdivided into three regular patches and one irregular patch. The corresponding automaton is presented in figure 3.17. Note that the irregular patch (F^{ir}) has two irregular edges (E^{ir}) as well as two regular ones (E). The irregular edge is subdivided ($T_{1,2}^{E^{ir}}$) into a regular and an irregular edge. Conditions that guarantee the continuity of the irregular patch can be deduced in the same manner as for its regular counterpart.

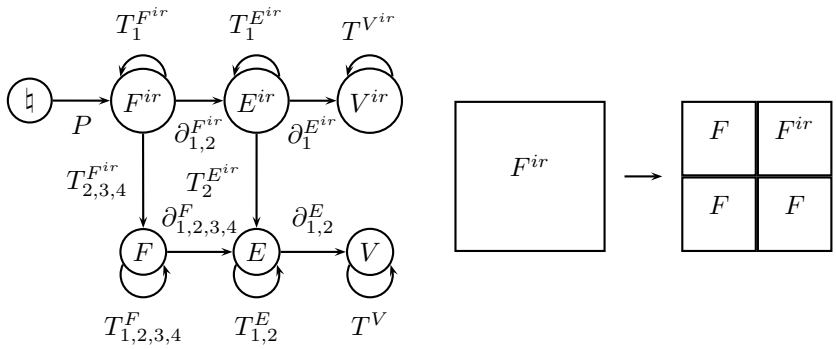

Figure 3.17: Left: An automaton for the irregular patch. Right: a schematic subdivision of the irregular patch.

A bi-quadratic spline patch with one irregular vertex would be an example of such a surface (see figure 3.18). For such a patch, the regular face subdivisions would be regular bi-quadratic subdivision matrices, while the matrix form of the irregular one can be deduced from the continuity constraints.

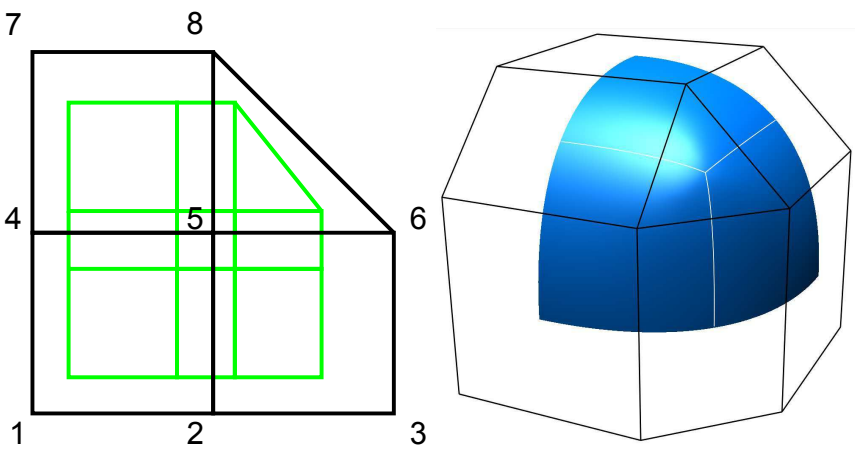

Figure 3.18: Left: a control mesh for a bi-quadratic spline patch with one irregular vertex. Green mesh represents the first step of the subdivision. Right: a control mesh for three irregular bi-quadratic patches that share their irregular vertex and the limit surface.

3.7 Generalised eigenvectors

In the later chapters, the notion of the generalised eigenvectors is used to work with the operators that do not have a complete set of eigenvectors. In this section we recall the definition of generalised eigenvectors and some of their properties. For a linear operator A acting on a vector space $\mathcal{X}$ an eigenvalue λ is a non-zero number for which a vector $\vec{v}$ exists such that $A\vec{v} = \lambda\vec{v}$. All eigenvectors corresponding to certain a eigenvalue λ lie within the kernel of the linear map $A-\lambda I$, where I is an identity map over $\mathcal{X}$. Similarly the generalised eigenvectors of order k lie in the kernel of $(A - \lambda I)^k$ where k is a positive integer. Note that for $k = 1$ we obtain the usual non-generalised eigenvectors. Also, since generalised eigenvectors of order k are the solutions of the linear equation

$$(A - \lambda I)^k \vec{x} = 0,$$

they are also related to eigenvectors of order $k - 1$ with the following relation:

$$(A - \lambda I)\vec{v}^k = \vec{v}^{k-1},$$

where $\vec{v}^k$ is a generalised eigenvector of order k. When there are not enough linearly independent eigenvectors to compose a basis of space, there are always enough linearly independent generalised eigenvectors that can be used to complete the basis.

3.7.1 Eigenvalues and multiplicities

Consider a matrix $A \in \mathbb{R}^{(n\times n)}$. The characteristic polynomial

$$P_A(\lambda) = |A - \lambda I|,$$

where I is an identity matrix. $P_A(\lambda)$ has m roots:

$$\lambda_0, \lambda_1, \ldots, \lambda_{m-1},$$

where $m \leq n$. The values λ_i are called eigenvalues of the matrix A. The characteristic polynomial can be decomposed as:

$$\prod_{i=0}^{m-1} (\lambda - \lambda_i)^{r_i}.$$

r_i is called the algebraic multiplicity of the eigenvalue λ_i. The sum of all algebraic multiplicities is equal to the degree of the characteristic polynomial:

$$\sum_{i=0}^{m-1} r_i = n.$$

Let $E_i = \{\vec{v} \in \mathbb{R}^n \text{ such that } Av = \lambda_i v\}$. E_i is called an eigenspace associated with an eigenvalue λ_i. The dimension of E_i (denoted as $dim(E_i)$) is always less than or equal to the algebraic multiplicity of λ_i. The dimension of E_i is also referred to as the geometric multiplicity of λ_i. Generalised eigenvectors associated with different eigenvalues are linearly independent.

If $dim(E_i) = r_i$ for all $i = 0, \ldots, n - 1$ then a linearly independent set of n eigenvectors can be found. This set forms a basis of R^n.

3.7.2 Chains of generalised eigenvectors

Vectors $\vec{v}^1, \dots, \vec{v}^k$ that are generalised eigenvectors of orders $1, \dots, k$ for an eigenvalue λ are said to form a chain of generalised eigenvectors of length k. If we consider a linear operator T on $\mathbb{R}^n$ with m eigenvalues $\lambda_0, \lambda_1, \dots, \lambda_{m-1}$ written with respect to their geometric multiplicity, i.e. such that for each λ_i exists an $\vec{v}_i$ and all $\vec{v}_i$ are linearly independent. Then for each λ_i there exists a chain of generalised eigenvectors, possibly limited to only one eigenvector.

$$\begin{array}{cccc} \vec{v}_0^0, & \vec{v}_1^0, & \dots, & \vec{v}_{m-1}^0 \\ \vec{v}_0^1 & \vec{v}_1^1 & \dots & \vec{v}_{m-1}^1 \\ \vdots & \vdots & & \vdots \\ \vdots & \vec{v}_1^{r_1} & & \vdots \\ \vec{v}_0^{r_0} & & & \vec{v}_{m-1}^{r_{m-1}} \end{array}$$

Here $\vec{v}_i^0 = \vec{v}_i$, while $\vec{v}_j^i$ are linearly independent and $\sum_{i=0}^{m-1}(r_i - 1) = n$. So for all $\vec{a} \in \mathbb{R}^n$ there exists $a_{i,j} \in \mathbb{R}$ such that

$$\vec{a} = \sum_{\substack{0 \le i \le m-1 \\ 0 \le j \le r_i}} a_{i,j} \vec{v}_i^j.$$

3.8 Eigenvalues, eigenvectors and barycentric spaces

In this subsection we point out a few properties of the eigenvectors and eigenvalues of the operators that act on barycentric spaces. Since a barycentric space is an invariant for such operators, the sum of all elements in each column equals 1.

The highest eigenvalue is always equal to 1. The eigenvalue 1 does not have a multiplicity greater than 1 because otherwise the operator is not contractive. Consider an operator with two non-collinear eigenvectors associated with eigenvalue 1. Both of them are fixed points and the distance between them does not diminish when we apply the operator, hence the operator cannot be contractive and have two or more eigenvalues equal to 1.

The fixed point of the operator acting on the barycentric space is defined by the dominant eigenvector, i.e. an eigenvector associated with greatest eigenvalues, in this case the eigenvalue 1.

For an operator to be contractive, is is necessary for all the other eigenvalues to be strictly less than 1 in absolute value. Consider the T operator with an eigenvalue λ that is greater than 1. Take any two different eigenvectors $\vec{v}_1$ and $\vec{v}_2$:

$$d(T(\vec{v}_1), T(\vec{v}_2)) = |T(\vec{v}_1 - \vec{v}_2)| = \lambda|\vec{v}_1 - \vec{v}_2| > |\vec{v}_1 - \vec{v}_2| = d(\vec{v}_1, \vec{v}_2).$$

Hence the operator T is not contractive.

All sub-dominant eigenvectors have the sum of their components equal to 0, i.e. they are parallel to the barycentric space. The contractive coefficient on the barycentric space is equal to the absolute value of the sub-dominant eigenvalue, i.e. the eigenvalue with the second largest absolute value.

3.9 Conclusion

In this chapter we reviewed the basic notion of an Iterated Function System. We also recalled different varieties of the basic IFS such as Projective IFS, Controlled IFS and Boundary Controlled IFS. We showed how continuity constraints can be derived using the BCIFS model and how they affect the structure of the transformations matrix form. Then we detailed how classic subdivision schemes can be modelled with BCIFS. Finally we recall some useful properties of the eigenvectors and eigenvalues that will come into use in the following chapters.

Chapter 4

Tangent space

This chapter is dedicated to the analysis of the differential properties of shapes defined as CIFS or BCIFS attractors. We define a notion of the tangent subspace that generalises the classic notions of tangent line and plane. Then we study the differential behaviour of self-similar sets in both classic and generalised senses. We base our study on the notion of the addresses function (see definition 7). Given the address of a point we can construct a sequence of subsets that encompasses the point. Later, we refer to these subsets as rings. Each symbol of the point's address corresponds to a specific ring and the next ring can be obtained by applying the respective transformation to the previous one. Together, the rings completely cover the neighbourhood of the point. So by studying how rings are transformed, we can obtain information on the differential behaviour of the attractor at the specified point.

We focus mainly on points with periodic addresses. Points with periodic addresses compose an everywhere dense subsets of the attractor. We provide a detailed analysis of the differential behaviour at the points with addresses (i^ω) and derive the necessary and sufficient conditions for differentiability. We also show how these conditions can be applied to other kinds of periodic points. Finally, we give several examples of different kinds of differential behaviour.

4.1 Tangent definition

In this section, we would like to give a definition of a tangent subspace from a purely geometrical standpoint. We also want to give such a definition that would generalise tangent lines of curves, tangent planes of surfaces and possibly objects of higher dimensions. We want to avoid defining the tangent depending on a parametrization, because given the complex natures of self-similar shapes it may be troublesome to find the correct parametrisation.

Definition 11 (Tangent subspace)**.** *Let p be a point of some set $\mathcal{A} \subset \mathbb{R}^m$. We consider all possible sequences $\{x_n\}_{n\in\mathbb{N}}$ such that $\forall n\ x_n \in \mathcal{A}$ and $x_n \to p \in \mathcal{A}$ as $n \to \infty$. A line that passes though points p and x_n is called a secant and is denoted by sx_n. An affine subspace E is called a tangent subspace if and only if*

1. $p \in E$,

2. *$dim(E) \geq 1$ and $dim(E)$ is a minimum of all possible subspaces E that satisfy the other conditions,*

3. *for all sequences x_n described above*

$$\lim_{n\to\infty} \widehat{sn_x E} = 0,$$

where

$$\widehat{sn_x E} = \arctan\left(\frac{\|q - q_E\|)}{\|p - q_E\|}\right),$$

$q \in sx_n$ and q_E is an orthogonal projection of q onto E.

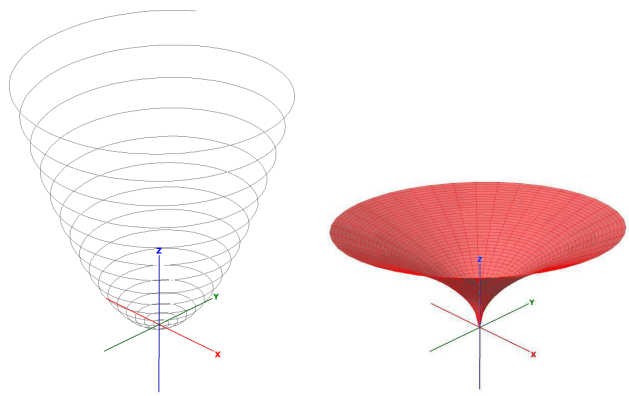

Figure 4.1: Left: the curve is tangent to the plane Oxy. Right: the surface is tangent to the z axis.

This definition generalises the classic notion of tangent line. Indeed, if we consider a set $\mathcal{A}$ that is a smooth curve, then the tangent subspace at any point of $\mathcal{A}$ is equal to the tangent line at the same point.

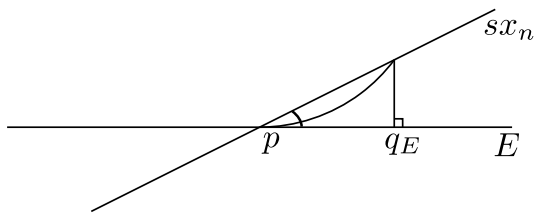

Figure 4.2: An angle between a secant and an affine subspace.

Our definition also includes the classic definition of a tangent plane. For any smooth curve on a surface that passes through the tangent point, the angle between a tangent plane and a secant converges to zero as we approach the tangent point. But our definition also includes other cases. Figure 4.1 provides an illustration. For example, a 3D parametric

curve $(t\cos t, t\sin t, t^2)$ does not possess a tangent line at the origin; however, the plane Oxy satisfies the definition of a tangent subspace. Another example is a 3D parametric surface $(u, v, (u^2+v^2)^{1/4})$ that is tangent to the z-axis at the point $(u, v) = (0, 0)$.

4.2 Rings

In this section we give the definition of a sequence of rings around a point. The definition of a sequence of rings depends on the address of the point, so we begin this section by classifying points based on the number and type of their addresses. After that we give the exact definitions and properties of a sequence of rings for a point and its address (see section 4.2.2).

4.2.1 Points and addresses

Based on the notion of address function (see Chapter 3) the points of any attractor can be placed into one of these three categories:

- points with dyadic addresses $p = \phi(\sigma)$, where $\sigma = \bar{\sigma}(i)^\omega$ and $\bar{\sigma}$ is a finite prefix,
- points with periodic addresses $p = \phi(\sigma)$, where $\sigma = \bar{\sigma}(i_0, \ldots, i_{n-1})^\omega$, $\bar{\sigma}$ is a finite prefix and $(i_0, \ldots, i_{n-1})$ is a period of length n,
- points with non-periodic addresses.

Example 4 (Double address point)**.** Consider a simple IFS with two transformations over $(\mathbb{R}, d_E)$, where d_E is the Euclidean metric. The two transformations are as follows:

$$T_0(x) = \frac{1}{2}x,$$
$$T_1(x) = \frac{1}{2}x + \frac{1}{2}.$$

The fixed points of the transformations T_0 and T_1 are points 0 and 1 respectively. The unit segment $[0, 1]$ is the attractor of this IFS. Both fixed points have a unique address. The corresponding addresses are $(0)^\omega$ and $(1)^\omega$ respectively. However point $\frac{1}{2}$ has two addresses. Indeed:

$$T_0(1) = T_1(0) = \frac{1}{2}.$$

So

$$\phi(1(0)^\omega) = \phi(0(1)^\omega) = \frac{1}{2},$$

where ϕ is an address function.

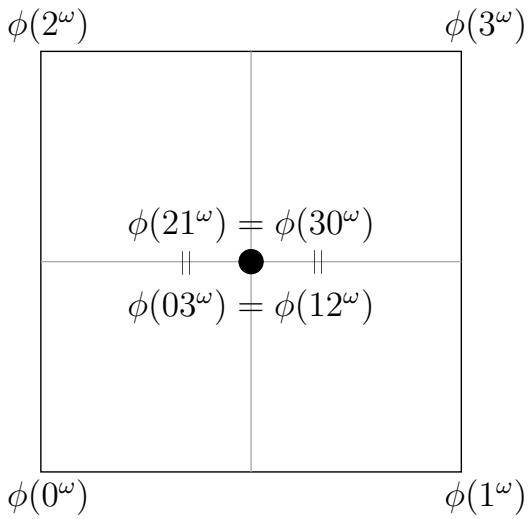

Figure 4.3: An illustration of example 5.

Example 5 (Quadruple address point)**.** Consider an IFS over $(\mathbb{R}^2, d_E)$ whose attractor is a unit square. Four transformations that map the square into four equal parts are as follows:

$$\begin{aligned}
T_0(x) &= \begin{pmatrix} 1/2 & 0 \\ 0 & 1/2 \end{pmatrix} x, \\
T_1(x) &= \begin{pmatrix} 1/2 & 0 \\ 0 & 1/2 \end{pmatrix} x + \begin{pmatrix} 1/2 \\ 0 \end{pmatrix}, \\
T_2(x) &= \begin{pmatrix} 1/2 & 0 \\ 0 & 1/2 \end{pmatrix} x + \begin{pmatrix} 0 \\ 1/2 \end{pmatrix}, \\
T_3(x) &= \begin{pmatrix} 1/2 & 0 \\ 0 & 1/2 \end{pmatrix} x + \begin{pmatrix} 1/2 \\ 1/2 \end{pmatrix}.
\end{aligned}$$

A unit square $[0,1]^2$ is an attractor of such IFS. All four corners of the attractor have unique addresses composed of single infinitely repeated symbol. Indeed, each corner is a fixed point for one of the transformations. Similarly to the previous example, midpoints of the edges have two addresses. But in the meantime, the point $(1/2, 1/2)$ has four different addresses:

$$T_0 \begin{pmatrix} 1 \\ 1 \end{pmatrix} = T_1 \begin{pmatrix} 0 \\ 1 \end{pmatrix} = T_2 \begin{pmatrix} 1 \\ 0 \end{pmatrix} = T_3 \begin{pmatrix} 0 \\ 0 \end{pmatrix} = \begin{pmatrix} 1/2 \\ 1/2 \end{pmatrix}.$$

Or in terms of address function:

$$\phi(0(3)^\omega) = \phi(1(2)^\omega) = \phi(2(1)^\omega) = \phi(3(0)^\omega) = \begin{pmatrix} 1/2 \\ 1/2 \end{pmatrix}.$$

The four addresses of this point represent four different ways to approach it and four possibly different quarter-tangent planes that may or may not exist.

4.2.2 Sequence of rings definition

Previously we discussed the notion of rings that enclose the point, that is based on the notion of the address function. In this subsection, we are going to give a formal definition of a sequence of rings both for unique address points as well as for points with multiple addresses.

The underlying idea is fairly straightforward. Given an attractor and a point on it, we calculate a sequence of images of the attractor with operators that correspond to each symbol of the address. The ring is then defined as a difference between two consecutive images.

Definition 12 (A set of rings)**.** *Let $\mathcal{A}$ be an attractor of some IFS. Let $p \in \mathcal{A}$ be a point with a corresponding address σ such that $\phi(\sigma) = p$. Then the sequence of rings for point p and its address σ is a sequence of subsets $R_i \subset \mathcal{A}$ such that:*

$$\forall i \geq 1 \; R_i = \overline{\mathcal{A}_{i-1} \setminus \mathcal{A}_i},$$

where

$$\forall i \geq 1, \mathcal{A}_i = T_{\sigma_i}(\mathcal{A}_{i-1})$$

and $\mathcal{A}_0 = \mathcal{A}$.

Since $\forall i \; T_{\sigma_i}$ is contractive $\mathcal{A}_i \subset A_{i-1}$, unless T_{σ_i} is degenerated. Hence $\forall i \; R_i \neq \emptyset$.

Property 1. *Now consider a sequence of points $x_n \in \mathcal{A}$ that converges to the point p, such that $\forall n \in \mathbb{N}$ there exists $j \in \mathbb{N}$ such that $x_n \in R_j$. Then for each i there exists $N \in \mathbb{N}$ such that $\forall n > N \; x_n \notin R_i$.*

Proof. Point $p \notin R_i$ and R_i is compact therefore exists $y_i \in R_i$ such that $\min_{y \in R_i} \|y - p\| = \|y_i - p\|$. For each i there exists $N \in \mathbb{N}$ such that $\forall n > N \; |x_n - p| < y_i$. Therefore $x_n \notin R_i$ for any $n > N$. □

Now let us consider points with multiple addresses. Let $\mathcal{A}$ be an attractor of some IFS. Let the point $p \in \mathcal{A}$ have multiple addresses $\sigma^1, \sigma^2, \ldots, \sigma^n$ such that $\phi(\sigma^1) = \phi(\sigma^2) = \ldots = \phi(\sigma^n) = p$. For a such point p we can define a sequence of rings $R^{\sigma^j} = \{R_i^{\sigma^j}\}$ for each address σ^j. Together these sets of rings completely encompass the point p. Any neighbourhood $V \subset \mathcal{A}$, $p \in V$ of the point p can be split into n parts according to which set of rings it intersects with:

$$V = \bigcup_{j=1}^{n} V \cap \left(\bigcup_{i=1}^{\infty} R_i^{\sigma^j} \right).$$

Figure 4.4 presents two examples of rings around a unique address point as well as around a dual address point.

For most of this chapter we will be focusing on points with unique uniform addresses like i^ω. Without loss of generality, any point with a periodic address like $(i_1 i_2 \ldots i_l)^\omega$ can be viewed as such if we consider the corresponding transformation $T_{i_1} T_{i_2} \ldots T_{i_l}$. Later in this chapter we generalise the results obtained for points with unique uniform addresses to other kinds of periodic points.

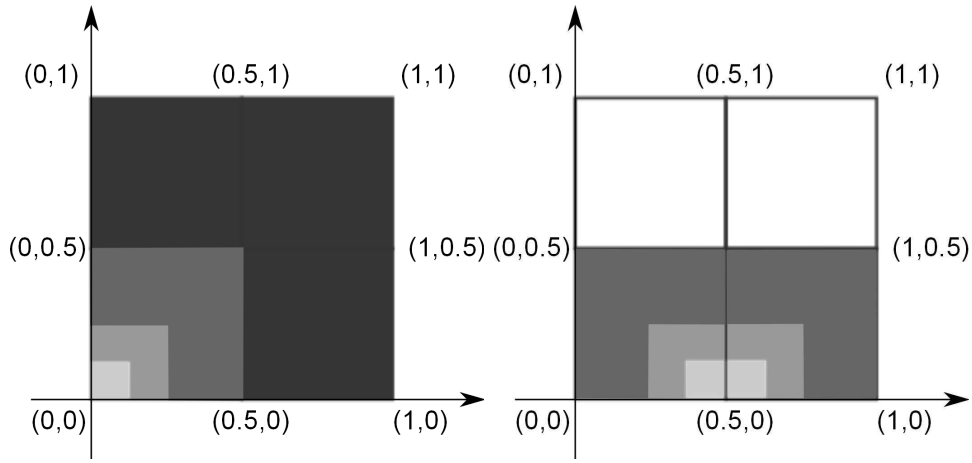

Figure 4.4: Left: one set of rings around the unique address point $(0, 0)$. Right: two sets of rings around the double address point $(1/2, 0)$.

4.2.3 Tangents, sequences of secants and rings

One may think of differentiability in terms of whether for all sequences converging to a point the corresponding secant sequence converges to the same limit.

Let us consider a point $p \in \mathcal{A}$ and the respective set of rings $\{R_i\}_{i=1}^{\infty}$. For any sequence of points $\{y_n\}_{n=0}^{\infty}$ such that $\lim_{n\to\infty} y_n = p$ there is only a finite number of elements that belong to a certain ring R_i. Indeed, if there exists $i \in \mathbb{N}$ such that there is an infinite number of elements of $\{y_n\}$ that belong to R_i than the sequence y_n cannot converge to p since $p \notin R_i$ and R_i is a closed set.

The set of rings can be studied more easily than arbitrary sequences that converge to the point of interest, since we know that each ring can be obtained from the previous one by means of an affine transformation. So by showing that the rings converge in a specific way we can show that the tangent space exists at the specific point.

In the next section we are going to study the convergence of rings around fixed points of transformation. We study two separate cases for transformations with a complete set of eigenvectors and for transformations with one.

4.3 Tangents and eigenvectors

In this section we explain why we are going to use eigenanalysis to study the differential properties of the attractor. Let us consider an arbitrary attractor $\mathcal{A}$ and some point $p \in \mathcal{A}$. The point p has at least one address $\sigma = \sigma_1\sigma_2\ldots$, such that σ has a period. Let us denote that transformation that corresponds to the period of σ as T. If we start applying the transformation T to the attractor $\mathcal{A}$ iteratively we obtain a set of its subsets $\mathcal{A}_i \subset \mathcal{A}$ such that:

$$A_1 = T(\mathcal{A}),$$
$$A_i = T^n(A_{i-1}).$$

All subsets A_i share the common point p, since p is a fixed point of T. So if there is a tangent subspace to the attractor $\mathcal{A}$ at the point p, the same tangent subspace is also a tangent subspace to all subsets A_i at the same point p. Therefore the tangent subspace is invariant to all the transformations T. Let σ contain only one unique symbol i. So if the tangent subspace exists at the point p it must be invariant of T_i, or in other words an eigenspace of T_i.

4.4 Angular deviation

In this section we give a formal definition to an angular deviation of a set from an affine subspace. This concept is later used to show the necessary and sufficient conditions for differentiability. The angular deviation generalises the notion of a field of view: how far does one need to turn one's eyes from the given direction to see the given set. Here is the more formal definition.

Definition 13 (Angular deviation)**.** *Let E be an affine subspace of $\mathbb{R}^m$ and p be a point in E. For any point q such that $q \neq p$ we denote the angle between line pq and E by $\alpha(E, q)$. More precisely, if q_E is an orthogonal projection of q onto E then*

$$\alpha(E,q) = \begin{cases} \arctan\left(\frac{\|q-q_E\|}{\|p-q_E\|}\right) & \text{if } p \neq q_E, \\ \frac{\pi}{2} & \text{if } p = q_E \end{cases}.$$

Then angular deviation of a compact set A from affine subspace E is denoted by $\alpha_{max}(E, A)$ is

$$\alpha_{max}(E, \mathcal{A}) = \max_{q \in \mathcal{A}} \alpha(E, q).$$

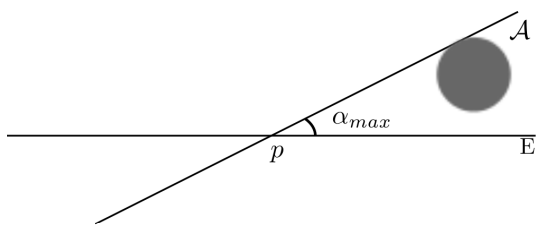

Figure 4.5: Angular deviation is the biggest possible angle between pq and E such that $q \in \mathcal{A}$.

Property 2. $0 \leq \alpha_{max}(E, \mathcal{A}) \leq \frac{\pi}{2}$

Knowing the angular deviation for a set gives us an idea of how far we would need to expand our field of view if we were standing at the point p looking at the subspace E to see the set $\mathcal{A}$. Let us consider an angular deviation of a set of nested neighbourhoods of a point p. If there exists a tangent line or plane to set $\mathcal{A}$ at point p then their respective angular deviations from the tangent line converge to zero as we consider the consecutive neighbourhoods.

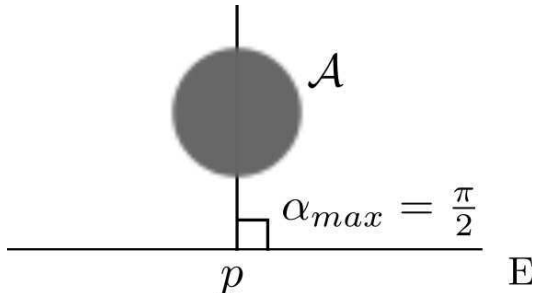

Figure 4.6: The maximum possible angular deviation is $\frac{\pi}{2}$.

Proposition 1. *Let $\mathcal{A}$ be an attractor of an IFS in $\mathbb{R}^m$. Let p be a point in $\mathcal{A}$ and R_i be a sequence of rings around the point p. If for some affine subspace E such that $p \in E$*

$$\alpha_{max}(E, R_i) \underset{i\to\infty}{\longrightarrow} 0$$

and E is the smallest of all subspaces that satisfy the previous condition, then E is a tangent subspace for attractor $\mathcal{A}$ at the point p.

Proof. The tangent depends on the convergence of secants. Any sequence of secants $\{sx_n\}_{n\in\mathbb{N}}$ will pass through each ring R_i only a finite number of times. For each secant sx_n such that $x_n \in R_i$ we can write the following:

$$\widehat{sx_n\ E} \leq \alpha_{max}(E, R_i).$$

□

Remark. *So to show that any sequence of secants converge it is enough to show that $\alpha_{max}(E, R_i) \to 0$ as $i \to \infty$.*

Proposition 2. *Let $\mathcal{A}$ be an attractor of an IFS in $\mathbb{R}^m$. Let p be a periodic point in $\mathcal{A}$, such that T is the transformation corresponding to its period and R_i is a sequence of rings around the point p. Let consider a point $x_0 \in R_0$ and a sequence of secants $\{sx_n\}_{n\in\mathbb{N}}$ that pass through points p and x_n, where $x_n = T(x_{n-1})$. So if $\widehat{sx_nE} \to 0$ for any $x_0 \in \mathbb{R}_0$ then $\alpha_{max}(E, R_i) \underset{i\to\infty}{\longrightarrow} 0$.*

Proof. Obvious. □

In the next two sections we are going to study the convergence of secants sx_n, where $x_n = T(x_{n-1})$. We are going to show that under specific conditions on T and x_0 there exists such a subspace E that $\widehat{sx_n\ E}$ converge to 0 as $n \to \infty$. Next section treats T with a complete set of eigenvectors, while the subsequent section deals with T that lacks a complete set of eigenvectors.

4.5 Complete set of eigenvectors

In this section we study the behaviour of a sequence of secants that is obtained with iterations of some transformation T. We give a series of lemmas, that describe this behaviour depending on the eigenvalues and eigenvectors of T. Given a point $p \in \mathcal{A}$, such that its address is $\sigma = (0)^\omega$, we consider an arbitrary point $x_0 \in \mathcal{A}$ such that $x_0 \neq p$. Then we consider a sequence of points $\{x_n\}_{n\in\mathbb{N}}$ such that $x_n = T(x_{n-1})$. The sequence $\{x_n\}$ defines a sequence of secants $\{sx_n\}$ such that each secant sx_n passes through the points x_n and p.

We have suggested above that if the tangent exists it is defined by eigenvectors of the transformation T. We are going to assume that T has a complete set of eigenvectors and show that sx_n converges to the subspace spanned by the sub-dominant eigenvector of T under certain conditions. We are going to denote this subspace as E. To show that $\widehat{sx_n\ E}$ indeed converges to zero we are going to study the convergence rate of different components of the vectors $\vec{px}_n$. Since T is a contractive mapping and p is its fixed point $|\vec{px}_n| \to 0$ as $n \to \infty$ we cannot simply calculate the limit of $\vec{px}_n$ to find the limit position of sx_n.

Lemma 1. *Let T be an operator on BI^m with a complete set of real eigenvectors $\vec{v}_0, \vec{v}_1, \ldots, \vec{v}_{m-1}$ along with their respective eigenvalues $\lambda_0 = 1 > \lambda_1 > |\lambda_2| \geq \ldots \geq |\lambda_{m-1}|$, $\forall i\ \lambda_i \in \mathbb{R}$. We denote the fixed point of T by p. Given a point $x_0 \neq p$, $x_0 \in BI^m$ we consider a sequence of secants sx_n that pass through the points p and x_n where $x_n = T^n(x_0)$. Let E be the subspace spanned by $\vec{v}_1$. If*

$$\vec{px}_0 = x_0^{(1)}\vec{v}_1 + \sum_{i=2}^{m-1} x_i^{(i)}\vec{v}_i$$

with $x_0^{(1)} \neq 0$, then

$$\widehat{sx_n\ E} \underset{n\to\infty}{\longrightarrow} 0.$$

Proof. The eigenvectors of T form a basis of $\mathbb{R}^m$. So any vector from $\mathbb{R}^m$ including $\vec{px}_n$ can be written as follows:

$$\vec{px}_n = \sum_{i=0}^{m-1} x_n^{(i)}\vec{v}_i.$$

In the previous chapter we demonstrated that all eigenvectors except the dominant one are parallel to the barycentric space (see section3.8). So for any point x_n of the barycentric space the corresponding vector $\vec{px}_n$ in the basis of the eigenvectors has its first component equal to 0 and we can omit the first term of the sum.

Since $x_n = T(x_{n-1}) = T^n(x_0)$ we can write the following:

$$\vec{px}_n = \sum_{i=1}^{m-1} \lambda_i^n x_0^{(i)}\vec{v}_i.$$

Now let us multiply each vector $\vec{px}_n$ by $\frac{1}{\lambda_1^n}$. We obtain:

$$\frac{\vec{px}_n}{\lambda_1^n} = \sum_{i=1}^{m-1} \frac{\lambda_i^n}{\lambda_1^n} x_0^{(i)}\vec{v}_i.$$

Note that since $\lambda_1 > 0$ this multiplication does not change the direction of vector $\vec{px}_n$. If we recall that $\forall i > 1\ \lambda_1 > |\lambda_i|$ we get that all the terms beside the first one converge to 0 as $n \to \infty$. In other words:

$$\frac{\vec{px}_n}{\lambda_1^n} \underset{n\to\infty}{\longrightarrow} x_0^{(1)}\vec{v}_1.$$

Henceforth, it is easy to see, that $\widehat{sx_n\ E}$ indeed converges to 0. □

Remark. *Note that if λ_1 is negative then $\widehat{sx_n\ E}$ also converges to zero, but as we are going to show later, a positive sub-dominant eigenvalues is necessary to obtain a tangent at the point p.*

4.5.1 Complex eigenvalue

We are now going to study the case in which a pair of complex sub-dominant eigenvalues is present. But first, le us review some facts about complex eigenvalues and eigenvectors. If $M \in \mathbb{R}^{(m\times m)}$ and $\lambda \in \mathbb{C}$ is an eigenvalue of M then $\bar{\lambda}$ is also an eigenvalue. The same goes for eigenvectors: if $\vec{v}$ is an eigenvector corresponding to the eigenvalue $\lambda \in \mathbb{C}$ then $\bar{\vec{v}}$ is an eigenvector that corresponds to the eigenvalue $\bar{\lambda}$. In addition, for every pair of complex eigenvalues $\lambda,\ \bar{\lambda}$ there exists a subspace of $\mathbb{R}^m$ that is invariant to T. Indeed let us consider a complex eigenvalue $\lambda = a+bi$ and the corresponding eigenvector $\vec{v} = \vec{x}+\vec{y}i$, where $a, b \in \mathbb{R}$ and $\vec{x}, \vec{y} \in \mathbb{R}^m$:

$$T(\vec{v}) = T(\vec{x}) + iT(\vec{y}) = (a+bi)(\vec{x}+\vec{y}i) = a\vec{x} - b\vec{y} + i(a\vec{y} + b\vec{x}).$$

So if we consider $T(\alpha\vec{x} + \beta\vec{y})$ we obtain:

$$T(\alpha\vec{x} + \beta\vec{y}) = \alpha(a\vec{x} - b\vec{y}) + \beta(a\vec{y} + b\vec{x}) = (a\alpha + b\beta)\vec{x} + (a\beta - b\alpha)\vec{y}.$$

So this way:

$$T(\mathrm{span}(\vec{x}, \vec{y})) = \mathrm{span}(\vec{x}, \vec{y}).$$

Note that $\vec{x}$ and $\vec{y}$ are also linearly independent from any real eigenvectors of T and from real or imaginary parts of other complex eigenvectors. This means that a set of all real eigenvectors of T can be completed with $\mathrm{Re}\,\vec{v}_i,\ \mathrm{Im}\,\vec{v}_i$ for each pair of complex eigenvectors $\vec{v}_i$ to form a complete basis of $\mathbb{R}^m$. If we consider $|T(\alpha\vec{x} + \beta\vec{y})|$ we obtain:

$$|T(\alpha\vec{x} + \beta\vec{y})| = |\lambda||\alpha\vec{x} + \beta\vec{y}|.$$

Lemma 2. *Let T be an operator on BI^m with a set of eigenvectors $\vec{v}_0, \vec{v}_1, \ldots, \vec{v}_{m-1}$ along with their respective eigenvalues $\lambda_0 = 1 > |\lambda_1| = |\lambda_2| > |\lambda_3| \geq \ldots \geq |\lambda_{m-1}|$, where $\lambda_1 = \bar{\lambda}_2$, $\lambda_1, \lambda_2 \in \mathbb{C}$. We denote the fixed point of T by p. Given a point $x_0 \neq p$, $x_0 \in BI^m$ we consider a sequence of secants sx_n that that pass through the points p and x_n where $x_n = T^n(x_0)$. Let E be a subspace spanned by $\mathrm{Re}\,\vec{v}_1$ and $\mathrm{Im}\,\vec{v}_1$. If*

$$\vec{px}_0 = x_0^{(1)}\,\mathrm{Re}\,\vec{v}_1 + x_0^{(2)}\,\mathrm{Im}\,\vec{v}_1 + \sum_{i=3}^{m-1} x_i^{(i)}\vec{v}_i$$

with $x_0^{(1)} \neq 0$ or $x_0^{(2)} \neq 0$, then

$$\widehat{sx_n\ E} \underset{n\to\infty}{\longrightarrow} 0.$$

Proof. Real eigenvectors of T along with $\operatorname{Re}\vec{v_1}$ and $\operatorname{Im}\vec{v_1}$ form a complete basis of $\mathbb{R}^m$. So for vector $p\vec{x}_0 \in \mathbb{R}^m$ we can write the following:

$$p\vec{x}_0 = x_0^{(1)} \operatorname{Re}\vec{v}_1 + x_0^{(2)} \operatorname{Im}\vec{v}_1 + \sum_{i=3}^{m-1} x_0^{(i)} \vec{v}_i.$$

If we apply the operator T we obtain:

$$T(p\vec{x}_0) = T(x_0^{(1)} \operatorname{Re}\vec{v}_1) + T(x_0^{(2)} \operatorname{Im}\vec{v}_1) + T\left(\sum_{i=3}^{m-1} x_0^{(i)} \vec{v}_i\right) = \tag{4.1}$$

$$= x_0^{(1)} T(\operatorname{Re}\vec{v}_1) + x_0^{(2)} T(\operatorname{Im}\vec{v}_1) + \sum_{i=3}^{m-1} x^{(i)} \lambda_i \vec{v}_i = \tag{4.2}$$

$$= x_0^{(1)} \operatorname{Re}(\lambda_1 \vec{v}_1) + x_0^{(2)} \operatorname{Im}(\lambda_1 \vec{v}_1) + \sum_{i=3}^{m-1} x_0^{(i)} \lambda_i \vec{v}_i. \tag{4.3}$$

So for $p\vec{x}_n = T^n(p\vec{x})$ we get:

$$p\vec{x}_n = x_0^{(1)} \operatorname{Re}(\lambda_1^n \vec{v}_1) + x_0^{(2)} \operatorname{Im}(\lambda_1^n \vec{v}_1) + \sum_{i=3}^{m-1} x_0^{(i)} \lambda_i^n \vec{v}_i.$$

Now if we multiply each vector $p\vec{x}_n$ by $\frac{1}{|\lambda_1^n|}$, we obtain:

$$\frac{p\vec{x}_n}{|\lambda_1^n|} = \frac{x_0^{(1)}}{|\lambda_1^n|} \operatorname{Re}(\lambda_1^n \vec{v}_1) + \frac{x_0^{(2)}}{|\lambda_1^n|} \operatorname{Im}(\lambda_1^n \vec{v}_1) + \sum_{i=3}^{m-1} x^{(i)} \frac{\lambda_i^n}{|\lambda_1^n|} \vec{v}_i.$$

Now if we consider the angle between sx_n and the plane spanned by $\operatorname{Re}\vec{v}_1$, $\operatorname{Im}\vec{v}_1$ we obtain:

$$\widehat{sx_n\ E} = \arctan\left(\frac{\|x_n - x_{n\,E}\|}{\|p - x_{n\,E}\|}\right),$$

where $x_{n\,E}$ is a projection of x_n onto E. So:

$$p - x_{n\,E} = x_0^{(1)} \operatorname{Re}(\lambda_1^n \vec{v}_1) + x_0^{(2)} \operatorname{Im}(\lambda_1^n \vec{v}_1)$$

and

$$x_n - x_{n\,E} = \sum_{i=3}^{m-1} x^{(i)} \lambda_i^n \vec{v}_i.$$

Also since for any $\vec{x} \in \operatorname{span}(\operatorname{Re}\vec{v}_1, \operatorname{Im}\vec{v}_2)$

$$|T(\vec{x})| = |\lambda_1||\vec{x}|$$

we can write:

$$\widehat{sx_n\ E} = \arctan\left(\frac{\left|\sum_{i=3}^{m-1} x_0^{(i)} \lambda_i^n \vec{v}_i\right|}{|\lambda_1^n||x_0^{(1)} \operatorname{Re}\vec{v}_1 + x_0^{(2)} \operatorname{Im}\vec{v}_1|}\right) = \tag{4.4}$$

$$= \arctan\left(\frac{\left|\sum_{i=3}^{m-1} x_0^{(i)} \frac{\lambda_i^n}{|\lambda_1^n|} \vec{v}_i\right|}{|x_0^{(1)} \operatorname{Re}\vec{v}_1 + x_0^{(2)} \operatorname{Im}\vec{v}_1|}\right). \tag{4.5}$$

Since $\forall i > 2,\ |\lambda_1| > |\lambda_i|$, the sum in the nominator converges to 0 as $n \to \infty$. However the denominator remains constant. This way we obtain

$$\widehat{sx_n\ E} \underset{n\to\infty}{\longrightarrow} 0$$

if $x_0^{(1)}$ or $x_0^{(2)}$ are not both equal to 0.

□

4.5.2 Double sub-dominant eigenvalues

Lemma 3. *Let T be an operator on BI^m with a complete set of real eigenvectors $\vec{v}_0, \vec{v}_1, \ldots, \vec{v}_{m-1}$ along with their respective eigenvalues $\lambda_0 = 1 > \lambda_1 = \lambda_2 \geq |\lambda_3| \geq \ldots \geq |\lambda_{m-1}|$. We denote the fixed point of T by p. Given a point $x_0 \neq p$, $x_0 \in BI^m$ we consider a sequence of secants sx_n that that pass through the points p and x_n where $x_n = T^n(x_0)$. Let E be a subspace spanned by $\vec{v}_1$ and $\vec{v}_2$. If*

$$\vec{px}_0 = x_0^{(1)}\vec{v}_1 + x_0^{(2)}\vec{v}_2 + \sum_{i=3}^{m-1} x_i^{(i)}\vec{v}_i$$

for some $x_0^{(1)} \neq 0$ or $x_0^{(2)} \neq 0$, then

$$\widehat{sx_n\ E} \underset{n\to\infty}{\longrightarrow} 0.$$

Proof. This proof is very similar to the proof of lemma 1. Since the eigenvectors of T form a complete basis of $\mathbb{R}^m$ and $x_n = T^n(x_0)$ we can write the following:

$$\vec{px}_n = \sum_{i=1}^{m-1} \lambda_i^n x_0^{(i)}\vec{v}_i.$$

By multiplying $\vec{px}_n$ by $\frac{1}{\lambda_1^n}$ we get:

$$\frac{\vec{px}_n}{\lambda_1^n} = \sum_{i=1}^{m-1} \frac{\lambda_i^n}{\lambda_1^n} x_0^{(i)}\vec{v}_i.$$

All but the first two terms of that sum always converge to 0 as $n \to \infty$. So

$$\frac{\vec{px}_n}{\lambda_1^n} \underset{n\to\infty}{\longrightarrow} x_0^{(1)}\vec{v}_1 + x_0^{(2)}\vec{v}_2.$$

Should we consider E a subspace spanned by $\vec{v}_1, \vec{v}_2$ we can see that:

$$\widehat{sx_n\ E} \underset{n\to\infty}{\longrightarrow} 0.$$

if $x_0^{(1)}$ and $x_0^{(2)}$ are not both equal to 0. □

4.5.3 Null component problem

In the previous lemmas we assumed, that the vector $\vec{px}_0$ has non-zero component(s) corresponding to the sub-dominants eigenvectors. Here we study the opposite case.

Lemma 4. *Let T be an operator on BI^m with a complete set of real eigenvectors $\vec{v}_0, \vec{v}_1, \ldots, \vec{v}_{m-1}$ along with their respective eigenvalues $\lambda_0 = 1 > \lambda_1 > \lambda_2 > |\lambda_3| \geq \ldots \geq |\lambda_{m-1}|$. We denote the fixed point of T by p. Given a point $x_0 \neq p$, $x_0 \in BI^m$ we consider a sequence of secants sx_n that that pass through the points p and x_n where $x_n = T^n(x_0)$. Let E be a subspace spanned by $\vec{v}_2$. If*

$$\vec{px}_0 = 0 \cdot \vec{v}_1 + x_0^{(2)}\vec{v}_2 + \sum_{i=3}^{m-1} x_i^{(i)}\vec{v}_i$$

for some $x_0^{(2)} \neq 0$, then

$$\widehat{sx_n\ E} \underset{n\to\infty}{\longrightarrow} 0.$$

Proof. As in the previous cases, we consider the basis decomposition of $x_n - p$:

$$\vec{px}_n = \sum_{i=2}^{m-1} \lambda_i^n x_0^{(i)}\vec{v}_i.$$

However this time we multiply the vectors $\vec{px}_n$ by $\frac{1}{\lambda_2^n}$ instead of $\frac{1}{\lambda_1^n}$. By doing this we obtain:

$$\frac{\vec{px}_n}{\lambda_n^1} = \sum_{i=2}^{m-1} \frac{\lambda_i^n}{\lambda_2^n}.$$

So if $x_0^{(2)} \neq 0$ we get:

$$\frac{\vec{px}_n}{\lambda_n^1} \underset{n\to\infty}{\longrightarrow} x_0^{(2)}\vec{v}_2.$$

Now if we consider E a subspace spanned by $\vec{v}_2$ we obtain:

$$\widehat{sx_n\ E} \underset{n\to\infty}{\longrightarrow} 0.$$

□

4.5.4 Mixed eigenvalues from $\mathbb{R}$ and $\mathbb{C}$

The next lemma treats a slightly more sophisticated case of an operator T with a real sub-dominant eigenvalue, but whose other eigenvalues are not necessarily real.

Lemma 5. *Let T be a operator on BI^m with a complete set of eigenvectors $\vec{v}_0, \vec{v}_1, \ldots, \vec{v}_{m-1}$ along with their respective eigenvalues $\lambda_0 = 1 > \lambda_1 > |\lambda_2| \geq \ldots \geq |\lambda_{m-1}|$. We denote the fixed point of T by p. Let us divide all the sub-dominant eigenvalues into three categories A, B and $\bar{B}$: $\lambda_i \in A$ if $\lambda_i \in \mathbb{R}$, $\lambda_i \in B$ if $\lambda_i \in \mathbb{C}$ and $\bar{\lambda}_i \in \bar{B}$ such that $B \cap \bar{B} = \emptyset$. Given*

a point $x_0 \neq p$, $x_0 \in BI^m$ we consider a sequence of secants sx_n that that pass through the points p and x_n where $x_n = T^n(x_0)$. Let E is a subspace spanned by $\vec{v}_1$. If

$$\vec{px}_0 = x_0^{(1)}\vec{v}_1 + \sum_{\lambda_i \in A} x_0^{(i)}\vec{v}_i + \sum_{\lambda_i \in B} (x_0^{(i)} \operatorname{Re}\vec{v}_i + x_0^{(i+1)} \operatorname{Im}\vec{v}_i)$$

for some $x_0^{(1)} \neq 0$, then

$$\widehat{sx_n\ E} \underset{n\to\infty}{\longrightarrow} 0.$$

Proof. Real eigenvectors of T along with the real and imaginary parts of complex eigenvectors form a basis of $\mathbb{R}^m$. So for any vector $\vec{px}_0$ we can write the following:

$$\vec{px}_0 = x_0^{(1)}\vec{v}_1 + \sum_{\lambda_i \in A} x_0^{(i)}\vec{v}_i + \sum_{\lambda_i \in B} (x_0^{(i)} \operatorname{Re}\vec{v}_i + x_0^{(i+1)} \operatorname{Im}\vec{v}_i).$$

Should we apply T^n we obtain:

$$\vec{px}_n = T^n(\vec{px}_0) = \lambda_1^n x_0^{(1)}\vec{v}_1 + \sum_{\lambda_i \in A} \lambda_i^n x_0^{(i)}\vec{v}_i + \sum_{\lambda_i \in B} (x_0^{(i)} \operatorname{Re}(\lambda_i^n\vec{v}_i) + x_0^{(i+1)} \operatorname{Im}(\lambda_i^n\vec{v}_i)).$$

Now let us consider the angle between sx_n and $E = \operatorname{span}(\vec{v}_1)$:

$$\widehat{sx_n\ E} = \arctan\left(\frac{\|x_n - x_{n\,E}\|}{\|p - x_{n\,E}\|}\right),$$

where $x_{n\,E}$ is a projection of x_n onto E, where

$$p - x_{n\,E} = \lambda_1^n x_0^{(1)}\vec{v}_1$$

and

$$x_n - x_{n\,E} = \sum_{\lambda_i \in A, i\neq 1} \lambda_i^n x_0^{(i)}\vec{v}_i + \sum_{\lambda_i \in B} (x_0^{(i)} \operatorname{Re}(\lambda_i^n\vec{v}_i) + x_0^{(i+1)} \operatorname{Im}(\lambda_i^n\vec{v}_i)).$$

Note that for any linear operator T

$$\|T(x)\| \leq |\lambda_{max}|\|x\|,$$

where λ_{max} is an eigenvalue of T with the greatest absolute value. Hence:

$$\frac{\|T^n(x_0 - x_{0\,E})\|}{\|\lambda_1^n x_0^{(1)}\vec{v}_1\|} \leq \frac{|\lambda_2^n|\|x_0 - x_{0\,E}\|}{\|\lambda_1^n x_0^{(1)}\vec{v}_1\|}$$

because λ_2 is the greatest absolute value of the restriction of T onto the orthogonal complement of E. Also since $|\lambda_1| > |\lambda_2|$ this fraction converges to 0 as long as $x_0^{(1)} \neq 0$ and

$$\widehat{sx_n\ E} \underset{n\to\infty}{\longrightarrow} 0$$

as well.

□

4.5.5 Summary

Now we can formulate a more general statement about the convergence of secants defined by iterations.

Theorem 2. *Let T be an operator on BI^m with a complete set of eigenvectors. Let p be a fixed point of T. Given a point $x_0 \neq p$, $x_0 \in BI^m$ we consider a sequence of secants sx_n that that pass through the points p and x_n where $x_n = T^n(x_0)$. Let E is a subspace spanned by $\vec{v}_i$ — eigenvectors of T corresponding to the first eigenvalue λ_i such that $\vec{px}_0$ has non-zero components in the eigen-basis decomposition corresponding to the eigenvectors $\vec{v}_i$. Then*

$$\widehat{sx_n\ E} \to 0.$$

Proof. For any point x_0 there exists an eigenvalue λ_i such that $\vec{px}_0$ has non-zero components at the corresponding positions of the eigen-basis decomposition, because if $\vec{px}_0$ has no non-zero components then $p = x_0$. To prove, this we apply lemma 4 i-times (1 for each zero component) and then apply either lemma 1, lemma 2 or lemma 3 depending on whether λ_i is real or complex and on its multiplicity. □

4.6 Incomplete set of eigenvectors

In this section we consider the convergence rate of different components of $T^n(\vec{v})$ using the generalised eigenvectors as a basis. We show that the following affect the convergence rate corresponding to a single generalised eigenvector: the absolute value of the eigenvalues, the order of the generalised eigenvector and the length of the chain it is a part of. We also show that the absolute value has the most significant effect on convergence rate.

At first we consider the convergence rate of different components $T^n(\vec{v})$ in a subspace spanned by generalised eigenvectors that form a single chain. We want to show that the component corresponding to the generalised eigenvector of order 1 has the slowest convergence rate within a chain.

Lemma 6. *Let us consider a linear operator T on $\mathbb{R}^k$. Let T be an eigenvalues λ with a geometric multiplicity 1 and an algebraic multiplicity k. We will denote one of its eigenvectors as $\vec{v}_0$:*

$$T\vec{v}_0 = \lambda\vec{v}_0.$$

There exist $k-1$ generalised eigenvectors $\vec{v}_1, \vec{v}_2, \dots \vec{v}_{k-1}$ such that:

$$T\vec{v}_i = \lambda\vec{v}_i + \vec{v}_{i-1},\ 1 \leq i \leq k-1,$$

and vectors $\vec{v}_0, \vec{v}_1, \dots, \vec{v}_{k-1}$ are linearly independent and therefore form a basis of $\mathbb{R}^k$.

Let us denote

$$y_j^{(n)} = \sum_{i=0}^{k-j-1} C_n^i a_{i+j} \lambda^{n-i},$$

where

$$C_n^i = \begin{cases} \frac{n!}{i!(n-i)!} & \text{if } i \leq n, \\ 0 & \text{else.} \end{cases}$$

Then:

$$T^n\vec{a} = \sum_{i=0}^{n} y_i^{(n)}\vec{v}_i.$$

Proof. So for any vector $\vec{a} \in \mathbb{R}^k$ exists $\{a_i\}_{i=0}^{k-1}$ such that $\vec{a} = \sum_{i=0}^{k-1} a_i\vec{v}_i$. Then for $n = 1$ we get:

$$\begin{aligned} T\vec{a} &= \sum_{i=0}^{k-1} a_i T\vec{v}_i = a_0 T\vec{v}_0 + \sum_{i=1}^{k-1} a_i T\vec{v}_i = \\ &= a_0\lambda\vec{v}_0 + \sum_{i=1}^{k-1} a_i(\lambda\vec{v}_i + \vec{v}_{i-1}) = \\ &= \sum_{i=0}^{k-2}(\lambda a_i + a_{i+1})\vec{v}_i + \lambda a_{k-1}\vec{v}_{k-1}. \end{aligned}$$

Now we are going to show that if our hypothesis is true for some n than is it also true for $n+1$. Consider

$$\begin{aligned} &T^{n+1}(\vec{a}) = T(T^n(\vec{a})) = \sum_{i=0}^{k-2}(\lambda y_i^{(n)} + y_{i+1}^{(n)})\vec{v}_i + \lambda y_{k-1}^{(n)}\vec{v}_{k-1} = \\ &= \sum_{i=0}^{k-2}\left(\lambda \sum_{j=0}^{k-i-1} C_n^j a_{i+j}\lambda^{n-j} + \sum_{j=0}^{k-i-2} C_n^j a_{i+j+1}\lambda^{n-j}\right)\vec{v}_i + \\ &+ \lambda C_n^0 a_{k-1}\lambda^n\vec{v}_{k-1}. \end{aligned}$$

Note that the last term equals $C_{n+1}^0 a_{k-1}\lambda^{n+1}\vec{v}_{k-1} = y_{k-1}^{(n+1)}\vec{v}_{k-1}$. The coefficient at $\vec{v}_i$ can be rewritten with the substitution in the second term $z = j+1$ as follows:

$$\begin{aligned} &\sum_{j=0}^{k-i-1} C_n^j a_{i+j}\lambda^{n-j+1} + \sum_{z=1}^{k-i-1} C_n^{z-1} a_{i+z}\lambda^{n-z+1} = \\ =&C_n^0 a_i\lambda^{n+1} + \sum_{j=1}^{k-i+1} a_{i+j}(C_n^j\lambda^{n-j+1} + C_n^{j-1}\lambda^{n-j+1}) = \\ =&C_n^0 a_i\lambda^{n+1} + \sum_{j=1}^{k-i+1} a_{i+j}\lambda^{n-j+1}(C_n^j + C_n^{j-1}) = \\ =&C_n^0 a_i\lambda^{n+1} + \sum_{j=1}^{k-i+1} a_{i+j}\lambda^{n-j+1}C_{n+1}^j = \\ =& \sum_{j=0}^{k-i+1} a_{i+j}\lambda^{n-j+1}C_{n+1}^j. \end{aligned}$$

So this way:

$$T^{n+1}(\vec{a}) = \sum_{j=0}^{k-1} \left(\sum_{i=0}^{k-j-1} C_{n+1}^{i} a_{i+j} \lambda^{n-i+1} \right) \vec{v}_j,$$

which confirms the initial hypothesis. □

Corollary 1.

$$\frac{1}{C_n^{k-1}\lambda^n} T^n(\vec{a}) \underset{n\to\infty}{\longrightarrow} (a_{k-1}\lambda^{-k+1}, 0, \ldots, 0)$$

if $a_{k-1} \neq 0$.

Proof. Let us consider $\frac{y_j^{(n)}}{C_n^{k-1}\lambda^n}$ and its limit at $n \to \infty$ at different values of j.

$$\frac{y_j^{(n)}}{C_n^{k-1}\lambda^n} = \frac{1}{C_n^{k-1}\lambda^n} \sum_{i=0}^{k-j-1} C_n^i a_{i+j} \lambda^{n-i} =$$
$$= \sum_{i=0}^{k-j-1} \frac{C_n^i}{C_n^{k-1}} (a_{i+j}\lambda^{-i}).$$

So the only n-dependent term here is $\frac{C_n^i}{C_n^{k-1}}$ which equals:

$$\frac{n!}{i!(n-i)!} \cdot \frac{(k-1)!(n-k+1)!}{n!} = \frac{(k-1)!(n-k+1)!}{i!(n-i)!}.$$

This expression converges to 0 for all $i < k-1$ and to 1 for $i = k-1$. So a term with a non-zero limit only exists in $\frac{y_j^{(n)}}{C_n^{k-1}\lambda^n}$ with $j = 0$ and if $a_{k-1} \neq 0$. Therefore

$$\frac{1}{C_n^{k-1}\lambda^n} T^n(\vec{a}) \underset{n\to\infty}{\longrightarrow} (a_{k-1}\lambda^{-k+1}, 0, \ldots, 0).$$

□

So we have shown that of all the components of $T^n(\vec{v})$ the first one, i.e. corresponding to the eigenvector of order 1, has the slowest convergence rate.

Also note that if we consider the limit of

$$\frac{1}{C_n^{k_2-1}\lambda_2^n} T^n(\vec{a})$$

for any $k_2 > k$ or for any $\lambda_2 > \lambda$ it would be equal to 0.

We can sum up the results as follows:

- component corresponding to the eigenvector of order 1 has the slowest convergence rate of all the corresponding chain
- should we compare two components corresponding to the base of different chains that correspond to the same eigenvalue, the one with the longer chain has the slowest rate of convergence

- if two components correspond to different eigenvalues, the one with the bigger eigenvalue converges more slowly, no matter the relative length of the chains.

If the initial vector has no zero component, then the component corresponding to the sub-dominant eigenvector of order 1 has the slowest convergence rate. As was shown in the previous section, the limit of the corresponding sequence of secants is then defined by the sub-dominant eigenvector. But if the initial vector has one or more zero component it can change the convergence rate of certain components. First, if the component corresponding to the last generalised eigenvector is equal to zero, then for the intent and purpose of calculating the rate of convergence we should treat it as a shorter chain. Second, if all the components corresponding to a single chain are equal to zero, then the first eigenvector of the chain cannot be the secants limit position.

Theorem 3. *Let T be an operator on BI^m with a positive sub-dominant eigenvalue λ. Let p be a fixed point of T. Given a point $x_0 \neq p$, $x_0 \in BI^m$ we consider a sequence of secants sx_n that that pass through the points p and x_n where $x_n = T^n(x_0)$. If E is a subspace spanned by $\vec{v}_i$ such that eigenvectors associated with the first eigenvalue of T such that $\vec{px}_0$ has non-zero components corresponding to the last generalised eigenvectors of the chain starting with $\vec{v}_i$ in the Jordan basis decomposition, then*

$$\widehat{sx_n\ E} \to 0.$$

Proof. Let us consider

$$\frac{\vec{px}_n}{C_n^{k-1}\lambda^n} = \frac{T^n(x_0)}{C_n^{k-1}\lambda^n},$$

where k is the length of chain of generalised eigenvectors that starts with $\vec{v}_i$ and λ is the corresponding eigenvalue. Consider the corresponding decomposition in the Jordan basis of T. Previously we have shown that all components except the one corresponding to $\vec{v}_i$ converge to 0. Since $\lambda > 0$ the angle between $\frac{1}{C_n^{k-1}\lambda^n}(p - x_n)$ and E is equal to

$$\widehat{sx_n\ E}.$$

Since all components of $\frac{1}{C_n^{k-1}\lambda^n}(p - T^n(x_0))$ except the one corresponding to $\vec{v}_i$ converge to 0 and $E = \mathrm{span}(\vec{v}_i)$ we obtain

$$\widehat{sx_n\ E} \to 0.$$

□

4.7 Convergence of the angular deviation.

In this section we consider the convergence of angular deviation for the sequence of rings. Let us consider a point $p \in \mathcal{A}$ such that p is a periodic point. Let T be the transformation that corresponds to the period of the point p. We denote the subspace spanned by sub-dominant eigenvectors as E.

Function $\alpha(E, x)$ that was used in the definition of angular deviation (see definition 13) is continuous because arctan and distance are continuous, and for any point such that the

value of the denominator converges to zero the value of $\alpha(E,x)$ converges to its value $\frac{\pi}{2}$. Therefore for each ring R_i there exists $x_i \in R_i$ such that

$$\alpha(x_i) = \max_{x \in R_i} \alpha(E,x),$$

since R_i is compact.

If $\nexists \vec{x} \in R_0$ such that x_0 has a null component corresponding to $\vec{v}_1$ then we can prove the following:

$$\alpha_{max}(E,R_i) \underset{i\to\infty}{\longrightarrow} 0.$$

To prove that it is sufficient to demonstrate that if $\alpha(E,x_i) = \max_{x\in R_i} \alpha(E,x_i)$ then $\alpha(E,x_{i+1}) = \max_{x\in R_{i+1}} \alpha(E,x)$, because we have already shown in sections 4.5 and 4.6 that under stated conditions $\alpha(E,x_i) \to 0$ when $i \to \infty$.

Lemma 7. *Consider an attractor $\mathcal{A}$ of some IFS. Let $p \in \mathcal{A}$ with a periodic address, where T is an affine transformation that corresponds to the period. Let us denote the set of rings that encompasses the point p by $\{R_i\}$ such that $R_i = T(R_{i-1})$. There exists a sequence $\{x_i\}$ such that $\alpha(E,x_i) = \max_{x\in R_i} \alpha(E,x)$ and $x_i = T^i(x_0)$ for some $x_0 \in R_0$.*

Proof. Since R_0 is a compact set and $\alpha(E,x)$ is continuous there exists $x_0 \in R_0$ such that $\alpha(E,x_0) = \max_{x\in R_0} \alpha(E,x)$.

Now let us consider the set of lines s_i such that each line $s \in s_i$ passes through the point p and some point from R_i. For each s_i there exists lines denoted by s^i_{min} and s^i_{max} such that

$$\widehat{s^i_{min}\ E} = \min_{s\in s_i} \widehat{s\ E}$$

and

$$\widehat{s^i_{max}\ E} = \max_{s\in s_i} \widehat{s\ E}$$

(see figure 4.7).

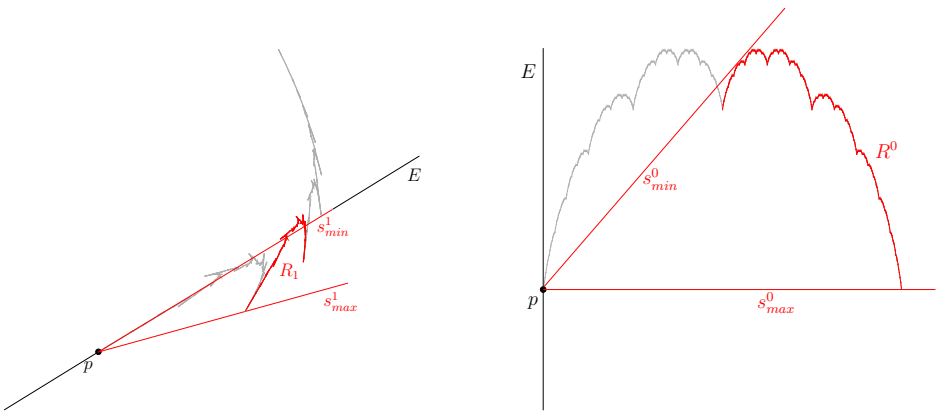

Figure 4.7: Two examples of lines s_i for rings R_i.

Suppose $x_i \in R_i$ such that $\alpha(E, x_i) = \max_{x \in R_i} \alpha(E, x)$ and $x_{i+1} = T(x_i) \neq \max_{x \in R_{i+1}} \alpha(E, x)$. Then T is not continuous because s^i_{max} belongs to the border of s_i while s^{i+1}_{max} does not belong to the border of s_{i+1}. Therefore there exists a sequence $\{x_i\}$ such that $\alpha(E, x_i) = \max_{x \in R_i} \alpha(E, x)$ and $x_i = T^i(x_0)$ for some $x_0 \in R_0$. □

4.8 Summary and points with non-uniform addresses

Now with the proof of lemma 7 we have a complete set of statements to derive the conditions for existence of a tangent subspace. Results from sections 4.5 and 4.6 give us a set of conditions that guarantee the convergence for a sequence of secants sx_n obtained with iterations of single transformation T ($x_n = T(x_0)$, $x_0 \in R_0$). According to theorems 2 and 3 the limit of sx_n is independent of x_0 if all points of R_0 have at least one non-zero component corresponding to the sub-dominant eigenvectors or generalised eigenvectors. In case R_0 contains no such points we can consider the restriction of T onto the sub-space spanned by all its (generalised) eigenvectors but the sub-dominant ones without any loss of generality. If this limit is indeed independent from the choice of $x_0 \in R_0$ then lemma 7 guarantees the convergence of $\alpha_{max}(E, R_i)$ for some affine subspace E spanned either by the sub-dominant eigenvector(s) of T (real sub-dominant eigenvalue) or by the pair of real and imaginary parts of the sub-dominant eigenvector (complex sub-dominant eigenvalue). Finally proposition 1 tells us that the convergence of $\alpha_{max}(R_i)$ for some affine subspace E means that subspace E is indeed a tangent subspace.

Previously we were studied points with uniform addresses i^ω. The following two propositions show how these results can be applied to other kinds of periodic points.

Proposition 3. *Let $\mathcal{A} \subset \mathbb{R}^m$ be an attractor of some CIFS. Let $p \in \mathcal{A}$ be periodic address i^ω. If E is a tangent subspace at the points p, then $T_\sigma(E)$ is the tangent subspace for the points p' with address σi^ω, where $\sigma = \sigma_1, \sigma_2, \ldots, \sigma_n$ is a finite prefix and $T_\sigma = T_{\sigma_1}, \ldots, T_{\sigma_n}$.*

Proof. Given the self-similarity of $\mathcal{A}$ points p' is can be obtained from point p by applying the corresponding linear map T_σ. Any neighbourhood of p is also mapped into the neighbourhood of p'. Hence the tangent subspace at p is mapped into the tangent subspace of p'. □

Proposition 4. *Let $\mathcal{A} \subset \mathbb{R}^m$ be an attractor of some CIFS. Let $p' \in \mathcal{A}$ be multiple addresses $\sigma_1 i_1^\omega, \sigma_2 i_2^\omega, \ldots, \sigma_n i_n^\omega$. Let E_j be the tangent subspaces at the points p_j with addresses 1_j^ω. Then the tangent space E at the point p' exists if E_j exist for all $j = 1, \ldots, n$ and*

$$T_{\sigma_1}(E_1) = T_{\sigma_2}(E_2) = \ldots = T_{\sigma_n}(E_n).$$

Proof. As was shown in section 4.2 each address corresponds to a specific way of approaching the point. Tangent subspace exists if the limit of secants is independent of the way the point is approached. So it is necessary that the resulting tangent subspace is independent of the choice of the address. □

Now the last part of this chapter is dedicated to applying these technique to various attractors of different IFS and CIFS.

4.9 Examples and applications

In this section we are going to apply theorem 2 and theorem 3 along with lemma 7 to attractors of different IFS and CIFS.

4.9.1 Curves

Throughout most of the following examples we are going to use the same technique to find the tangent at the specific point. We illustrate the technique with a quadratic B-spline curve, please refer to figure 4.8. Given an IFS $\{T_1, \ldots, T_n\}$ we choose a point we are interested

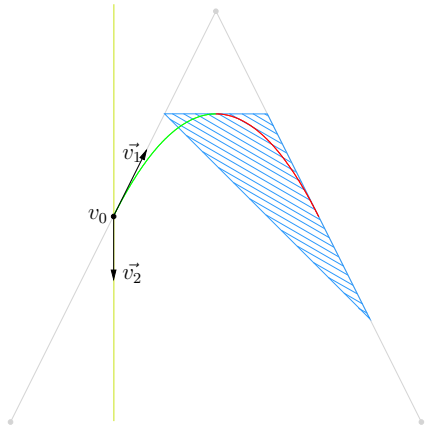

Figure 4.8: Study of the differential behaviour of a quadatic B-spline curve: the standard basis of BI^3 is shown in gray; the eigenbasis of T_1 in black. The yellow line is the sub-space of BI^3 with coordinates $(\cdot, 0, \cdot)$ in the eigenbasis. Ring R_0 of the point v_0 is shown in red and the hatched blue polygon is the convex set that contains ring R_0.

in. In most of the examples we choose the fixed point of some transformation T_i. For the quadratic B-spline curve the IFS consists of two transformations on BI^3:

$$T_1 = \begin{pmatrix} 3/4 & 1/4 & 0 \\ 1/4 & 3/4 & 3/4 \\ 0 & 0 & 1/4 \end{pmatrix}, \; T_2 = \begin{pmatrix} 1/4 & 0 & 0 \\ 3/4 & 3/4 & 1/4 \\ 0 & 1/4 & 3/4 \end{pmatrix}.$$

We study the behaviour of the curve at the fixed point of T_1. We calculate the eigenvectors and eigenvalues of respective transformation. For the given example we obtain the following eigenvectors:

$$\vec{v_0} = \begin{pmatrix} 1/2 \\ 1/2 \\ 0 \end{pmatrix}, \; \vec{v_1} = \begin{pmatrix} -1 \\ 1 \\ 0 \end{pmatrix}, \; \vec{v_2} = \begin{pmatrix} 1 \\ -2 \\ 1 \end{pmatrix},$$

and the corresponding eigenvalues:

$$\lambda_0 = 1, \; \lambda_1 = 1/2, \; \lambda_2 = 1/4.$$

After that we try to establish whether the outermost ring R_0 contains any points with zero components in the direction of the sub-dominant eigenvector(s). Lemma 1 (along with theorem 2 and lemma 7) states that if it is not the case then the tangent direction is given by the sub-dominant eigenvector(s).

For the quadratic b-spline example the ring R_0 of the point v_0 is shown in red in figure 4.8. The sub-dominant eigenvector is $\vec{v_1}$, thus the yellow line gives the set of points with coordinates $(\cdot, 0, \cdot)$ in the eigenbasis. In general it is difficult to test whether R_0 intersects the set of points with 0 along the sub-dominant eigenvectors. So we will try to find a polyhedron that includes our R_0.

Throughout all our examples the IFS matrices have non-negative entries, therefore we can conclude that our curve $\mathcal{A}$ is contained in the simplex BI^3. In other words, the quadratic b-spline lies within the control triangle shown in gray in figure 4.8. The coordinates of the initial simplex that contains all the curve $\mathcal{A}$ is just the identity matrix $I_{3\times 3}$. Next, we can find a (set of) polyhedron containing ring R_0. In our B-spline example there is one polygon (hatched blue in figure 4.8) containing R_0. Since here $R_0 = T_2(\mathcal{A})$, the coordinates of the polygon vertices in the standard bases are given by the matrix $T_2 \times I_{3\times 3}$. Now it is easy to check if the (set of) polyhedron intersects the subspace with zero coordinates in the sub-dominant components of the eigenbasis. The eigenmatrix S gives the change of basis from the standard one to the eigenbasis.

$$S = \begin{pmatrix} 1/2 & -1 & 1 \\ 1/2 & 1 & -2 \\ 0 & 0 & 1 \end{pmatrix}.$$

Then the coordinates of the bounding polygon in the eigenbasis can be obtained as

$$S^{-1} \times T_2 = \begin{pmatrix} 1 & 1 & 1 \\ 1/4 & 3/4 & 5/4 \\ 0 & 1/4 & 3/4 \end{pmatrix}.$$

Note that the second row is of the matrix is the second coordinate of the bounding polygon vertices in the eigenbasis. Since it is strictly positive the polygon is separated from the subspace $(\cdot, 0, \cdot)$. Indeed, the hatched polygon does not intersect the yellow line in figure 4.8.

So we can conclude that the conditions of lemma 1 are satisfied and the tangent direction is given by the vector $\vec{v_1}$.

Double address point

In this example we are going to study differential behaviour at a point with a double address. Let us consider the following IFS:

$$T_1 = \begin{pmatrix} 1 & 7/10 & 7/20 \\ 0 & 3/10 & 3/10 \\ 0 & 0 & 7/20 \end{pmatrix}, \; T_2 = \begin{pmatrix} 7/20 & 0 & 0 \\ 3/10 & 3/10 & 0 \\ 7/20 & 7/10 & 1 \end{pmatrix}.$$

The corresponding attractor is presented in figure 4.9. The midpoint of the curve has two addresses $1(2)^\omega$ and $2(1)^\omega$. To compute the two half tangents we are going to compute the

tangents at the endpoints of the curve (endpoints have $(1)^\omega$) and $(2)^\omega$ as their respective addresses) and apply T_1 and T_2 respectively.

First let us find the tangent at the fixed point of T_1. Here are the eigenvectors and eigenvalues of T_1:

$$\lambda_0 = 1,\ \lambda_1 = 7/20,\ \lambda_2 = 3/10,$$

$$\vec{v}_0 = \begin{pmatrix} 1 \\ 0 \\ 0 \end{pmatrix},\ \vec{v}_1 = \begin{pmatrix} 1 \\ -6/7 \\ -1/7 \end{pmatrix},\ \vec{v}_2 = \begin{pmatrix} 1 \\ -1 \\ 0 \end{pmatrix}.$$

So if the corresponding change of basis matrix is S then

$$S^{-1} = \begin{pmatrix} 1 & 1 & 1 \\ 0 & 0 & -7 \\ 0 & -1 & 6 \end{pmatrix}.$$

Since the IFS has only two transformations we can compute the polygon containing R_0 as follows:

$$S^{-1}T_2 = \begin{pmatrix} 1 & 1 & 1 \\ -49/20 & -49/10 & -7 \\ 9/5 & 39/10 & 6 \end{pmatrix}.$$

So all vertices of the polygon have a negative coordinate that corresponds to the sub-dominant eigenvector (second row of the above matrix). This means that there is no point with a zero component corresponding to the sub-dominant eigenvector and sub-dominant eigenvector gives the direction of the tangents. Let us denote this vector as $\vec{t_1}$:

$$\vec{t_1} = \begin{pmatrix} 1 \\ -6/7 \\ -1/7 \end{pmatrix}.$$

In a similar manner we can compute the tangent at the fixed point of T_2 which is

$$\vec{t_2} = \begin{pmatrix} 1 \\ 6 \\ -7 \end{pmatrix}.$$

Now to find the two half-tangents at the midpoint we calculate $T_1(\vec{t_2})$ and $T_2(\vec{t_1})$:

$$T_1(\vec{t_2}) = \begin{pmatrix} 11/4 \\ -3/10 \\ -49/20 \end{pmatrix},\ T_2(\vec{t_1}) = \begin{pmatrix} 7/20 \\ 3/70 \\ -11/28 \end{pmatrix}.$$

Now should we compute the cross product between the two we can see that two half-tangent are not collinear:

$$T_2(\vec{t_1}) \times T_1(\vec{t_2}) = \begin{pmatrix} -39/175 \\ -39/175 \\ -39/175 \end{pmatrix}.$$

The curve and all computed tangent along with respective control points is presented in figure 4.9.

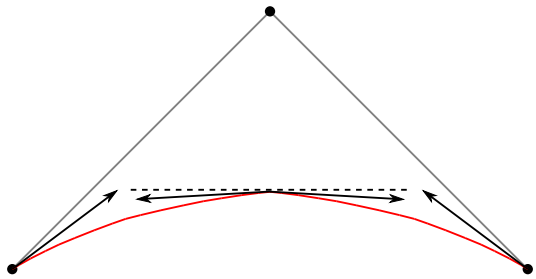

Figure 4.9: A curve with two different half-tangent at the double address point.

Spiral touching a tangent plane

In this section we study a curve which does not have a tangent line but a tangent plane. The curve will be obtained by a modified Doo-Sabin scheme, refer to figure 4.10 for an illustration. The control mesh consists of two faces: a triangle and a quad; subdivided mesh converges to the limit curve. We express this subdivision in terms of CIFS, namely, the limit curve is the attractor of a CIFS with control graph provided in figure 4.11.

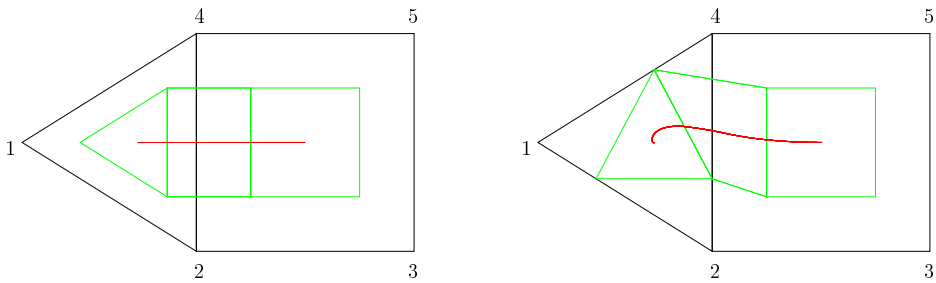

Figure 4.10: Left-hand image shows the Doo-Sabin subdivision scheme applied on the control mesh shown in black, the green mesh is obtained by one iteration and the red curve is the limit curve. Right-hand image shows the subdivision with modified weights.

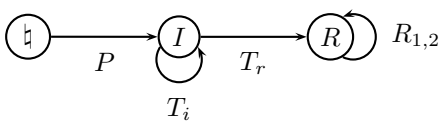

Figure 4.11: A projective IFS as a CIFS automaton.

The barycentric space associated with the state I has 5 dimensions, whereas R has 6 dimensions. The matrices corresponding to the Doo-Sabin subdivision scheme can be

expressed as follows:

$$T_i = \begin{pmatrix} 2/3 & 1/6 & 0 & 1/6 & 0 \\ 1/6 & 2/3 & 9/16 & 1/6 & 3/16 \\ 0 & 0 & 3/16 & 0 & 1/16 \\ 1/6 & 1/6 & 3/16 & 2/3 & 9/16 \\ 0 & 0 & 1/16 & 0 & 3/16 \end{pmatrix}, \; T_r = \begin{pmatrix} 1/6 & 0 & 0 & 1/6 & 0 & 0 \\ 2/3 & 9/16 & 3/16 & 1/6 & 3/16 & 1/16 \\ 0 & 3/16 & 9/16 & 0 & 1/16 & 3/16 \\ 1/6 & 3/16 & 1/16 & 2/3 & 9/16 & 3/16 \\ 0 & 1/16 & 3/16 & 0 & 3/16 & 9/16 \end{pmatrix}$$

Matrices R_1 and R_2 are obtained as a tensor product of quadratic B-spline and quadratic B-spline vertex. The left-hand image of figure 4.10 shows one subdivision. For example, the green triangle is obtained from the black one with the weights defined in the 1st, 2nd and 4th columns of the matrix T_i.

For this section we modify the scheme, namely the green triangle is slightly rotated (refer to the right-hand image of figure 4.10). The modified matrices are as follows:

$$T_i = \begin{pmatrix} 2/3 & 0 & 0 & 1/3 & 0 \\ 1/3 & 2/3 & 9/16 & 0 & 3/16 \\ 0 & 0 & 3/16 & 0 & 1/16 \\ 0 & 1/3 & 3/16 & 2/3 & 9/16 \\ 0 & 0 & 1/16 & 0 & 3/16 \end{pmatrix}, \; T_r = \begin{pmatrix} 0 & 0 & 0 & 1/3 & 0 & 0 \\ 2/3 & 9/16 & 3/16 & 0 & 3/16 & 1/16 \\ 0 & 3/16 & 9/16 & 0 & 1/16 & 3/16 \\ 1/3 & 3/16 & 1/16 & 2/3 & 9/16 & 3/16 \\ 0 & 1/16 & 3/16 & 0 & 3/16 & 9/16 \end{pmatrix}$$

Let us study the differential behaviour of the curve at the fixed point of T_i. The operator T_i has 5 eigenvalues:

$$\lambda_0 = 1, \; \lambda_1 = 1/2 - i\sqrt{3}/6, \; \lambda_2 = 1/2 + i\sqrt{3}/6, \; \lambda_3 = 1/4, \; \lambda_4 = 1/8$$

and the correspondig eigenmatrix is

$$(\vec{v}_0, \vec{v}_1, \vec{v}_2, \vec{v}_3, \vec{v}_4) = \begin{pmatrix} 1 & 1 & 1 & 1 & 1 \\ 1 & -1/2 + i\sqrt{3}/2 & -1/2 - i\sqrt{3}/2 & -41/4 & 5/8 \\ 0 & 0 & 0 & 21/4 & -43/24 \\ 1 & -1/2 - i\sqrt{3}/2 & -1/2 + i\sqrt{3}/2 & -5/4 & -13/8 \\ 0 & 0 & 0 & 21/4 & 43/24 \end{pmatrix}$$

Lemma 2 tells us that the plane spanned on $(\operatorname{Re}\vec{v}_1, \operatorname{Im}\vec{v}_2)$ is the tangent plane to our curve if there is no point belonging to the ring R_0 with zero coordinates along the vectors $\operatorname{Re}\vec{v}_1, \operatorname{Im}\vec{v}_2$ in the basis

$$(\vec{v}_0, \operatorname{Re}\vec{v}_1, \operatorname{Im}\vec{v}_2, \vec{v}_3, \vec{v}_4) = \begin{pmatrix} 1 & 1 & 1 & 1 & 1 \\ 1 & -1/2 & -\sqrt{3}/2 & -41/4 & 5/8 \\ 0 & 0 & 0 & 21/4 & -43/24 \\ 1 & -1/2 & \sqrt{3}/2 & -5/4 & -13/8 \\ 0 & 0 & 0 & 21/4 & 43/24 \end{pmatrix}$$

We know that the curve belongs to the convex hull of its control points (black mesh in figure 4.10). The coordinates of the control points in the standard basis are given by a 5×5 identity matrix $I_{5\times 5}$. Therefore the ring R_0 belongs to the convex hull of 6 control

points with coordinates $I_{5\times5} \times T_r$ in the standard basis (two green quads in figure 4.10). The coordinates in the eigenbasis can be obtained as follows:

$$(\vec{v_0}, \operatorname{Re}\vec{v}_1, \operatorname{Im}\vec{v}_2, \vec{v}_3, \vec{v}_4)^{-1} \times I_{5\times5} \times T_r = \begin{pmatrix} \frac{1}{3} & \frac{1}{3} & \frac{1}{3} & \frac{1}{3} & \frac{1}{3} & \frac{1}{3} \\ -\frac{1}{3} & -\frac{97}{301} & -\frac{271}{903} & 0 & -\frac{118}{301} & -\frac{460}{903} \\ -\frac{\sqrt{3}}{9} & -\frac{67\sqrt{3}}{301} & -\frac{302\sqrt{3}}{903} & \frac{2\sqrt{3}}{9} & \frac{24\sqrt{3}}{301} & -\frac{85\sqrt{3}}{903} \\ 0 & \frac{1}{42} & \frac{1}{14} & 0 & \frac{1}{42} & \frac{1}{14} \\ 0 & -\frac{3}{86} & -\frac{9}{86} & 0 & \frac{3}{86} & \frac{9}{86} \end{pmatrix}$$

Second and third rows give coordinates of 6 control points along the vectors $(\operatorname{Re}\vec{v}_1, \operatorname{Im}\vec{v}_2)$. We need to check if there is a point with coordinates $(\cdot, 0, 0, \cdot, \cdot)$ in the convex hull. Any point of the convex hull can be expressed as a weighted sum of hull vertices. Thus our problem can be restated as follows: find weights $(\alpha_0, \alpha_1, \alpha_2, \alpha_3, \alpha_4, \alpha_5)$ and coordinates $(\beta_0, \beta_3, \beta_4)$ subject to constraints $\sum\limits_{i=0}^{5} \alpha_i = 1$, $\alpha_i \geq 0$ such that

$$\begin{pmatrix} \frac{1}{3} & \frac{1}{3} & \frac{1}{3} & \frac{1}{3} & \frac{1}{3} & \frac{1}{3} \\ -\frac{1}{3} & -\frac{97}{301} & -\frac{271}{903} & 0 & -\frac{118}{301} & -\frac{460}{903} \\ -\frac{\sqrt{3}}{9} & -\frac{67\sqrt{3}}{301} & -\frac{302\sqrt{3}}{903} & \frac{2\sqrt{3}}{9} & \frac{24\sqrt{3}}{301} & -\frac{85\sqrt{3}}{903} \\ 0 & \frac{1}{42} & \frac{1}{14} & 0 & \frac{1}{42} & \frac{1}{14} \\ 0 & -\frac{3}{86} & -\frac{9}{86} & 0 & \frac{3}{86} & \frac{9}{86} \end{pmatrix} \times \begin{pmatrix} \alpha_0 \\ \alpha_1 \\ \alpha_2 \\ \alpha_3 \\ \alpha_4 \\ \alpha_5 \end{pmatrix} = \begin{pmatrix} \beta_0 \\ 0 \\ 0 \\ \beta_3 \\ \beta_4 \end{pmatrix}.$$

The second row of the linear system implies $\alpha_0 = \alpha_1 = \alpha_2 = \alpha_4 = \alpha_5 = 0$ and therefore from the third row we have $\alpha_3 \frac{2\sqrt{3}}{9} = 0 \Rightarrow \alpha_3 = 0$. This is incompatible with the constraint $\sum\limits_{i=0}^{5} \alpha_i = 1$ and thus the convex hull does not include points with coordinates $(\cdot, 0, 0, \cdot, \cdot)$.

So, the conditions of the lemma 2 are verified and the plane spanned by the vectors $(\operatorname{Re}\vec{v}_1, \operatorname{Im}\vec{v}_2)$ is indeed a tangent plane. To better illustrate the existence of such a plane, the right-hand image of figure 4.12 shows the suitcase corner subdivision. The studied curve (present 3 times) is highlighted in the limit surface. Any secant s^i will rotate infinitely around the fixed point of T_i, converging to the plane.

Null component problem

Here we are going to study a pair of IFS that share a common transformation. We are going to show that it is possible to obtain different tangents at the fixed point of the common transformation to the different attractors.

Let us consider two IFS $\{T_1, T_2\}$ and $\{T_1, T_2'\}$ and their attractors $\mathcal{A}$ and $\mathcal{A}'$. Let

$$T_1 = \begin{pmatrix} 1/2 & 0 & 0 \\ 0 & 1/4 & 0 \\ 0 & 0 & 1 \end{pmatrix}, \; T_2 = \begin{pmatrix} 1/2 & 0 & 0 \\ 0 & 3/4 & 1/4 \\ 0 & 0 & 1 \end{pmatrix}, \; T_2' = \begin{pmatrix} 1/2 & 0 & \epsilon/2 \\ 0 & 3/4 & 1/4 \\ 0 & 0 & 1 \end{pmatrix}.$$

Please note that here were express affine transformations on $\mathbb{R}^2$ as linear transformation in $\mathbb{R}^3$ via homogeneous coordinates.

The respective attractors are presented in figure 4.13. Two attractors share a common point — the fixed point of T_1. However they have different tangents at this common point.

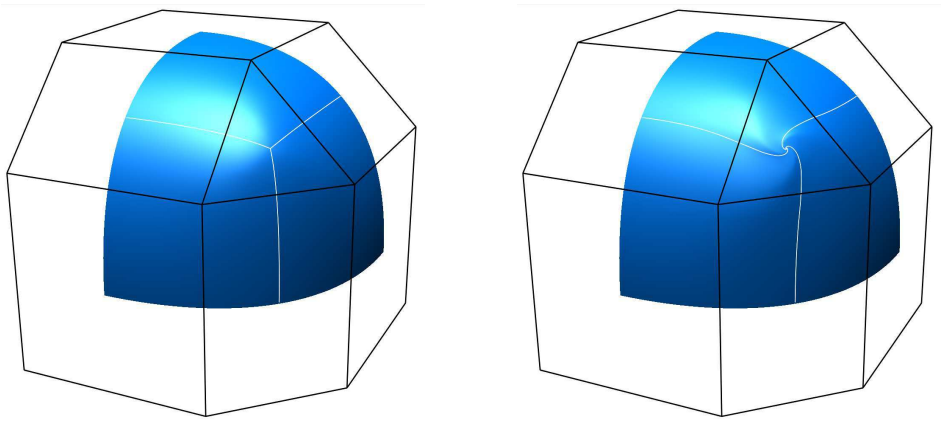

Figure 4.12: Left-hand image: Doo-Sabin subdivision scheme applied on the suitcase corner mesh; right-hand image: the subdivision with modified weights, the studied curves (patch borders) are highlighted.

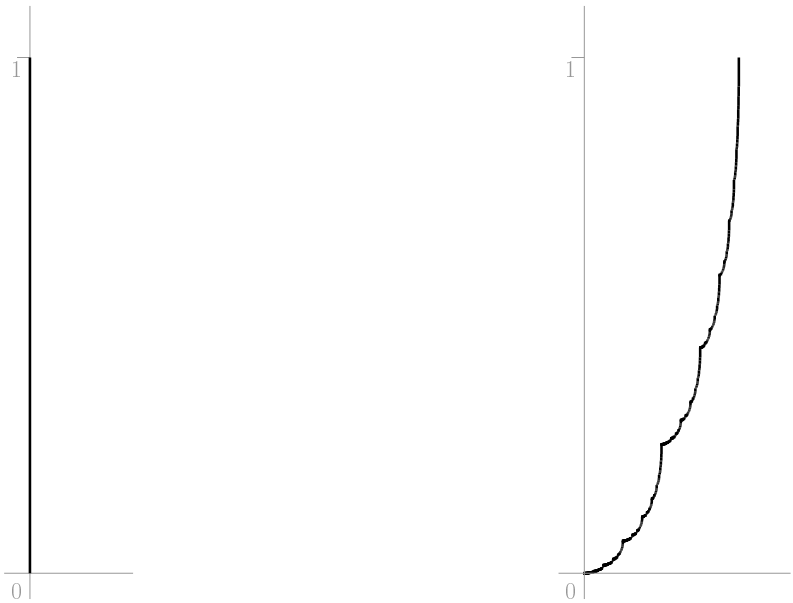

Figure 4.13: Left: attractor of the IFS $\{T_1, T_2\}$; right: attractor of $\{T_1, T_2'\}$. Even if both IFS share the transformation T_1, the tangents are different at the origin.

Previously we showed the possible tangent at the fixed point are eigenvectors of the respective transformation. The eigenvalues of T_1 are $\lambda_1 = 1/4$ and $\lambda_2 = 1/2$. The respective eigenvectors are $(1, 0)$ and $(0, 1)$.

First let us study the tangent of $\mathcal{A}$ at the fixed point $(0, 0)$. We are going to show that there is no points $x \in \mathcal{A}$ such that is has a non-zero component corresponding to the

sub-dominant eigenvector of T_1. If we consider a set of points with addresses that end in $(1)^\omega$ or $(2)^\omega$ we get a everywhere dense subset of the attractor [Bar88, Theorem 2.4]. Points with addresses that end in $(1)^\omega$ or $(2)^\omega$ can be obtained from the fixed points of T_1 and T_2 by applying some combination of transformations T_1 and T_2. So if we show that both fixed points of T_1 and T_2 have a zero component for the sub-dominant eigenvector we could prove that all the points in $\mathcal{A}$ have a zero component. Therefore all points in R_0 have a zero component and according to lemma 7 the tangent corresponds to the second sub-dominant eigenvector $(0, 1)$. The fixed point of T_1 is $(0, 0)$ while the fixed point T_2 is $(1, 0)$. Indeed:

$$T_1(0, 0) = (0, 0), T_2(1, 0) = (1, 0).$$

Since both for fixed points have first coordinate of their eigenbasis decomposition is equal to zero, we can conclude that the tangent to $\mathcal{A}$ at the point $(0, 0)$ is given by the second sub-dominant eigenvector $(0, 1)$.

Now we study the tangent of $\mathcal{A}'$ at $(0, 0)$. To show that the tangent for this attractor at the fixed point of T_1 is given by the respective sub-dominant eigenvector we are going to show that no point of R_0 has a zero component corresponding to the sub-dominant eigenvector. For that we are going to calculate a rectangular box that contains R_0. From that is easy to demonstrate that no point of R_0 has the undesired zero component. First let us calculate fixed point of T_2:

$$T_2(fix_2) = fix_2, fix_2 = (\epsilon, 1).$$

Note that all the eigenvalues of T_1 and T_2 are positive. This implies that $\mathcal{A}'$ is bounded by the rectangle with fixed points of T_1 and T_2 as two of the four vertices. So no point in $\mathcal{A}'$ has a strictly greater coordinates than the fixed point of T_2. So since $R_0 = \mathcal{A}' \setminus T_1(\mathcal{A}')$ we can conclude that R_0 is bounded by the rectangle with fix_2 and $T_1(fix_2)$. Since fix_2 has a non-zero sub-dominant component in the eigenbasis decomposition so does $T_1(fix_2)$. Therefore so do all point in R_0. So according to the theorem 2 the tangent corresponds to the first sub-dominant eigenvector $(1, 0)$.

We want to note that despite the fact that for both attractors, the rings around the point $(0, 0)$ are transformed with the same transformation T_1, the resulting differential behaviour is different because of the difference in the position of the outer rings.

Takagi curve

In this paragraph we are going to show how our theoretical results apply to such a well-known attractor as the Takagi curve. The Takagi curve is an example of an IFS with an operator that does not have a complete set of eigenvectors (see figure 4.14).

For Takagi curve we chose to use 4 control points (one for each vertex of the rectangle it is projected into) (see figure 4.14). In BI^4 the Takagi curve is an attractor of the following IFS:

$$T_1 = \begin{pmatrix} 1 & 1/2 & 0 & 1/4 \\ 0 & 1/2 & 1/2 & 1/4 \\ 0 & 0 & 1/2 & 1/4 \\ 0 & 0 & 0 & 1/4 \end{pmatrix}, \; T_2 = \begin{pmatrix} 1/4 & 0 & 0 & 0 \\ 1/4 & 1/2 & 0 & 0 \\ 1/4 & 1/2 & 1/2 & 0 \\ 1/4 & 0 & 1/2 & 1 \end{pmatrix}.$$

Let us study the tangent at the fixed point of T_1. Transformation T_1 has three different eigenvalues $1, 1/2, 1/4$ with $1/2$ being a double eigenvalue. Here are the corresponding

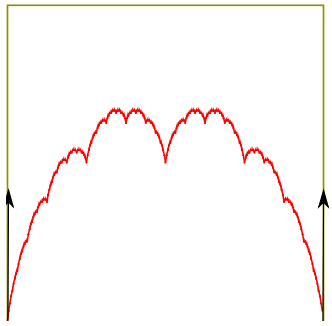

Figure 4.14: The Takagi curve is an attractor of an IFS without a complete set of eigenvectors.

eigenvectors:

$$\vec{v}_0 = \begin{pmatrix} 1 \\ 0 \\ 0 \\ 0 \end{pmatrix}, \vec{v}_1 = \begin{pmatrix} 0.5 \\ -0.5 \\ 0 \\ 0 \end{pmatrix}, \vec{v}_2 = \begin{pmatrix} 1 \\ -1 \\ 1 \\ -1 \end{pmatrix}.$$

We need one generalise eigenvector to obtain a complete basis:

$$\vec{v}_1^1 = \begin{pmatrix} 1 \\ 0 \\ -1 \\ 0 \end{pmatrix}.$$

To show that the sub-dominant eigenvector gives the tangent we need to verify, that R_0 for the fixed point of T_1 does not have any point with null components corresponding to the generalised eigenvector $\vec{v}_1^1$. To verify this we are going to calculate the control polygon for R_0.

Now we can calculate the control polygon for R_0 using the same method as before.

$$S = \begin{pmatrix} 1 & 1 & 1/2 & 1 \\ 0 & -1 & -1/2 & 0 \\ 0 & 1 & 0 & -1 \\ 0 & -1 & 0 & 0 \end{pmatrix}, \; S^{-1} = \begin{pmatrix} 1 & 1 & 1 & 1 \\ 0 & 0 & 0 & -1 \\ 0 & -2 & 0 & 2 \\ 0 & 0 & -1 & -1 \end{pmatrix}.$$

So the vertices of the control polygon for R_0 in the basis of generalised eigenvectors are as follows:

$$S^{-1} \times T_2 = \begin{pmatrix} 1 & 1 & 1 & 1 \\ -1/4 & 0 & -1/2 & -1 \\ 0 & -1 & 1 & 2 \\ -1/2 & -1/2 & -1 & -1 \end{pmatrix}$$

. Note that the fourth component for all four vertices is negative. Therefore there is no point in R_0 with a zero component corresponding to the generalised eigenvector $\vec{v}_1^1$. So the tangent at the fixed point of T_1 is given by the sub-dominant eigenvector $\vec{v}_1$. Thus

the tangent passes through the first and second control points. If we project the attractor from BI^4 into the unit square using the vertices of the square as control points we obtain a vertical tangent (see figure 4.14).

Since the curve is symmetric the half-tangent at the other endpoint is given by the third and fourth control points.

4.9.2 Surfaces

Null components

In this section we consider an example of a surface where the null component problem discussed before leads to a peculiar differential behaviour. Consider a quadrangular surface

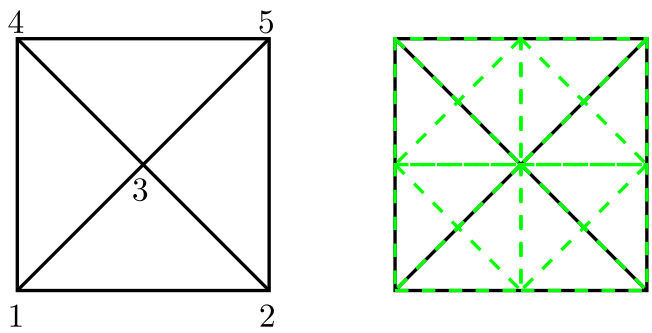

Figure 4.15: One step of the pyramidal subdivision. One patch with 5 control points is subdivided into 4 patches. Each pair of new patches share 2 edge control points.

subdivision with 5 control points. Let each of the 4 vertices depend only on 1 control point. Let each edge depend on two control points corresponding to its vertices. Finally, let the last control point influence the interior of the surface, but not the vertices or edges. This subdivision is represented in figure 4.15. Here are the corresponding matrices:

$$T_1 = \begin{pmatrix} 1 & 1/2 & 0 & 1/2 & 2/3 \\ 0 & 1/2 & 0 & 0 & 0 \\ 0 & 0 & 0 & 0 & 0 \\ 0 & 0 & 0 & 1/2 & 0 \\ 0 & 0 & 1 & 0 & 1/3 \end{pmatrix}, \; T_2 = \begin{pmatrix} 1/2 & 0 & 0 & 0 & 0 \\ 1/2 & 1 & 1/2 & 0 & 2/3 \\ 0 & 0 & 1/2 & 0 & 0 \\ 0 & 0 & 0 & 0 & 0 \\ 0 & 0 & 0 & 1 & 1/3 \end{pmatrix},$$

$$T_3 = \begin{pmatrix} 0 & 0 & 0 & 0 & 0 \\ 0 & 1/2 & 0 & 0 & 0 \\ 0 & 1/2 & 1 & 1/2 & 2/3 \\ 0 & 0 & 0 & 1/2 & 0 \\ 1 & 0 & 0 & 0 & 1/3 \end{pmatrix}, \; T_4 = \begin{pmatrix} 1/2 & 0 & 0 & 0 & 0 \\ 0 & 0 & 0 & 0 & 0 \\ 0 & 0 & 1/2 & 0 & 0 \\ 1/2 & 0 & 1/2 & 1 & 2/3 \\ 0 & 1 & 0 & 0 & 1/3 \end{pmatrix}.$$

Let us consider the differential behaviour at the fixed point of T_1. If we compute the eigenvalues and eigenvectors we obtain the following:

$$\lambda_0 = 1, \; \lambda_1 = 1/2, \; \lambda_2 = 1/2, \; \lambda_3 = 1/3, \; \lambda_4 = 0$$

and

$$\vec{v}_0 = \begin{pmatrix}1\\0\\0\\0\\0\end{pmatrix},\ \vec{v}_1 = \begin{pmatrix}1\\0\\0\\-1\\0\end{pmatrix},\ \vec{v}_2 = \begin{pmatrix}0\\1\\0\\-1\\0\end{pmatrix},\ \vec{v}_3 = \begin{pmatrix}1\\0\\0\\0\\-1\end{pmatrix},\ \vec{v}_4 = \begin{pmatrix}1\\0\\1/2\\0\\-3/2\end{pmatrix}.$$

Here we have two sub-dominant eigenvectors. However let us consider the fifth control point that we denote as c_5. The fixed point of T_1 denoted as p obviously belongs to the attractor. So does the c_5 since

$$T_3(p) = c_5.$$

Should we consider the vector $\vec{pc}_5$ in the eigenbasis decomposition we obtain:

$$c_5 - p = -\vec{v}_3.$$

So we have found a point that has a null components that correspond to the sub-dominant eigenspace (vector $-\vec{v}_3$ is linearly independent from $\vec{v}_1$ and $\vec{v}_2$). This means that a sequence of secants that pass through points p and $T^n(c_5)$ does not converge to $\mathrm{span}(\vec{v}_1, \vec{v}_2)$. In fact it converges to $\mathrm{span}(\vec{v}_3)$. So we obtain three geometrical "edges" on the surface: two of them correspond to the sub-dominant eigenvectors $\vec{v}_1,\ \vec{v}_2$ and the third corresponds to the $\vec{v}_3$ (see figure 4.16.)

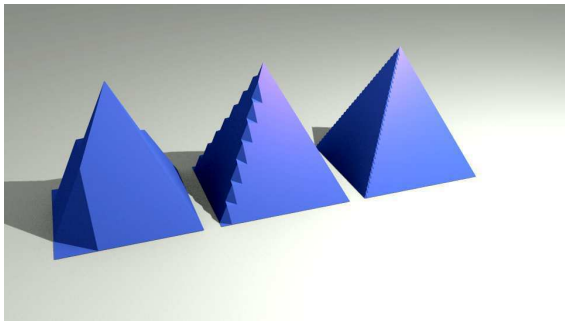

Figure 4.16: Three different iterations of pyramidal surface.

Takagi tensor product

In this section we study an IFS obtained by tensor product of two Takagi curves. We take two identical IFS from one of the previous sections:

$$\mathbb{T} = \{T_1, T_2\},\ \mathbb{T}' = \{T_1, T_2\},$$

where

$$T_1 = \begin{pmatrix}1 & 1/2 & 0 & 1/4\\0 & 1/2 & 1/2 & 1/4\\0 & 0 & 1/2 & 1/4\\0 & 0 & 0 & 1/4\end{pmatrix},\ T_2 = \begin{pmatrix}1/4 & 0 & 0 & 0\\1/4 & 1/2 & 0 & 0\\1/4 & 1/2 & 1/2 & 0\\1/4 & 0 & 1/2 & 1\end{pmatrix}.$$

Now we consider an IFS composed of the pairwise tensor product of T_1 and T_2:

$$\bar{\mathbb{T}} = \mathbb{T} \otimes \mathbb{T}' = \{T_{11}, T_{12}, T_{21}, T_{22}\},$$

where

$$\begin{aligned} T_{11} &= T_1 \otimes T_1, \\ T_{12} &= T_1 \otimes T_2, \\ T_{21} &= T_2 \otimes T_1, \\ T_{22} &= T_2 \otimes T_2. \end{aligned}$$

We want to study the tangent behaviour at one for the four vertices, so let us consider the fixed point of T_{11}. Should we calculate its eigenvalues we obtain:

$$\begin{aligned} &\lambda_0 = 1, \lambda_1 = 1/16, \lambda_2 = 1/2, \lambda_3 = 1/2, \lambda_4 = 1/2, \lambda_5 = 1/2, \lambda_6 = 1/8, \lambda_7 = 1/8, \\ &\lambda_8 = 1/8, \lambda_9 = 1/8, \lambda_{10} = 1/4, \lambda_{11} = 1/4, \lambda_{12} = 1/4, \lambda_{13} = 1/4, \lambda_{14} = 1/4, \lambda_{15} = 1/14. \end{aligned}$$

If we also calculate the matrix of corresponding eigenvectors and generalised eigenvectors we obtain the following matrix:

$$S = \begin{pmatrix}
1 & 1 & 1/2 & 1 & 0 & 0 & 1/4 & 1 & 1/8 & 0 & 1/8 & 1/2 & 1 & 1 & 0 & 0 \\
0 & -1 & 0 & 0 & 1/2 & 0 & -1/4 & 0 & -1/8 & 1 & -1/8 & -1/4 & 0 & 0 & 0 & 0 \\
0 & 1 & 0 & 0 & 0 & 1 & 1/8 & 0 & 0 & 0 & 0 & -1/4 & 0 & 0 & 1 & 0 \\
0 & -1 & 0 & 0 & 0 & 0 & -1/8 & -1 & 0 & -1 & 0 & 0 & 0 & 0 & 0 & 1 \\
0 & -1 & -1/2 & 0 & -1/2 & 0 & -1/4 & 0 & -1/8 & 0 & -1/8 & -1/4 & 0 & -1 & 1 & 0 \\
0 & 1 & 0 & 0 & 0 & 0 & 1/4 & -1 & 1/8 & -1 & 1/8 & 0 & 0 & 0 & -1 & 0 \\
0 & -1 & 0 & 0 & 0 & 0 & -1/8 & 1 & 0 & 0 & 0 & 1/4 & -1 & 0 & -1 & -1 \\
0 & 1 & 0 & 0 & 0 & 0 & 1/8 & 0 & 0 & 1 & 0 & 0 & 0 & 0 & 0 & 0 \\
0 & 1 & 0 & -1 & 0 & -1 & 1/8 & -1 & 1/8 & -1 & 0 & -1/4 & 0 & 1 & 0 & 0 \\
0 & -1 & 0 & 0 & 0 & 0 & -1/8 & 2 & -1/8 & 2 & 0 & 1/4 & 0 & 0 & 1 & 1 \\
0 & 1 & 0 & 0 & 0 & 0 & 0 & -2 & 0 & -1 & 0 & 0 & 1 & 0 & 0 & 0 \\
0 & -1 & 0 & 0 & 0 & 0 & 0 & 1 & 0 & 0 & 0 & 0 & 0 & 0 & 0 & 0 \\
0 & -1 & 0 & 0 & 0 & 0 & -1/8 & 0 & -1/8 & 1 & 0 & 0 & -1 & -1 & -1 & -1 \\
0 & 1 & 0 & 0 & 0 & 0 & 1/8 & -1 & 1/8 & -2 & 0 & 0 & 0 & 0 & 0 & 0 \\
0 & -1 & 0 & 0 & 0 & 0 & 0 & 1 & 0 & 1 & 0 & 0 & 0 & 0 & 0 & 0 \\
0 & 1 & 0 & 0 & 0 & 0 & 0 & 0 & 0 & 0 & 0 & 0 & 0 & 0 & 0 & 0
\end{pmatrix}.$$

Here note that the third and fifth columns are eigenvectors corresponding to the sub-dominant eigenvalues 1/2. With it we can calculate the three polygons which cover the whole R_0:

$$S^{-1} \times T_{12} = \begin{pmatrix}
1 & 1 & 1 & 1 & 1 & 1 & 1 & 1 & 1 & 1 & 1 & 1 & 1 & 1 & 1 & 1 \\
0 & 0 & 0 & 0 & 0 & 0 & 0 & 0 & 0 & 0 & 0 & 0 & 1/16 & 0 & 1/8 & 1/4 \\
0 & -1 & 1 & 2 & -1 & -2 & 0 & 1 & -1 & -2 & 0 & 1 & 0 & -1 & 1 & 2 \\
-1/2 & -1/2 & -1 & -1 & -1/2 & -1/2 & -1 & -1 & -1 & -1 & -3/2 & -3/2 & -1 & -1 & -3/2 & -3/2 \\
0 & 1 & -1 & -2 & 0 & 1 & -1 & -2 & 0 & 1 & -1 & -2 & 0 & 1 & -1 & -2 \\
1/2 & 1/2 & 1 & 1 & 1/2 & 1/2 & 1 & 1 & 1/2 & 1/2 & 1 & 1 & 1/2 & 1/2 & 1 & 1 \\
0 & 0 & 0 & 0 & 1 & 0 & 2 & 4 & 2 & 0 & 4 & 8 & 0 & -1 & 0 & 2 \\
0 & 0 & 0 & 0 & 0 & 0 & 0 & 0 & 1/8 & 0 & 1/4 & 1/2 & 1/8 & 0 & 1/4 & 1/2 \\
0 & 0 & 0 & 0 & -1 & 0 & -2 & -4 & -3 & 0 & -6 & -12 & 1 & 4 & 1 & -4 \\
0 & 0 & 0 & 0 & 0 & 0 & 0 & 0 & -1/8 & 0 & -1/4 & -1/2 & 0 & 1/8 & 0 & -1/4 \\
-2 & 0 & -4 & -8 & -3 & 1 & -8 & -14 & -4 & 1 & -11 & -18 & -3 & 0 & -7 & -12 \\
0 & 0 & 0 & 0 & 1/2 & 1/2 & 1 & 1 & 1 & 3/2 & 3/2 & 1 & 1/2 & 1 & 1/2 & 0 \\
0 & 0 & 0 & 0 & 0 & 0 & 0 & 0 & 1/4 & 1/4 & 1/2 & 1/2 & 1/4 & 1/4 & 1/2 & 1/2 \\
0 & 0 & 0 & 0 & 1/8 & 1/8 & 1/4 & 1/4 & 0 & -1/8 & 1/8 & 1/4 & -3/8 & -1/2 & -3/8 & -1/4 \\
-1/4 & 0 & -1/2 & -1 & -3/8 & -1/8 & -3/4 & -5/4 & -1/2 & -1/8 & -9/8 & -7/4 & -3/8 & 0 & -7/8 & -3/2 \\
1/4 & 0 & 1/2 & 1 & 1/4 & 0 & 1/2 & 1 & 1/4 & 0 & 1/2 & 1 & 1/4 & 0 & 1/2 & 1
\end{pmatrix},$$

$$S^{-1} \times T_{21} = \begin{pmatrix}
1 & 1 & 1 & 1 & 1 & 1 & 1 & 1 & 1 & 1 & 1 & 1 & 1 & 1 & 1 & 1 \\
0 & 0 & 0 & 1/16 & 0 & 0 & 0 & 0 & 0 & 0 & 0 & 1/8 & 0 & 0 & 0 & 1/4 \\
0 & -1 & -1 & 0 & -1 & -2 & -2 & -1 & 1 & 0 & 0 & 1 & 2 & 1 & 1 & 2 \\
-1/2 & -1/2 & -1 & -1 & -1/2 & -1/2 & -1 & -1 & -1 & -1 & -3/2 & -3/2 & -1 & -1 & -3/2 & -3/2 \\
0 & 1 & 1 & 0 & 0 & 1 & 1 & 0 & 0 & 1 & 1 & 0 & 0 & 1 & 1 & 0 \\
0 & 0 & 1/2 & 1/2 & 0 & 0 & 1/2 & 1/2 & 0 & 0 & 1/2 & 1/2 & 0 & 0 & 1/2 & 1/2 \\
0 & 0 & -1 & 0 & 0 & 0 & 0 & 2 & 0 & 0 & -2 & -1 & 0 & 0 & -4 & -4 \\
0 & 0 & 0 & 1/8 & 0 & 0 & 0 & 1/8 & 0 & 0 & 0 & 1/4 & 0 & 0 & 0 & 1/4 \\
0 & 1 & 4 & 1 & 0 & 0 & 0 & -3 & 0 & 2 & 8 & 3 & 0 & 4 & 16 & 10 \\
0 & 0 & 1/8 & 0 & 0 & 0 & 0 & -1/8 & 0 & 0 & 1/4 & 0 & 0 & 0 & 1/2 & 1/4 \\
0 & 1 & 0 & -3 & 0 & 3 & 1 & -4 & 0 & 0 & -1 & -3 & 0 & -2 & -2 & -2 \\
0 & 1/2 & 1 & 1/2 & 0 & 1/2 & 3/2 & 1 & 0 & 1 & 3/2 & 1/2 & 0 & 1 & 1 & 0 \\
0 & 0 & 1/4 & 1/4 & 0 & 0 & 1/4 & 1/4 & 0 & 0 & 1/2 & 1/2 & 0 & 0 & 1/2 & 1/2 \\
-1/4 & -3/8 & -1/2 & -3/8 & 0 & -1/8 & -1/8 & 0 & -1/2 & -3/4 & -9/8 & -7/8 & -1 & -5/4 & -7/4 & -3/2 \\
0 & 1/8 & 0 & -3/8 & 0 & 1/8 & -1/8 & -1/2 & 0 & 1/4 & 1/8 & -3/8 & 0 & 1/4 & 1/4 & -1/4 \\
0 & 0 & 0 & 1/4 & 0 & 0 & 0 & 1/4 & 0 & 0 & 0 & 1/4 & 0 & 0 & 0 & 1/4
\end{pmatrix},$$

$$S^{-1} \times T_{22} = \begin{pmatrix}
1 & 1 & 1 & 1 & 1 & 1 & 1 & 1 & 1 & 1 & 1 & 1 & 1 & 1 & 1 & 1 \\
1/16 & 0 & 1/8 & 1/4 & 0 & 0 & 0 & 0 & 1/8 & 0 & 1/4 & 1/2 & 1/4 & 0 & 1/2 & 1 \\
0 & -1 & 1 & 2 & -1 & -2 & 0 & 1 & 1 & 0 & 2 & 3 & 2 & 1 & 3 & 4 \\
-1 & -1 & -3/2 & -3/2 & -1 & -1 & -3/2 & -3/2 & -3/2 & -3/2 & -2 & -2 & -3/2 & -3/2 & -2 & -2 \\
0 & 1 & -1 & -2 & 0 & 1 & -1 & -2 & 0 & 1 & -1 & -2 & 0 & 1 & -1 & -2 \\
1/2 & 1/2 & 1 & 1 & 1/2 & 1/2 & 1 & 1 & 1/2 & 1/2 & 1 & 1 & 1/2 & 1/2 & 1 & 1 \\
0 & -1 & 0 & 2 & 2 & 0 & 4 & 8 & -1 & -2 & -2 & 0 & -4 & -4 & -8 & -8 \\
1/8 & 0 & 1/4 & 1/2 & 1/8 & 0 & 1/4 & 1/2 & 1/4 & 0 & 1/2 & 1 & 1/4 & 0 & 1/2 & 1 \\
1 & 4 & 1 & -4 & -3 & 0 & -6 & -12 & 3 & 8 & 4 & -4 & 10 & 16 & 16 & 8 \\
0 & 1/8 & 0 & -1/4 & -1/8 & 0 & -1/4 & -1/2 & 0 & 1/4 & 0 & -1/2 & 1/4 & 1/2 & 1/2 & 0 \\
-3 & 0 & -7 & -12 & -4 & 1 & -11 & -18 & -3 & -1 & -6 & -10 & -2 & -2 & -2 & -4 \\
1/2 & 1 & 1/2 & 0 & 1 & 3/2 & 3/2 & 1 & 1/2 & 3/2 & 0 & -1 & 0 & 1 & -1 & -2 \\
1/4 & 1/4 & 1/2 & 1/2 & 1/4 & 1/4 & 1/2 & 1/2 & 1/2 & 1/2 & 1 & 1 & 1/2 & 1/2 & 1 & 1 \\
-3/8 & -1/2 & -3/8 & -1/4 & 0 & -1/8 & 1/8 & 1/4 & -7/8 & -9/8 & -1 & -3/4 & -3/2 & -7/4 & -7/4 & -3/2 \\
-3/8 & 0 & -7/8 & -3/2 & -1/2 & -1/8 & -9/8 & -7/4 & -3/8 & 1/8 & -1 & -7/4 & -1/4 & 1/4 & -3/4 & -3/2 \\
1/4 & 0 & 1/2 & 1 & 1/4 & 0 & 1/2 & 1 & 1/4 & 0 & 1/2 & 1 & 1/4 & 0 & 1/2 & 1
\end{pmatrix}.$$

Note that for all vertices of all the polygons among the components corresponding to the sub-dominant chains there is always a non-zero component. Therefore we obtain a tangent plane spanned by two sub-dominant eigenvectors (see figure 4.17). However if we project the attractor into a "cube" (by merging pairs of respective control points) then two sub-dominant eigenvectors are projected onto the one edge of the cube. So the tangent plane collapses into a tangent line. This way we obtain a surface commonly known as the Takagi surface (see figure 4.18).

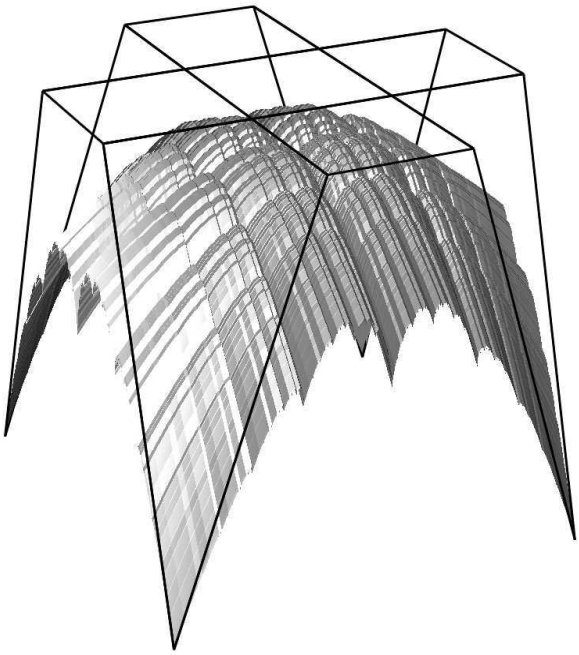

Figure 4.17: Tensor product of Takagi curves defined in the barycentric space BI^{16}.

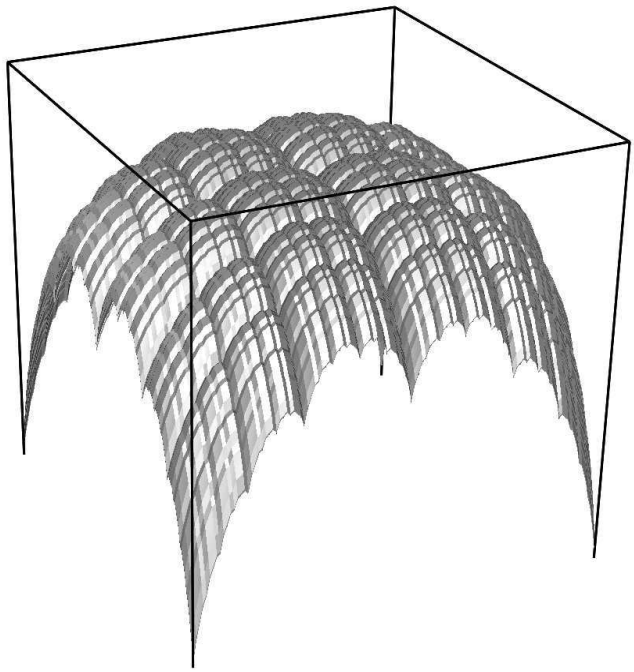

Figure 4.18: The tensor product of Takagi curves projected into the cube gives the same surface as the product of two classical 2D curves. Note that the surface does not have tangent planes but tangent lines at the corners.

4.9.3 Surfaces as tensor product of curves

In the previous example we calculated the tangent plane at one of the corners of the surface obtained as the tensor product of two Takagi curves. The computations were straightforward but cumbersome. In this section we show how to use the fact that the surface is obtained as the tensor product to find the same result more easily.

Generalised eigenvectors and tensor product of curves

Let us we consider two different curves defined by two different Barycentric IFS. From the operators on the initial curve we can construct a set of operators that will define a continuous surface in a barycentric space (its dimension is a product of the initial curves dimension), such that the edges of the surface are initial curves. To obtain said set of operators we take pairwise tensor products of the operators of initial curves. This was described in details in [ZT96]. It was also shown that this method produces continuous surfaces from continuous curves. The operators obtained by tensor product are contracting on the barycentric space, since they can be expressed as a sum of sums of initial matrix elements (which sums up to one) multiplied by a coefficient, which also sums up to one. The IFS formed with the resulting operators will define a continuous surface. Using the properties of the tensor product we can analyse the differential behaviour of the resulting surface.

Property 3. *The eigenvalues of the product are pairwise products of the operands eigenvalues.*

Lets consider two subdivision operators A, B defined on two different barycentric spaces of dimension n and m respectively. Since both operands have an eigenvalue equal to 1, the eigenvalues of the product will include the eigenvalues 1, all the eigenvalues of both operands that are smaller than 1 and all pairwise products of the eigenvalues with absolute value that is less than 1. All the pairwise products have smaller absolute values than individual eigenvalues of the operands. Hence the sub-dominant eigenvalue of the product is equal to the sub-dominant eigenvalue of one of the operands. If the operands have equal sub-dominant eigenvalues then the product will have a double sub-dominant eigenvalue.

Property 4. *The tensor product of eigenvectors is an eigenvector of the product which corresponds to the eigenvalue equal to the product of the initial eigenvalues.*

Proof. Consider the following:

$$(A - \lambda E)x = 0, (B - \mu E)y = 0.$$

Then

$$(A \otimes B)(x \otimes y) = Ax \otimes B = \lambda x \otimes \mu y = \lambda\mu(x \otimes y)$$

Therefore $x \otimes y$ is a eigenvector with an eigenvalue $\lambda\mu$. □

This property however does not hold for generalised eigenvectors, except for the special case of eigenvalue 1. Consider the following generalised eigenvectors:

$$(A - \lambda E)x' = x$$

Then

$$(A \otimes B)(x' \otimes y) = Ax` \otimes By = (x + \lambda x') \otimes \mu y = x \otimes \mu y + \lambda x' \otimes \mu y.$$

Now if $\mu = 1$ then

$$(A \otimes B)(x' \otimes y) = (x \otimes y + \lambda x' \otimes y).$$

So we have a chain of eigenvectors $x \otimes y, x' \otimes y$ corresponding to the eigenvalue λ. We can generalise this to chains of any order since we started with the equation $(A - \lambda E)x' = x$, that describes the relation between any two neighbouring eigenvectors of the chain. Therefore if an operand has a chain of generalised eigenvectors corresponding to its eigenvalue, then the product will have a chain of the same length corresponding to the respective eigenvalue.

Tensor product and null components

Let us consider two projected IFS $\mathbb{T} = \{T_1, T_2\}$ and $\mathbb{T}' = \{T_1', T_2'\}$, where the transformations operate on $\mathbb{R}^n$ and $\mathbb{R}^m$ respectively. We denote their attractors as $\mathcal{A}$ and $\mathcal{A}'$ respectively. Now we consider the tensor product of these IFS $\mathbb{T} \otimes \mathbb{T}'$ and its attractor $\mathcal{A}^{\otimes} = \mathcal{A} \otimes \mathcal{A}'$. Any vector $x \otimes y \in \mathcal{A}^{\otimes}$ corresponds to a pair (x, y) such that $x \in \mathcal{A}$ and $y \in \mathcal{A}'$. Let $x \otimes y$ be a fixed point of $T_{11} = T_1 \otimes T_1'$. Then x is the fixed point of T_1 and y is the fixed point of T_1'. Consider the first ring around $x \otimes y$ that we denote by $R_0^{\otimes}$:

$$R_0^{\otimes} := T_{12}(\mathcal{A}^{\otimes}) \cup T_{21}(\mathcal{A}^{\otimes}) \cup T_{22}(\mathcal{A}^{\otimes}).$$

Let us also consider the first rings around x and y in their respective attractors:

$$R_0 = T_2(\mathcal{A}),$$

$$R_0' = T_2'(\mathcal{A}').$$

See figure 4.19.

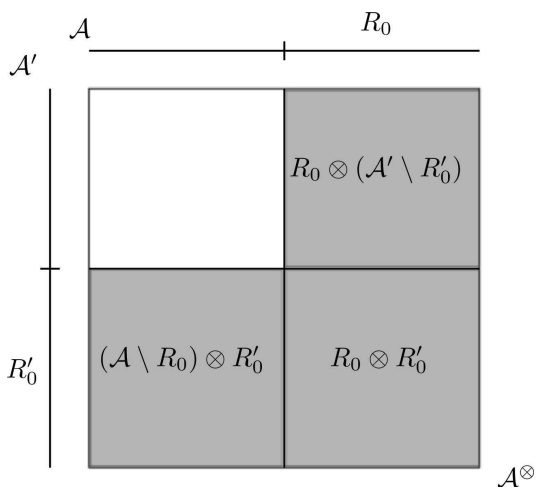

Figure 4.19: A schematic representation of a ring on a tensor product of curves.

From this figure we can deduce the following relation between R_0, R_0' and $R_0^{\otimes}$:

$$R_0^{\otimes} = (R_0 \otimes R_0') \cup (R_0 \otimes (\mathcal{A}' \setminus R_0')) \cup (R_0' \otimes (A \setminus R_0)).$$

In other words $x \otimes y$ belongs to $R_0^{\otimes}$ as long as either $x \in R_0$ or $y \in R_0'$.

Suppose that $(\vec{e}_0, \ldots, \vec{e}_n)$ and $(\vec{u}_0, \ldots, \vec{u}_m)$ are the eigenvectors of T_1 and T_1' ordered by the absolute value of the corresponding eigenvalues.

Then $x = \vec{e}_0 + \sum_{i=1}^{n} x_i \vec{e}_i$, $y = \vec{u}_0 + \sum_{i=1}^{n} y_i \vec{u}_i$ and

$$x \otimes y = \vec{e}_0 \otimes \vec{u}_0 + x_1(\vec{e}_1 \otimes \vec{u}_0) + y_1(\vec{e}_0 \otimes \vec{u}_1) + \sum_{i,j \geq 2}^{i,j \leq n} x_i y_j (\vec{e}_i \otimes \vec{u}_j).$$

Let us suppose the following:

$$\forall x \in R_0 \ x_1 \neq 0,$$

$$\forall y \in R_0' \ y_1 \neq 0.$$

Or in other words no point in either R_0 or R_0' has a zero components along the corresponding sub-dominant eigenvector. Then any point $x \otimes y \in R_0^{\otimes}$ has at least one non-zero coordinate corresponding to the eigenvectors $\vec{e}_0 \otimes \vec{u}_1$ or $\vec{e}_1 \otimes \vec{u}_0$. If the sub-dominant eigenvalues of T_1 and T_1' are equal, then the eigenvalues that correspond to $\vec{e}_0 \otimes \vec{u}_1$ and $\vec{e}_1 \otimes \vec{u}_0$ are also equal. In that case the tangent sub-space at the fixed point of T_{11} is spanned by these vectors.

4.10 Conclusion

In this chapter we have given a definition of a tangent subspace that generalises the notion of a tangent line and plane. We also have defined the notion of a rings: a set of nested neighbourhoods of a point on an attractor using the notion of a point's address. We have derived the necessary and sufficient conditions for the existence of a tangent subspace at a point with periodic addresses. These conditions show the relation between the eigenvector and eigenvalues of a transformation and the differential behaviour of an attractor at the fixed point of that transformation. In chapter 5 we are going to deal with the problem of constructing a junction between different curves and surfaces and we will use these conditions to analyse the differential behaviour of the constructed shapes.

Chapter 5

Joining shapes

In this chapter we consider the problem of constructing an intermediate shape between two different shapes defined with iterative processes. In many aspects this problem is similar to joining different subdivision schemes that arise quite often in subdivision modelling. Subdivision schemes are tailored only to work on specific mesh configurations, such as quad meshes for the Catmull-Clarck scheme or triangle meshes for the Loop scheme. But different subdivision schemes produce surfaces with different visual properties. So it maybe beneficial to be able to define different parts of the shape with different types of subdivisions. Thus there arises the need to join shapes defined with different subdivision schemes.

The first part of this chapter is dedicated to constructing an intermediate curve between two curves. We use the BCIFS formalism to define the intermediate curve as an attractor, that has the same type of vertex subdivision as the initial curves. Such approach allows the connection of the initial curves with the intermediate one. Then we study the differential properties of the newly constructed curve. After that we provide modifications to the basic automaton to provide a more direct and user-friendly control over the shape of the intermediate curve. Finally we give some examples using the proposed method.

In the second part of this chapter we discuss the construction of the intermediate surface between two surfaces. This study is limited to quad patches, but a similar approach can be taken to deal with other types of surfaces. Please note that quad patches refers to the surfaces patches with four edges and four vertices, and not to the surfaces defined as a limit of a subdivision scheme on a quad mesh. Here we follow the same steps as for curves. We describe a subdivision of the intermediate surface and derive the continuity constraints. Then we analyse the differential properties of the new surface using the method described in chapter 4. After that we modify the basic automaton in a specific way to provide a more straightforward way of controlling the differential properties of the junction. Finally we give some examples of connecting well-known subdivision schemes as well as fractal surfaces.

5.1 Joining curves

5.1.1 Constructing the intermediate curve

In this section we are going to use the BCIFS formalism to describe a set of two curves and construct a third curve between them. We start with a BCIFS for two disjoint curves (see figure 5.1) and build a joining curve between the right endpoint of the left curve and the left endpoint of the right curve. The initial BCIFS consists of 5 states: one state corresponding to the modelling space $\natural$, two states corresponding respectively to the initial curves l and r and two states for their respective vertices v^l and v^r. P^l and P^r are the vectors of control

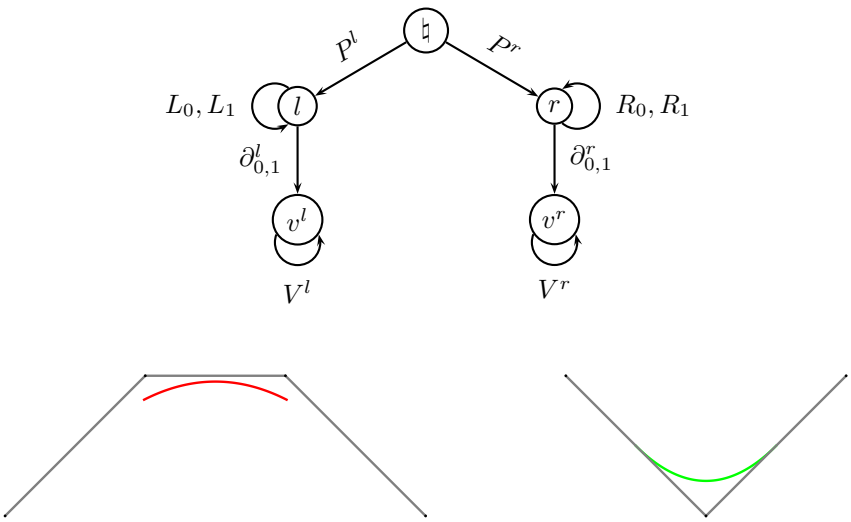

Figure 5.1: Top: initial BCIFS. Each branch of the automaton corresponds to an initial curve. Bottom: Possible attractor of that BCIFS: two B-splines of different degrees.

points for the initial curves. L_0, L_1 and R_0, R_1 are the subdivision operators for their respective curves and $\partial^l_{0,1}$ and $\partial^r_{0,1}$ are the boundary operators. We denote the barycentric space for any state s as BI^s and the dimensions of BI^{v^l} and BI^{v^l} as n_l and n_r respectively.

The intermediate curve

Now for the purpose of building a joining curve we add an intermediate state i and three new transitions T^l, T^r, P^i as well as vertex states v^{il}, v^{ir} and their respective boundary operators $\partial^i_0, \partial^i_1$(see figure 5.2). At this point our intermediate curve is not yet a curve, but two disjoint images of the initial curves placed somewhere in the modelling space (by applying $T^l P^i$ and $T^r P^i$ respectively), but we will introduce conditions on transitions T^l, T^i and P^i so that the new curves become a continuation of our initial curves. To do that we need to determine the dimension of BI^i (i.e. how many control points the intermediate curve depends on) and therefore the dimensions of T^l and T^r. We know that the endpoints of the initial curves respectively depend on n_l and n_r control points. As we seek the way to

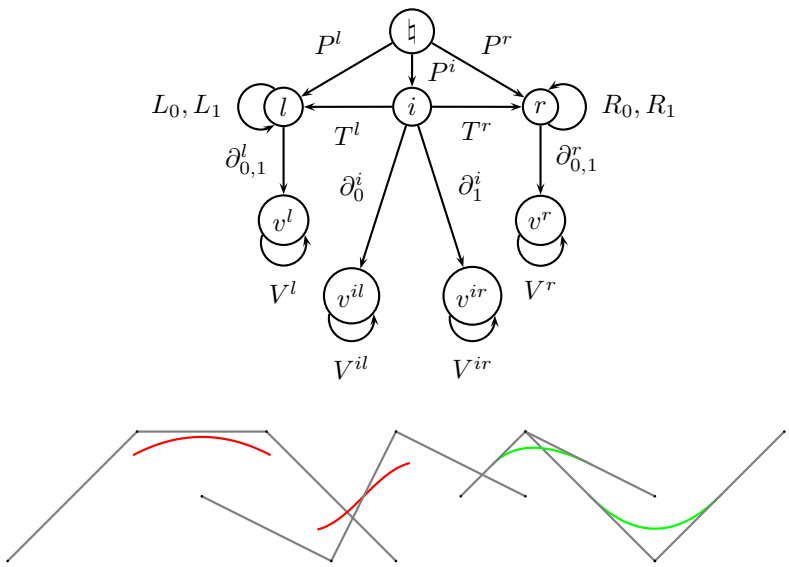

Figure 5.2: Top: modified BCIFS, with an intermediate state i and additional transitions leading to and from it. Bottom: The attractor of this BCIFS: two initial curves and their two copies.

connect those points with our intermediate curve, it has to be controlled by at least $n_l + n_r$ control points.

The necessity to join the intermediate curve to the initial curves means that the left vertex of the intermediate curve must be equal to the right vertex of the left curve. It provides the following equations:

$$v^l = v^{il}$$

$$V^l = V^{il}$$

Similar equations have to be held true for the right curve:

$$v^r = v^{ir}$$

$$V^r = V^{ir}$$

To derive the other conditions we use the graph depicting the unfolding of the automaton. It is presented in figure 5.3. Note that state v^{il} is merged with v^l as well as v^{ir} is merged with v^r. The constraints for the left-hand part of the curve can be written as follows:

$$P^i \partial^i_0 = P^l \partial^l_1 \tag{5.1}$$

$$T^l \partial^l_0 = \partial^i_0 V^l \tag{5.2}$$

$$\partial^l_1 V^l = L_1 \partial^l_1 \tag{5.3}$$

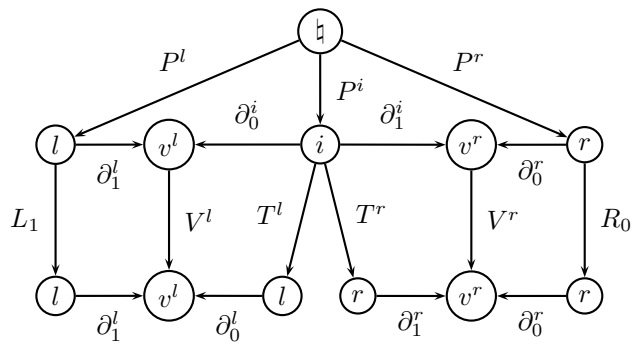

Figure 5.3: Unfolding of the automaton from figure 5.2.

Analogous conditions can be written down for the right-hand part:

$$P^i \partial_1^i = P^r \partial_0^r \tag{5.4}$$

$$T^r \partial_1^r = \partial_1^i V^r \tag{5.5}$$

$$\partial_0^r V^r = R_0 \partial_0^r \tag{5.6}$$

The equations (5.2),(5.3),(5.5) and (5.6) fixate n_l leftmost columns for T^l and n_r rightmost columns for T^r:

$$T^L = \begin{pmatrix} V^l & \\ 0 & \mathrm{X} \end{pmatrix},$$

$$T^R = \begin{pmatrix} \mathrm{Y} & 0 \\ & V^r \end{pmatrix}.$$

Here V^l and V^r are blocks equal to the respective vertex subdivisions, while X and Y consists of arbitrary columns, such that the sum of the all elements for each column is equal to 1.

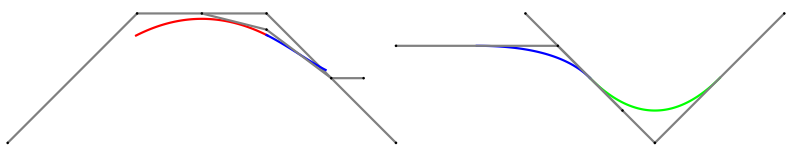

Figure 5.4: Possible attractor of the automaton from figure 5.2 with adjacency and incidence constraints in place. Two initial curves and two segment of the new intermediate curve are connected pairwise.

At this point the BCIFS presented in figure 5.2 plus the aforementioned conditions still yield us a disjoint curve (see figure 5.4). But if we keep the X and Y blocks of T^l and T^r

within certain bounds, we can ensure that the gap between the curves is smaller than the gap between the initial two. These bounds are derived after we introduce another transition into our automaton.

We add one more transition, applying the approach described before to the newly obtained curves. The new transformation acts on the image of the initial curves in BI^i and its effect is similar to what we had achieved before by adding T^l, T^r, P^i. This transformation leads from the state i to itself and is denoted as T^i. The modified BCIFS is presented in figure 5.5. To obtain the constraints on T^i we use the graph depicting the unfolding of the

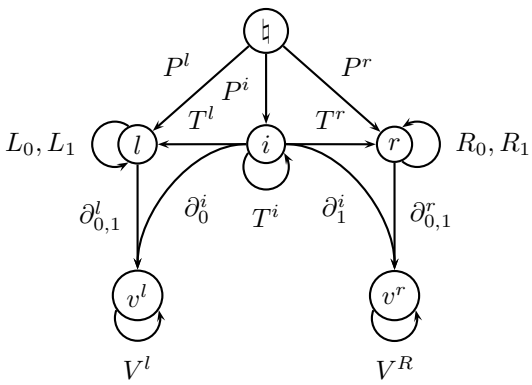

Figure 5.5: Final BCIFS with an intermediate state and all required transitions.

new automaton (see figure 5.6.) And then we can deduce the following constraints on T^i:

$$T^r \partial^r_0 = T^i \partial^i_1 \tag{5.7}$$

$$T^l \partial^l_1 = T^i \partial^i_0 \tag{5.8}$$

As we already know the form of T^l, T^r, ∂^i_0 and ∂^i_1, T^i can be described as follows: T^i has n_l first columns equal to the last n_l columns of T^l and the n_r last columns equal to the first n_r columns of T^r.

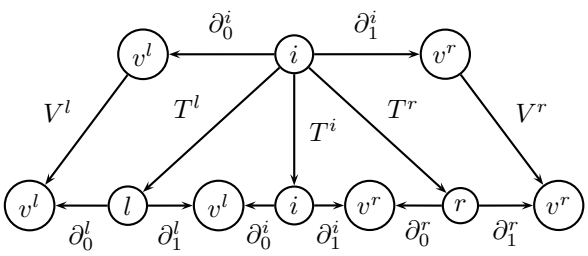

Figure 5.6: Unfolding of the automaton from figure 5.5.

5.1.2 Differential properties of the intermediate curve

In this subsection we study the differential properties of the intermediate curve that are defined by the automaton we described in the previous section. Let us consider the intermediate curve. For each state L, I and R let us denote the respective attractor as $\mathcal{A}^l$, $\mathcal{A}^i$ or $\mathcal{A}^r$ respectively. According to the definition 9 of the CIFS state attractor:

$$\mathcal{A}^i = T^l(\mathcal{A}^l) \cup T^i(\mathcal{A}^i) \cup T^r(\mathcal{A}^r).$$

So the intermediate curve is composed of the initial curves images ($T^r(\mathcal{A}^r)$ and $T^l(\mathcal{A}^l)$ respectively) that get smaller and smaller (transformed by repetitive applications of T^i) toward the fixed point of T^i. Hence the differential behaviour almost everywhere depends on the nature of the initial curves, since for the most part of the curve a tangent can be computed as an image of the tangent at the corresponding point to one of the initial curve.

However there are two kinds of points which are exceptions to this. First it is the junction between two copies of the same kind of initial curve. Here the left and right half-tangents exists only if the initial curves have the corresponding tangents at their respective endpoints. Depending on the initial curves the half-tangents at this kind of junction may or may not coincide. For example they will coincide for B-splines, but not for necessary Bézier curves.

The second kind of special points is the fixed point of T^i. The differential behaviour at that point depends on the nature of the initial curves, while the differential behaviour at the fixed point of T^i depends on its eigenvalues and eigenvectors.

Let us take two specific examples. Both examples present a junction between a cubic and a quadratic splines, however we choose a different set of parameters values for each example. Choosing a specific initial curve means that we choose the corresponding transformations. So for the transformations L_1, L_2, R_1, R_2 we choose the standard cubic and quadratic B-spline subdivisions respectively:

$$L_1 = \begin{pmatrix} 1/2 & 1/8 & 0 & 0 \\ 1/2 & 3/4 & 1/2 & 1/8 \\ 0 & 1/8 & 1/2 & 3/4 \\ 0 & 0 & 0 & 1/8 \end{pmatrix}, \; L_2 = \begin{pmatrix} 1/8 & 0 & 0 & 0 \\ 3/4 & 1/2 & 1/8 & 0 \\ 1/8 & 1/2 & 3/4 & 1/2 \\ 0 & 0 & 1/8 & 1/2 \end{pmatrix},$$

$$R_1 = \begin{pmatrix} 3/4 & 1/4 & 0 \\ 1/4 & 3/4 & 3/4 \\ 0 & 0 & 1/4 \end{pmatrix}, \; R_2 = \begin{pmatrix} 1/4 & 0 & 0 \\ 3/4 & 3/4 & 1/4 \\ 0 & 1/4 & 3/4 \end{pmatrix}.$$

Now we can use equations (5.2),(5.3),(5.5) and (5.6) to derive the matrix form of T^l and T^r. Solving the equations we obtain:

$$T^l = \begin{pmatrix} 1/2 & 1/8 & 0 & a \\ 1/2 & 3/4 & 1/2 & b \\ 0 & 1/8 & 1/2 & c \\ 0 & 0 & 0 & d \\ 0 & 0 & 0 & e \end{pmatrix}, \; T^r = \begin{pmatrix} k & 0 & 0 \\ l & 0 & 0 \\ m & 0 & 0 \\ n & 3/4 & 1/4 \\ p & 1/4 & 3/4 \end{pmatrix},$$

where $a + b + c + d + e = 1$ and $k + l + m + n + p = 1$. After that we can solve equations

(5.7) and (5.8) to derive T^i:

$$T^i = \begin{pmatrix} 1/8 & 0 & a & k & 0 \\ 3/4 & 1/2 & b & l & 0 \\ 1/8 & 1/2 & c & m & 0 \\ 0 & 0 & d & n & 3/4 \\ 0 & 0 & e & p & 1/4 \end{pmatrix}.$$

In the following example we study the differential behaviour of the intermediate curve defined by the above matrices. Each time we choose some random values for parameters and proceed to apply the results obtained in chapter 4 to the curve at hand.

Example 1

Let us choose the following values for the free variables: $a = 0.131$, $b = 0.2$, $c = 0.38$, $d = 0.289$, $k = 0.11$, $l = 0.12$, $m = 0.1$, $n = 0.12$. With these values we can calculate the eigenvalues of T^i:

$$\lambda_0 = 1,\ \lambda_1 \approx -0.4775,\ \lambda_2 \approx 0.696,$$

$$\lambda_3 \approx 0.0782 - i0.2472,\ \lambda_4 \approx 0.0782 + i0.2472.$$

and the matrix composed of the respective eigenvectors:

$$(\vec{v}_0, \vec{v}_1, \vec{v}_2, \vec{v}_3, \vec{v}_4) \approx$$

$$\approx \begin{pmatrix} 1 & 1 & 1 & 1 & 1 \\ 3.8485 & -0.1335 & 11.175 & -0.7996 + 1.3368i & -0.7996 - 1.3368i \\ 3.8489 & 0.6629 & 14.322 & -0.5475 - 1.6877i & -0.5475 + 1.6877i \\ 3.3707 & -6.2671 & -11.866 & 0.2271 - 0.2377i & 0.2271 + 0.2377i \\ 2.4718 & 4.7377 & -14.632 & 0.1199 + 0.5886i & 0.1199 - 0.5886i \end{pmatrix}.$$

with the λ_2 being the sub-dominant eigenvalue. Since $\lambda_{3,4} \in \mathbb{C}$ we can choose vectors

$$S_i = (\vec{v}_0, \vec{v}_1, \vec{v}_2, \mathrm{Re}(\vec{v}_3), \mathrm{Im}(\vec{v}_3))$$

as a complete basis.

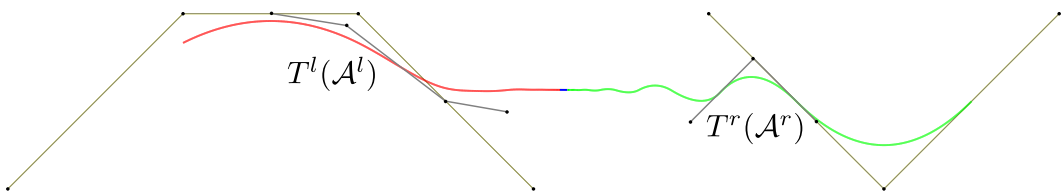

Figure 5.7: Control points for two splines that compose R_0.

According to theorem 2 and lemma 1 the tangent at the fixed points is given by the respective sub-dominant eigenvector $\vec{v}_2$ unless there exists a point in R_0 that has a zero coordinate along the sub-dominant eigenvector $\vec{v}_2$. Since

$$\mathcal{A} = T^r(\mathcal{A}) \cup T^i(\mathcal{A}) \cup T^l(\mathcal{A}),$$

we conclude that

$$R_0 = T^r(\mathcal{A}) \cup T^l(\mathcal{A}).$$

So R_0 consists of two separate subsets, a quadratic and a cubic B-spline (our initial curves) (for reference see figure 5.7). The position of these splines is dictated by transformations T^r and T^l. Namely the columns of their matrix form are the control points for the respective splines. Here we are going to consider a convex hull of control points for each spline. If we can manage to show that none of these hulls has a point with coordinates $(\cdot, \cdot, 0, \cdot, \cdot)$ in the basis $(\vec{v}_0, \vec{v}_1, \vec{v}_2, \operatorname{Re}\vec{v}_3, \operatorname{Im}\vec{v}_3)$, then R_0 does not contain such points, since the convex hulls of the control points contain the respective curves. Now we need to calculate the coordinates of the control points in that basis. To do that we need to multiply the respective matrices T^r or T^l by the inverse to the basis change matrix S_i.

$$S_i^{-1} \times T^r \approx \begin{pmatrix} 0.0687 & 0.0687 & 0.0687 \\ 0.0412 & -0.0425 & 0.0452 \\ -0.0122 & -0.0206 & -0.0266 \\ 0.0121 & -0.0055 & -0.0873 \\ 0.0057 & -0.0331 & -0.0230 \end{pmatrix},$$

$$S_i^{-1} \times T^l \approx \begin{pmatrix} 0.0687 & 0.0687 & 0.0687 & 0.0687 \\ -0.0012 & -0.0063 & 0.0075 & -0.0147 \\ 0.0235 & 0.0191 & 0.0136 & 0.0053 \\ 0.4089 & 0.0434 & -0.0899 & 0.0715 \\ 0.2235 & 0.2285 & 0.0087 & -0.0518 \end{pmatrix}.$$

Note that the highlighted coordinates correspond to the sub-dominant eigenvector. For the first convex hull the highlighted coordinates are strictly negative, while they are strictly positive for the second one. Since the points within the hull are weighted sums of its vertices, no points inside any of the hull has its third coordinate equal to 0. So according to lemma 1 the tangent is given by the sub-dominant eigenvector $\vec{v}_2$.

The resulting curve as well as the sub-dominant eigenvector of T^i are presented in figure 5.8.

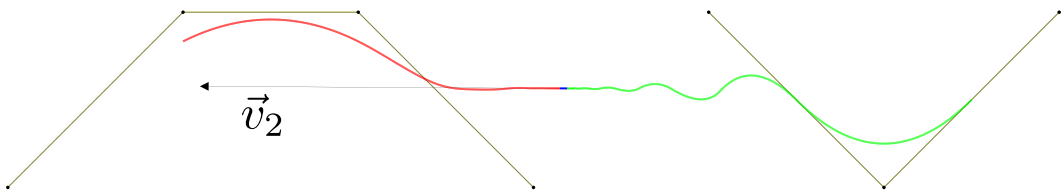

Figure 5.8: A connection between a cubic and a quadratic spline. Positive sub-dominant eigenvalue yields G_1-continuity. $a = 0.131$, $b = 0.2$, $c = 0.38$, $d = 0.289$, $k = 0.11$, $l = 0.12$, $m = 0.1$, $n = 0.12$, sub-dominant eigenvalues $\lambda_1 \approx 0.696$.

Example 2

In this example we choose another set of parameters and proceed to study the differential behaviour at the fixed point of T^i. Let $a = 0.065$, $b = 0.115$, $c = 0.115$, $d = 0.675$, $k = 0.6$,

$l = 0.35$, $m = 0$, $n = 0.09$. This way we obtain the following eigenvalues of T^i:

$$\lambda_0 = 1,\ \lambda_1 \approx -0.296,\ \lambda_2 \approx 0.211,$$

$$\lambda_3 \approx 0.082 + 0.602i,\ \lambda_4 \approx 0.082 - 0.602i,$$

as well as the following eigenvectors:

$$(\vec{v}_0, \vec{v}_1, \vec{v}_2, \vec{v}_3, \vec{v}_4) \approx$$

$$= \begin{pmatrix} 1 & 1 & 1 & 1 & 1 \\ 2.785 & -0.684 & -1.309 & -0.124 + 1.009i & -0.124 - 1.009i \\ 1.714 & 0.528 & -5.484 & -0.841 + 0.058i & -0.841 - 0.058i \\ 1.272 & -0.759 & 0.738 & 0.019 - 1.010i & 0.019 + 1.010i \\ 0.0007 & -0.084 & 5.056 & -0.053 - 0.058i & -0.053 + 0.058i \end{pmatrix},$$

where $\lambda_{3,4}$ are the sub-dominant eigenvalues.

According to lemma 5 the plane spanned by $(\operatorname{Re}\vec{v}_3, \operatorname{Im}\vec{v}_4)$ is the tangent plane to our curve if there is no point in the ring R_0 with zero coordinates along the vectors $\operatorname{Re}\vec{v}_1, \operatorname{Im}\vec{v}_2$ in the basis $(\vec{v}_0, \vec{v}_1, \vec{v}_2, \operatorname{Re}\vec{v}_3, \operatorname{Im}\vec{v}_4)$.

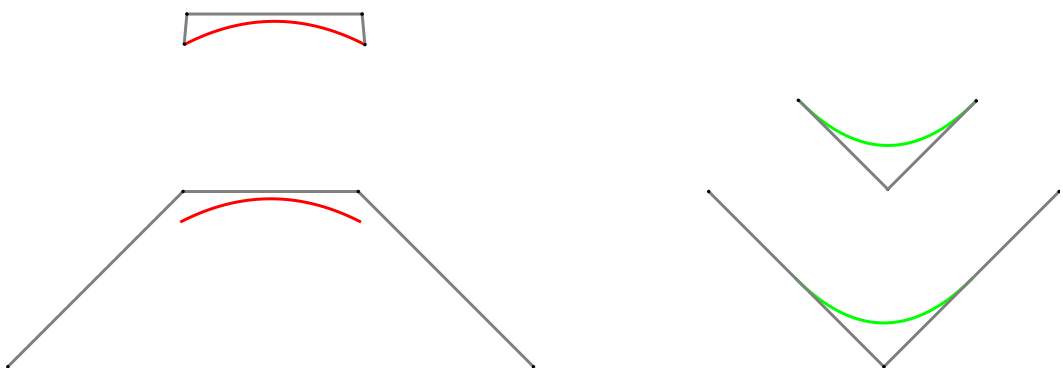

Figure 5.9: Top: new control points. Bottom: old control points. The control points reposition used to obtain tighter convex hulls.

As in the previous example R_0 consists of two spline curves. We can try to compute the convex hulls of control points as we did in the previous example, but both hulls computed this way contain points with coordinates $(\cdot, \cdot, \cdot, 0, 0)$. To alleviate this issue we need to choose a set of points that has a smaller convex hull that still contains the splines. This can be done by shifting the position of the control points relative to the curves. We choose to move the first and last control points of our initial curves to the position of their respective endpoints. For reference see figure 5.9. This corresponds to the basis change in the respective iterative spaces BI^L and BI^R. To compose the basis change matrix one must write the coordinates of the new basis vector in the old basis as columns of the new matrix. Since we wish to use the fixed points of L_1, L_2 as new basis vectors we must find their coordinates in the Euclidean basis. By definition the fixed point of an operator T is a solution to the following equation:

$$T(x) = x.$$

So by solving the corresponding equations we can find the fixed points of L_1, L_2, R_1, R_2. Since we do not alter the remaining basis vectors, we can write down the basis change matrices:

$$S_l = \begin{pmatrix} 1/6 & 0 & 0 & 0 \\ 2/3 & 1 & 0 & 1/6 \\ 1/6 & 0 & 1 & 2/3 \\ 0 & 0 & 0 & 1/6 \end{pmatrix}, \; S_r = \begin{pmatrix} 1/2 & 0 & 0 \\ 1/2 & 1 & 1/2 \\ 0 & 0 & 1/2 \end{pmatrix}.$$

In turn these changes also force a corresponding basis change in the iterative space of the intermediate curve BI^I:

$$S_i = \begin{pmatrix} 1 & 0 & 1/6 & 0 & 0 \\ 0 & 1 & 2/3 & 0 & 0 \\ 0 & 0 & 1/6 & 0 & 0 \\ 0 & 0 & 0 & 1/2 & 0 \\ 0 & 0 & 0 & 1/2 & 1 \end{pmatrix}.$$

So the coordinates of the new control points for each spline can be computed as:

$$S_i^{-1} \times T^r \times S_r,$$

$$S_i^{-1} \times T^l \times S_l.$$

Now we can calculate the coordinates of these control points in the basis $S = (\vec{v}_0, \vec{v}_1, \vec{v}_2, \operatorname{Re}\vec{v}_3, \operatorname{Im}\vec{v}_4)$ as

$$S^{-1} \times S_i^{-1} \times T^r \times S_r \approx \begin{pmatrix} 0.147 & 0.147 & 0.147 \\ -0.299 & -0.621 & -0.284 \\ -0.067 & -0.113 & -0.0100 \\ 0.518 & 0.587 & 0.146 \\ -0.459 & -0.903 & -0.594 \end{pmatrix},$$

$$S^{-1} \times S_i^{-1} \times T^l \times S_l \approx \begin{pmatrix} 0.147 & 0.147 & 0.147 & 0.147 \\ 0.459 & 0.272 & 1.621 & 1.086 \\ -0.000 & -0.000 & -0.009 & -0.029 \\ -0.606 & -0.419 & -2.259 & -1.546 \\ -0.171 & -0.027 & -1.084 & -0.906 \end{pmatrix}.$$

Here we highlighted components corresponding to the $\operatorname{Re}\vec{v}_3, \operatorname{Im}\vec{v}_4$. Since the points inside the hulls are weighted sums of the vertices and each highlighted row is either strictly positive or strictly negative, neither of the hull can contain the points with coordinates $(\cdot, \cdot, \cdot, 0, 0)$. Therefore $\operatorname{span}(\operatorname{Re}\vec{v}_3, \operatorname{Im}\vec{v}_4)$ is the tangent plane at the fixed point of T^i. The corresponding curve is presented in figure 5.10.

It is worth noting that T^i has 8 degrees of freedom, and all of them affect the eigenvalues of the matrix, and therefore affect the shape and differential properties of the final curve. In the next section we refine our automaton to create a more user-friendly configuration.

5.1.3 Refinement of the BCIFS

While the automaton described above solves the problem, it is not very convenient in practice. Although free parameters give a flexible control of the curve, the influence of each separate parameter can not be singled out and described. Also establishing a parameter

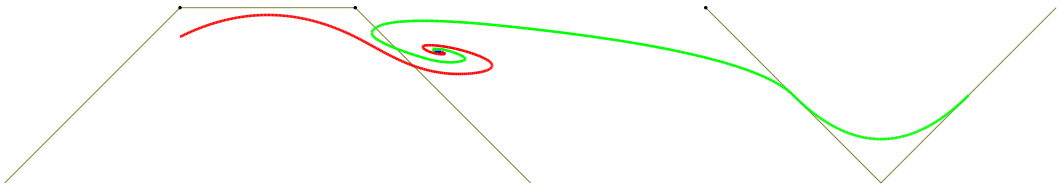

Figure 5.10: A connection between a cubic and a quadratic spline. The sub-dominant eigenvalue is complex and both parts of the curve are spiralling towards the fixed point. $a = 0.065$, $b = 0.115$, $c = 0.115$, $d = 0.675$, $k = 0.6$, $l = 0.35$, $m = 0$, $n = 0.09$, sub-dominant eigenvalues $\lambda_{3,4} \approx 0.082 \pm 0.602i$.

domain that guarantees a smooth curve is difficult to provide as it requires symbolic evaluation of the eigenvectors and eigenvalues. In the following section we describe modifications to the automaton as well as additional constraints to eliminate these flaws.

Previously we have shown that the sub-dominant eigenvector usually gives the tangent direction. Here we are going to change the automaton, so that the direction of the sub-dominant eigenvector will depend on the position of two control points.

The intermediate curve consists of copies of the initial curves. We are going to split the intermediate curve in two parts, such that each part will be composed of copies of one initial curve. This will also give us a more direct form of control over the curve shape. We replace the intermediate state i with two states il and ir. The new states have a shared vertex denoted as v^i. The modified automaton is presented in figure 5.11.

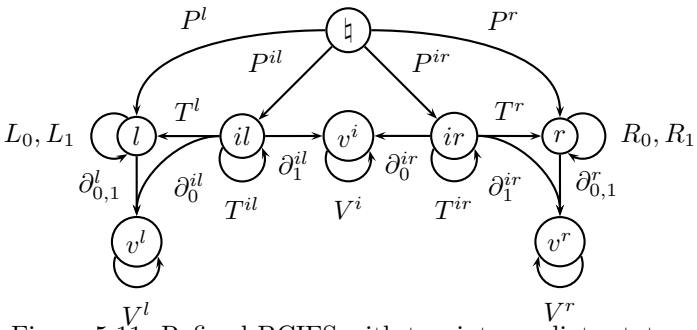

Figure 5.11: Refined BCIFS with two intermediate states.

Here we are free to choose any dimension for BI^{v^i}. For the sake of simplicity we choose to make it equal to 1. There is only one 1×1 matrix possible in an IFS — an identity matrix. An identity matrix as a vertex subdivision essentially means that the vertex will be located exactly at the control point position. It gives us a direct control of the curve, as the curve always passes through the vertex and therefore will always pass through the corresponding control point.

Now we can repeat the process seen in section 5.2 and deduce the form of T^{il}, T^{ir}, T^l and T^r. We illustrate it with the cubic-quadratic splines from section 5.1.2.

Let us first consider transformations T^l and T^{il}. The left-hand curve is a cubic spline. There are 3 control points for the vertex of the initial curve and 1 for the intermediate

vertex. To better control the curve we can add another control point. We will later use it to explicitly control the half-tangent at the intermediate vertex. This means that the final dimension of BI^{il} is $3+1+1=5$.

We can write down the constraints and fix the form of T^{il}:

$$\begin{pmatrix} 1/8 & 0 & a & f & 0 \\ 3/4 & 1/2 & b & g & 0 \\ 1/8 & 1/2 & c & h & 0 \\ 0 & 0 & d & j & 0 \\ 0 & 0 & e & k & 1 \end{pmatrix},$$

where $a+b+c+d+e=1$ and $f+g+h+j+k=1$.

Now we would like to set the tangent at the intermediate vertex in the direction of the segment between the two rightmost control points. To achieve this the sub-dominant eigenvector must have the given direction. For this we assign values to the parameters of T^{il}. We would also like to simplify the dependency between parameters and eigenvalues. So we assign 0 to a, b, c, e, f, g, h and 1 to d and obtain the following structure:

$$\begin{pmatrix} 1/8 & 0 & 0 & 0 & 0 \\ 3/4 & 1/2 & 0 & 0 & 0 \\ 1/8 & 1/2 & 0 & 0 & 0 \\ 0 & 0 & 1 & j & 0 \\ 0 & 0 & 0 & 1-j & 1 \end{pmatrix}$$

The idea behind this is to create a 2×2 sub-matrix in the bottom left corner and to restrict the free variables outside of it. This means that free variables only affect eigenvalues of the sub-matrix. Sub-matrix $\begin{pmatrix} j & 0 \\ 1-j & 1 \end{pmatrix}$ has two eigenvalues 1 and j. These eigenvalues are also eigenvalues of T^{il}. The eigenspace corresponding to the eigenvalue j is $(t, -t)$, where $t \in \mathbb{R}$. So the original 5×5 matrix has the following eigenspace: $(0, 0, 0, t, -t)$. Note that $\forall t \in \mathbb{R}$ the corresponding eigenvector is collinear to $\vec{e_4} - \vec{e_5}$ (where $\vec{e_i}$ is a component of the canonical basis) which is a desired tangent direction. Now we only have to ensure that j is the sub-dominant eigenvalue. Because all other eigenvalues are constant it is easy to establish a domain for j. In the provided example $j \in (1/2, 1)$.

We can now apply the same ideas to the right half of the curve and obtain the following:

$$T^{ir} = \begin{pmatrix} 1 & 1-r & 0 & 0 \\ 0 & r & 1 & 0 \\ 0 & 0 & 0 & 3/4 \\ 0 & 0 & 0 & 1/4 \end{pmatrix}.$$

It is easy to deduct a domain for r which turns out to be $(1/4, 1)$.

We have built an intermediate curve with 3 control points. It passes through one of them, and we can use the other two to control the half-tangents at the first control point.

To verify that we indeed get the desired tangent behaviour, we need to check for the existence of vectors with null components along the sub-dominant eigenvectors. As an example we choose $j = 3/4$ and $r = 3/4$. Since each half of the intermediate curve is an

attractor of either il or il we can treat each half separately. Let us denote the corresponding attractors as $\mathcal{A}^{ir}$ and $\mathcal{A}^{il}$. The structures of each attractor are quite similar:

$$\mathcal{A}^{il} = T^{il}(\mathcal{A}^{il}) \cup T^{l}(\mathcal{A}^{l}),$$

$$\mathcal{A}^{ir} = T^{ir}(\mathcal{A}^{ir}) \cup T^{r}(\mathcal{A}^{r}),$$

where $\mathcal{A}^l$ and $\mathcal{A}^r$ are the attractor of the states l and r respectively. Now we calculate the tangents at the fixed points of T^{il} and T^{ir}.

First we consider $\mathcal{A}^{il}$ and the fixed points of T^{il}. We are going to use the same method as we used in section 4.9. Here is the matrix composed of the eigenvectors of T^{il}:

$$S_l = \begin{pmatrix} 0 & 0 & 0 & 1 & 0 \\ 0 & 0 & 1 & -2 & 0 \\ 0 & 0 & 1 & -5 & 1 \\ 0 & 1 & -4 & 8 & -4/3 \\ 1 & -1 & 2 & -16/7 & 1/3 \end{pmatrix}.$$

The corresponding eigenvectors are as follows:

$$\lambda_0 = 1, \lambda_1 = 3/4, \lambda_2 = 1/2, \lambda_3 = 1/8, \lambda_4 = 0.$$

We denote the first ring around the fixed points of T^{il} as R_0^l. The ring R_0^l is composed of of a single cubic b-spline since $R_0^l = T^l(\mathcal{A}^l)$. We can use the control points of this B-spline to construct a convex hull that contains the ring itself. The control points are columns of the matrix T^r, and we can calculate their coordinates in the basis of eigenvectors of T^{il} if we multiply T^r by the inverse basis change matrix S_l:

$$S_l^{-1} \times T_l = \begin{pmatrix} 8/7 & 29/28 & 1 & 1 \\ 10/3 & 8/3 & 2 & 1 \\ 3/2 & 1 & 1/2 & 0 \\ 1/2 & 1/8 & 0 & 0 \\ 1 & -1/4 & 0 & 0 \end{pmatrix}.$$

The highlighted row, which corresponds to the component along the sub-dominant eigenvector, has strictly positive components. Since the points of the hull are weighted combination of its vertices no point inside can have its second coordinate equal to 0. Therefore according to lemma 1 the left half-tangent is indeed along the sub-dominant eigenvector.

Now we can repeat the same process for the right half of the curve. Let us calculate the eigenvector and eigenvalues of T^{ir}:

$$S_r = \begin{pmatrix} 1 & 1 & 1 & 1 \\ 0 & -1 & -3 & -4 \\ 0 & 0 & 3/2 & 3 \\ 0 & 0 & 1/2 & 0 \end{pmatrix},$$

and

$$\lambda_0 = 1, \lambda_1 = 3/4, \lambda_2 = 1/4, \lambda_3 = 0.$$

The first ring around the fixed point of T^{ir} that we denote as R_0^r is composed of a single quadratic b-spline since $R_0^r = T^r(\mathcal{A}^r)$. So the control points give us a convex hull that contains R_0^r. We can calculate the coordinates of these control points in the basis of eigenvectors of T^{ir} as

$$S_r^{-1} \times T^r = \begin{pmatrix} 1 & 1 & 1 \\ -1 & -3/2 & -11/6 \\ 0 & 1/2 & 3/2 \\ 0 & 0 & -2/3 \end{pmatrix}.$$

As we can see here all components of the second row are negative. These are the coordinates that correspond to the sub-dominant eigenvector $\vec{v}_1$. As in the previous case no point inside the hull can have its second coordinate equal to 0 and according to lemma1 the right half-tangent is indeed along the sub-dominant eigenvector $\vec{v}_1$.

5.1.4 Examples

Here are some examples demonstrating curves obtained with the modified automaton from section 5.1.3. These examples illustrates an intermediate curve between the fractal curve and a B-spline (figures 5.12, 5.13). The control points control the shape of the curve. The curve passes through the second control points, while the half-tangents are defined by the direction given by the first and third control point in relation to the second one. The first two examples illustrate curves with collinear half-tangents as all three control points are aligned. (figure 5.12). The third example illustrates the same curve, but with a different control point configuration (figure 5.13). As the control point are not aligned, they define two non-collinear half-tangents.

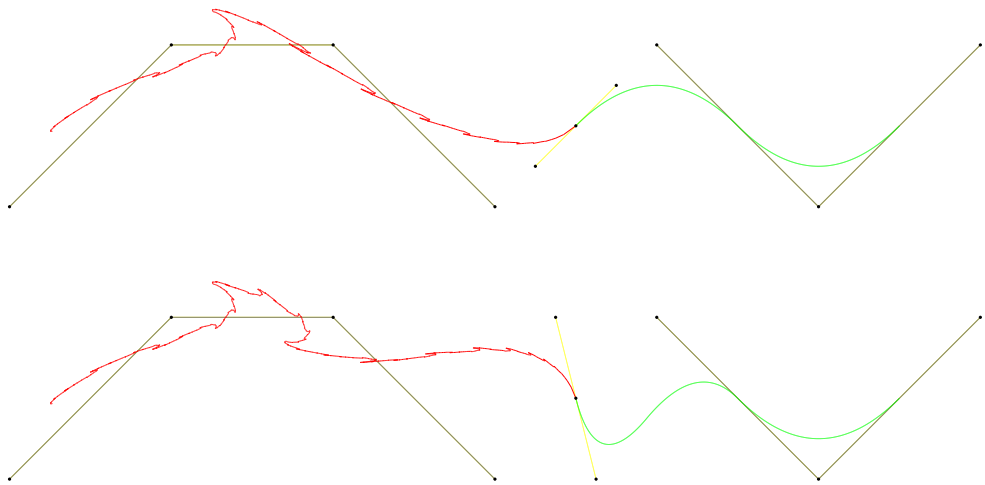

Figure 5.12: Two intermediate curves between the fractal curve and B-spline. Three control point are used to control the shape of the curve.

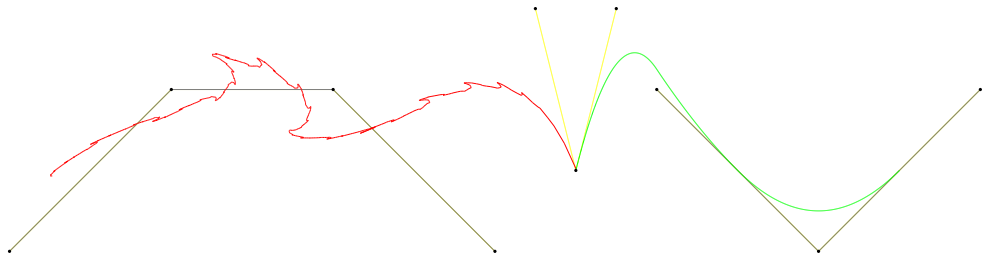

Figure 5.13: Intermediate curve between the fractal curve and B-spline. Such configuration of control points defines different half-tangents.

5.2 Joining surfaces

In this section we study the problem of connecting two surfaces defined as attractors of different BCIFS. Here our approach is similar to the one presented in the previous section. Using the BCIFS formalism we describe the intermediate surface with the desired properties. After deriving all the necessary conditions we proceed to refine the automaton to provide a more user-friendly tool to design the intermediate surface. Finally we proceed to analyse the differential behaviour of the final surface using tools the developed in chapter 4.

Initial problem

As in the previous section we consider the automaton that defines two initial shapes, in this case they are surfaces. Here we restrict the topology of the initial surfaces to quadrangular patches: four edges and four vertices, but the same method can be easily applied to surfaces with more a complex configuration. The initial automaton is presented in figure 5.14. The initial state is denoted by $\natural$, while L and R denote the states corresponding to the respective initial surfaces.

Intermediate surface topology subdivision

Now we introduce a state I for the intermediate surface. For this surface we propose the following subdivision. The intermediate surface is subdivided into six parts: two of them have the same nature as the first initial surface, another are similar to the second initial surface and the last two are similar to the intermediate surface itself. This subdivision and the corresponding graph are shown in figure 5.15. In the next subsection we use the BCIFS to deduce the condition on the transformations of the intermediate patch to ensure its continuity. To do this we need to guarantee that the edges of the patch are continuous curves and that the patches obtained after the subdivision are connected with one another, as described below.

5.2.1 Continuity constraints

In this subsection we derive the C^0-continuity constraints for the intermediate surface.

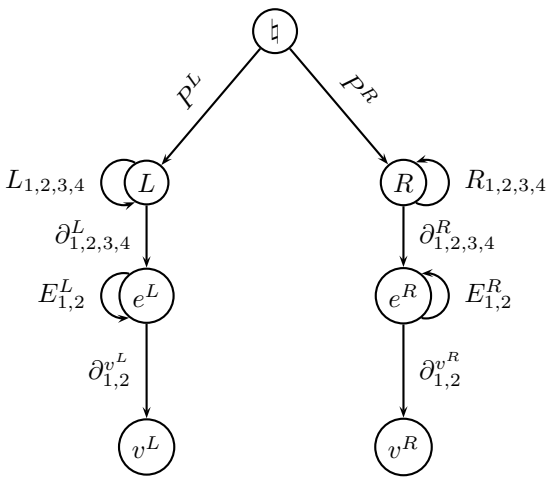

Figure 5.14: Initial BCIFS. Each branch of the automaton corresponds to an initial surface.

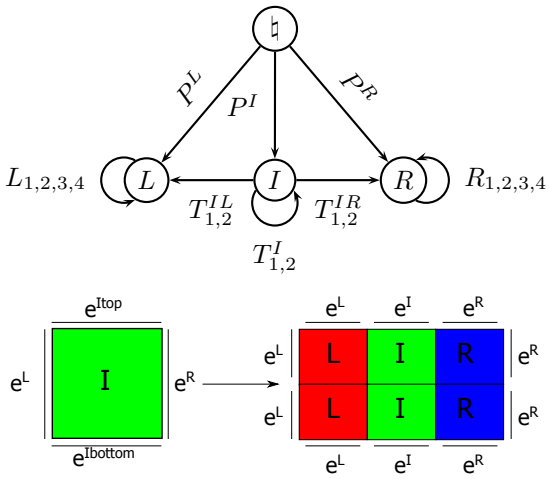

Figure 5.15: Top: Automaton describing the subdivision of the intermediate patch. Note that edge and vertex states are omitted to conserve space. Bottom: Schematic representation of the same subdivision.

Outer edges

The intermediate surface has four edges: e^L, e^R (for the left and right edges respectively) and e^{Itop}, e^{Ibot} (for the top and bottom edges) as can be seen in figure 5.15. Note that e^L (and e^R) is actually subdivided into two smaller edges, while each of them is the edge of an L-patch (or R-patch respectively). We can use the subdivision of the edges of the initial

patches for e^L and e^R to guarantee their continuity, as well as to provide with us an easy way to connect the intermediate surface with the initial ones (see section 5.2.1).

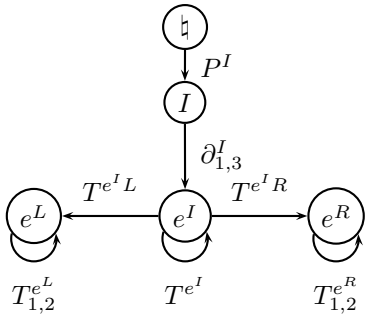

Figure 5.16: The automaton depicting top and bottom edges subdivision of the intermediate patch.

Edges e^{Itop}, e^{Ibot} differ from e^L and e^R as they are subdivided into three different parts instead of two uniform parts. Also note that after one iteration two intermediate patches are produced and they share a common edge (see figure 5.15). This means that e^{Itop}, e^{Ibot} must have the same subdivision, so that the surface is indeed continuous. Thus $e^{Itop} = e^{Ibot} = e^I$.

Now we want to deduce the constraints on the subdivision of e^I. It is presented in figure 5.16. Here $\partial^I_{1,3}$ are the boundary operators that selects the edges in question, e^I is the state which corresponds to them, $T^{e^I L}, T^{e^I R}$ and T^{e^I} are the operators of the edge subdivision, while $T^{e^R}_{1,2}$ and $T^{e^L}_{1,2}$ are the subdivision operators for the edges of respected initial surfaces.

To guarantee the continuity of the edge we use the same method as in section 3.5.3. We can deduce both adjacency and incidence constraints from the graph representing one step of the edge subdivision (see figure 5.17). Using the equivalent paths in this graph we can

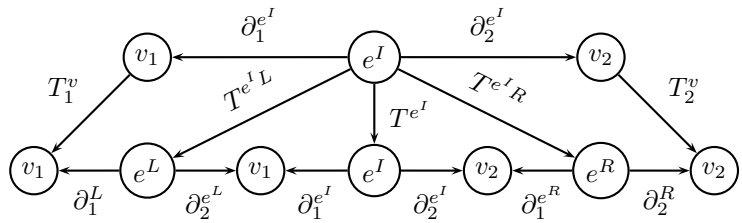

Figure 5.17: Part of the graph representing one iteration of the automaton.

deduce the following constraints:

$$T^{e^I L}\partial^{e^L}_2 = T^{e^I}\partial^{e^I}_1,$$

$$T^{e^I}\partial^{e^I}_2 = T^{e^I R}\partial^{e^R}_1,$$

$$\partial^{e^I}_1 T^v_1 = T^{e^I L}\partial^L_1,$$

$$\partial^{e^I}_2 T^v_2 = T^{e^I R}\partial^R_2.$$

Inner edges

There are 7 shared edges between the patches obtained after the first iteration (see figure 5.15). For each of them we need to write a constraint on the subdivision operators.

At first we consider two R-patches. One step of the subdivision that produces these two patches is presented in figure 5.18. Note that nodes not related to the considered patches or to the common edge are not presented. From the equivalent paths in this graph we can

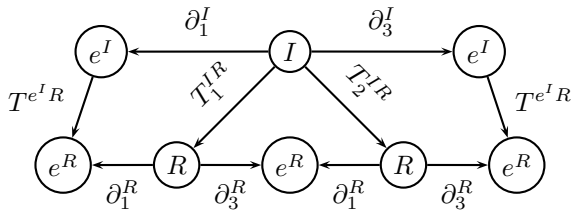

Figure 5.18: Part of the graph representing one step of the subdivision. This part shows two R patches and the common edge between them.

deduce the following equations:

$$T_1^{IR}\partial_3^R = T_2^{IR}\partial_1^R,$$
$$\partial_1^I T^{e^I R} = T_1^{IR}\partial_1^R,$$
$$\partial_3^I T^{e^I R} = T_2^{IR}\partial_3^R.$$

In the same way we can deduce the condition on edges between the I-patches:

$$T_1^I\partial_3^I = T_2^I\partial_1^I,$$
$$\partial_1^I T^{e^I} = T_1^I\partial_1^I,$$
$$\partial_3^I T^{e^I} = T_2^I\partial_3^I.$$

And between the L-patches:

$$T_1^{IL}\partial_3^L = T_2^{IL}\partial_1^L,$$
$$\partial_1^I T^{e^I L} = T_1^{IL}\partial_1^L,$$
$$\partial_3^I T^{e^I L} = T_2^{IL}\partial_3^L.$$

Now we proceed to treat edges between two adjacent patches of different nature. At first we consider the top row of the patches (see figure 5.15). The corresponding graph is presented in figure 5.19. From that graph we deduce the following equations:

$$T_1^{IL}\partial_2^L = T_1^I\partial_4^I,$$
$$T_1^I\partial_2^I = T_1^{IR}\partial_4^R.$$

Note that the top row of the intermediate patch is similar to the bottom one. This means that to obtain the condition on the last two inner edges, we need to substitute T_1^{IL}, T_1^I and T_1^{IR} with T_2^{IL}, T_2^I and T_2^{IR} respectively. This way we obtain the following equations:

$$T_2^{IL}\partial_2^L = T_2^I\partial_4^I,$$
$$T_2^I\partial_2^I = T_2^{IR}\partial_4^R.$$

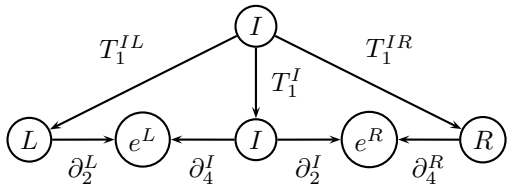

Figure 5.19: Part of the graph representing one step of the subdivision. This part shows the top row of three patches and the edges between them.

Connection to the initial surfaces

Finally we need to ensure that the intermediate patch actually connects two initial surfaces. Since we chose to use the subdivision of the initial surfaces edges for e^L and e^R, we can connect the initial surface to the intermediate one by using the same control points for the respective edges. This can be written as following:

$$P^I \partial_2^I = P^R \partial_4^R,$$

$$P^I \partial_4^I = P^L \partial_2^L,$$

where P^I, P^R, P^L are vectors of control points for respective surfaces. From these conditions we can also deduce the minimum dimension of BI^I. That is a sum of dimension for initial surfaces respective edges. The said dimension can be increased, therefore introducing additional control points to the intermediate patch.

5.2.2 Approximation of the limit surface

The adjacency and incidence condition described above only guarantee the continuity of the limit shape. Hence approximations obtained with a finite number of iterations of an arbitrary compact set as a starting point are not necessarily continuous. However with a correct starting set, we can obtain a continuous surface that approximates the limit shape for any number of iterations. For each face state a quad is chosen as compact set to be transformed accordingly with the rules of the BCIFS. Said quads of course lie within the corresponding barycentric space. The vertices of each quad must be chosen specifically so that incidence and adjacency conditions are met for each level of approximation. This is true if each vertex of the tetragon lies within the barycentric subspace which corresponds to that vertex iterative subspace and has the same coordinates within the subspaces. One way to satisfy that condition is to choose the fixed points of respective transformations as quads vertices. Then after each iteration the corresponding quads will share the edges and vertices that correspond to the specific continuity constraints.

Different iterations of approximation of the intermediate surface are presented in figure 5.20. The different quads are color coded to show their "origin" from different barycentric spaces. Green is for an image of the quad from BI^I (barycentric space corresponding to state I), red is for BI^R and blue is for BI^L.

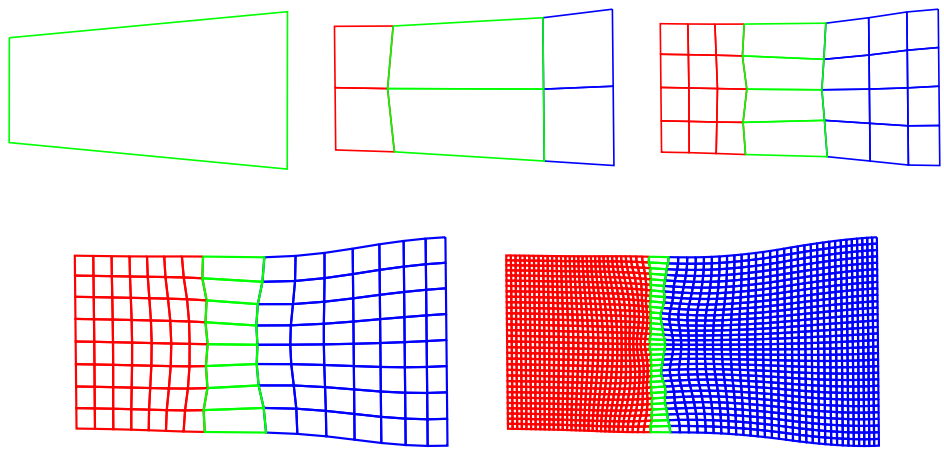

Figure 5.20: Continuous approximation of the limit surface.

5.2.3 Differential properties of the intermediate surface

The intermediate patch is subdivided into four regular patches and two intermediate ones.

$$\mathcal{A}^I = T_1^{IR}(\mathcal{A}^R) \cup T_2^{IR}(\mathcal{A}^R) \cup T_1^{IL}(\mathcal{A}^L) \cup T_2^{IL}(\mathcal{A}^L) \cup T_1^I(\mathcal{A}^I) \cup T_2^I(\mathcal{A}^I).$$

The regular patches are copies of the respective initial surfaces ($\mathcal{A}^R$ and $\mathcal{A}^L$). So the limit surface consists of regular patches stitched together. The regular patches get smaller and smaller as we approach the intermediate curve (see figure 5.21). So the differential behaviour for most of the surface depends solely on the nature of the initial surfaces, that define the subdivision of the regular patches. There exists a curve that separates two regions tiles with regular patches. This curve is a sub-attractor of our automaton. Namely it is an attractor of $\{T_1^I, T_2^I\}$. So the differential behaviour of the surface at the points of that curve does depend not on the initial surfaces nature, but on the sub-dominant eigenvectors of T_1^I and T_2^I.

Unfortunately the degrees of freedom allowed by continuity constraints for T_1^I, T_2^I do not allow for a straight forward modelling of a smooth intermediate surface. So in the next subsection we are going to improve the automaton the will become a more convenient tool for modelling a smooth intermediate surface.

5.2.4 Refinement of the BCIFS

So far we have deduced a BCIFS that produces a variety of limit surfaces satisfying the initial conditions. A specific surface can be chosen by specifying the parameter values for the BCIFS operators. Unfortunately, specifying a parameter directly can have a somewhat unpredictable effect on the final shape. In the previous section we have shown, that the shape of the surface depends on the sub-dominant eigenvectors of the operators $T_{1,2}^I$. Now

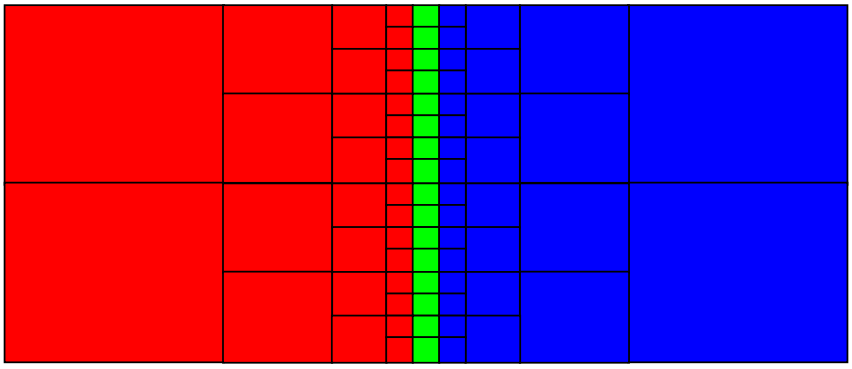

Figure 5.21: A schematic representation of several subdivision steps of the intermediate surface. Red and blue squares present the regular patches, green ones represent the irregular patches.

we are going to show how control points can be added to provide more intuitive way of designing the intermediate surface.

As was already noted before a special curve (an attractor of $T^I_{1,2}$) runs across the intermediate surface. We are going to reflect this in the BCIFS and assign new control points to directly influence the shape of this curve and therefore the surface itself. Explicit specification of the special curve allows us to view the intermediate surface as two quadrangular patches that share a common edge. This allows us to redefine its subdivision as presented in figure 5.22. As these two patches are mirrored copies of each other we can use the same automaton to resolve the adjacency and incidence constraints.

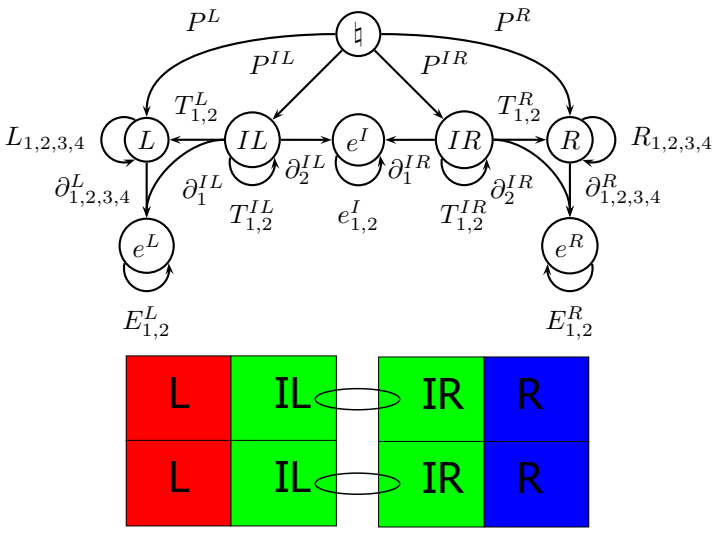

Figure 5.22: Top: Refined BCIFS with two intermediate states. Bottom: Corresponding subdivision scheme.

But before we can resolve the constraints we need to specify the subdivision of the common edge. Virtually any subdivision may be chosen, but our goal is to build a smooth surface, so some restrictions apply. First of all the curve needs to be C^1 itself. For more studies on the differentiability of self-similar curves please refer to [BGN09], [PGSL13a] and [SGB12].

In the previous section we showed that the existence of the tangent quarter-planes depend on the eigenvalues of $T^{IL}_{1,2}$ or $T^{IR}_{1,2}$ respectively. If two equal positive sub-dominant eigenvalues exist then the tangent plane is collinear to the respective two dimensional eigenspace. In turn, the tangent plane position in the modelling space depends on those control points which correspond to the smallest subspace containing the tangent plane. So to be able to guarantee C^1-continuity between two patches the tangent planes must depend on the control points shared by two patches - control points of the common edge.

These can be further exploited if we consider the structure of the subdivision matrices. When we consider two matrices that are constrained by a boundary condition, e.g., a face and an edge subdivision, the face subdivision will always have a block-triangular structure, with one block equal to the edge subdivision. For example:

$$T^{IL}_1 = \begin{pmatrix} e^I_1 & A_1 \\ 0 & B_1 \end{pmatrix}, \quad T^{IL}_2 = \begin{pmatrix} e^I_2 & A_2 \\ 0 & B_2 \end{pmatrix}$$

where e^I_1, e^I_2 are matrices of the edge subdivision.

The eigenvalues of the edge subdivision are also eigenvalues of the face subdivision, while the corresponding eigenvectors are embedded into the higher dimensional space. Note that if two patches share the same edge and hence the same edge subdivision, their face subdivision will have common blocks. In our case:

$$T^{IR}_1 = \begin{pmatrix} e^I_1 & A_3 \\ 0 & B_3 \end{pmatrix}, \quad T^{IR}_2 = \begin{pmatrix} e^I_2 & A_4 \\ 0 & B_4 \end{pmatrix}.$$

So to guarantee the C^1-continuity the edge subdivision block must provide two sub-dominant eigenvalues, so that the same tangent plane can be obtained on both sides of the special curve.

5.2.5 Example

Here we are going to provide a specific example and study its differential properties. For our initial surfaces we are going to choose Doo-Sabin and Catmull-Clark regular patches. This gives us the matrix form of the transformations $L_{1,2,3,4}$ and $R_{1,2,3,4}$. You can find these matrices in appendix A.1.

For the intermediate curve we choose the curve obtained as the tensor product of cubic B-spline subdivision and quadratic vertex:

$$e_1^I = \begin{pmatrix} \frac{3}{4} & \frac{1}{4} \\ \frac{1}{4} & \frac{3}{4} \end{pmatrix} \otimes \begin{pmatrix} \frac{1}{2} & \frac{1}{8} & 0 & 0 \\ \frac{1}{2} & \frac{3}{4} & \frac{1}{2} & \frac{1}{8} \\ 0 & \frac{1}{8} & \frac{1}{2} & \frac{3}{4} \\ 0 & 0 & 0 & \frac{1}{8} \end{pmatrix} = \begin{pmatrix} \frac{3}{8} & \frac{3}{32} & 0 & 0 & \frac{1}{8} & \frac{1}{32} & 0 & 0 \\ \frac{3}{8} & \frac{9}{16} & \frac{3}{8} & \frac{3}{32} & \frac{1}{8} & \frac{3}{16} & \frac{1}{8} & \frac{1}{32} \\ 0 & \frac{3}{32} & \frac{3}{8} & \frac{9}{16} & 0 & \frac{1}{32} & \frac{1}{8} & \frac{3}{16} \\ 0 & 0 & 0 & \frac{3}{32} & 0 & 0 & 0 & \frac{1}{32} \\ \frac{1}{8} & \frac{1}{32} & 0 & 0 & \frac{3}{8} & \frac{3}{32} & 0 & 0 \\ \frac{1}{8} & \frac{3}{16} & \frac{1}{8} & \frac{1}{32} & \frac{3}{8} & \frac{9}{16} & \frac{3}{8} & \frac{3}{32} \\ 0 & \frac{1}{32} & \frac{1}{8} & \frac{3}{16} & 0 & \frac{3}{32} & \frac{3}{8} & \frac{9}{16} \\ 0 & 0 & 0 & \frac{1}{32} & 0 & 0 & 0 & \frac{3}{32} \end{pmatrix},$$

$$e_2^I = \begin{pmatrix} \frac{3}{4} & \frac{1}{4} \\ \frac{1}{4} & \frac{3}{4} \end{pmatrix} \otimes \begin{pmatrix} \frac{1}{8} & 0 & 0 & 0 \\ \frac{3}{4} & \frac{1}{2} & \frac{1}{8} & 0 \\ \frac{1}{8} & \frac{1}{2} & \frac{3}{4} & \frac{1}{2} \\ 0 & 0 & \frac{1}{8} & \frac{1}{2} \end{pmatrix} = \begin{pmatrix} \frac{3}{32} & 0 & 0 & 0 & \frac{1}{32} & 0 & 0 & 0 \\ \frac{9}{16} & \frac{3}{8} & \frac{3}{32} & 0 & \frac{3}{16} & \frac{1}{8} & \frac{1}{32} & 0 \\ \frac{3}{32} & \frac{3}{8} & \frac{9}{16} & \frac{3}{8} & \frac{1}{32} & \frac{1}{8} & \frac{3}{16} & \frac{1}{8} \\ 0 & 0 & \frac{3}{32} & \frac{3}{8} & 0 & 0 & \frac{1}{32} & \frac{1}{8} \\ \frac{1}{32} & 0 & 0 & 0 & \frac{3}{32} & 0 & 0 & 0 \\ \frac{3}{16} & \frac{1}{8} & \frac{1}{32} & 0 & \frac{9}{16} & \frac{3}{8} & \frac{3}{32} & 0 \\ \frac{1}{32} & \frac{1}{8} & \frac{3}{16} & \frac{1}{8} & \frac{3}{32} & \frac{3}{8} & \frac{9}{16} & \frac{3}{8} \\ 0 & 0 & \frac{1}{32} & \frac{1}{8} & 0 & 0 & \frac{3}{32} & \frac{3}{8} \end{pmatrix}.$$

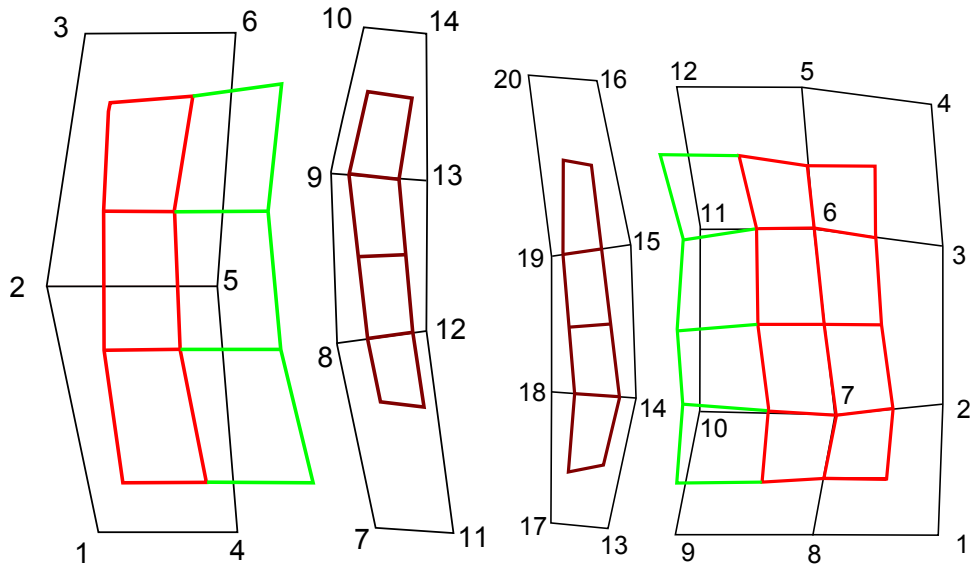

Figure 5.23: Control meshes for two intermediate patches. Left: Doo-Sabin side. Right: Catmull-Clark Side. Colored meshes represent different parts of the first step of the subdivision. Please note that since the two intermediate patches are independent we treat them separately, thus the mesh for the intermediate curve is presented twice.

After we choose the initial surface and the intermediate curve we can solve the constraints and derive the subdivision matrices for the intermediate patches. The control meshes with ordered control points are presented in figure 5.23. The first step of the subdivision is also

presented in that picture. We use different colors to highlight different types of control points. The brown mesh depends only on the control points of the intermediate curve, the red one depends on the control points initial surfaces, while the green depends on both. The configuration of the brown and red meshes is fixed once we chose our initial surfaces and intermediate curve. The positions of the vertices of the green mesh change when we change the values of the free parameters allowed by the degrees of freedom. The matrices satisfying the continuity constraints can be found in appendix A.2. To ensure the continuity we must ensure that the two sub-dominant eigenvectors are the eigenvectors of the intermediate edge subdivision embedded into the higher dimension space. The parameter values that satisfy that condition are listed in appendix A.2.

Next we consider the differential behaviour at fixed points of $T^{IR}_{1,2}$ and $T^{IL}_{1,2}$. Let us study the Catmull-Clark side first.

Catmull-Clark side

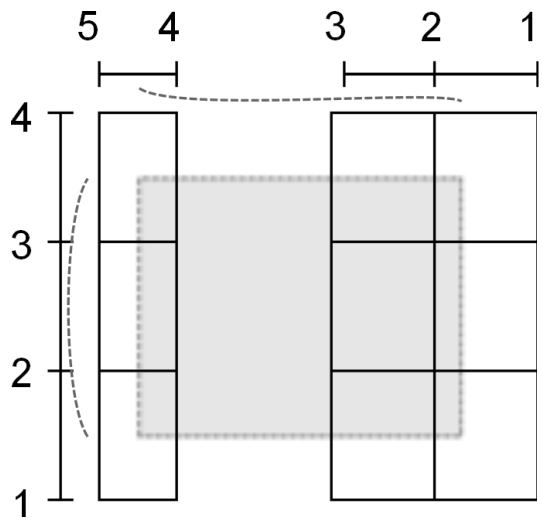

Figure 5.24: Catmull-Clark intermediate patch as tensor product of its edges.

.

Let us note that the Catmull-Clark intermediate patch is, in fact, a tensor product of a cubic B-spline and a special curve that has a quadratic vertex and a cubic one (see figure 5.24). It can be directly verified by computing the tensor products of the respective edge's subdivisions. So here to study the differential behaviour at the fixed points of $T^{IR}_{1,2}$ we can use the properties of tensor product attractors described in section 4.9.3. Let us consider the subdivision of the horizontal edge. This edge is an attractor of the BCIFS presented in figure 5.25. It turns out that the edge subdivision is very similar to the curve described in section 5.1.3. The edge is tiled with cubic B-splines that converge towards the fixed point of e^i. Here $e^r_{1,2}$ are standard cubic b-spline subdivisions:

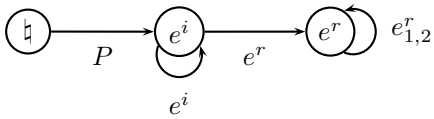

Figure 5.25: An automaton representing the subdivision of the irregular edge.

$$e^r_1 = \begin{pmatrix} \frac{1}{2} & \frac{1}{8} & 0 & 0 \\ \frac{1}{2} & \frac{3}{4} & \frac{1}{2} & \frac{1}{8} \\ 0 & \frac{1}{8} & \frac{1}{2} & \frac{3}{4} \\ 0 & 0 & 0 & \frac{1}{8} \end{pmatrix}, \; e^r_2 = \begin{pmatrix} \frac{1}{8} & 0 & 0 & 0 \\ \frac{3}{4} & \frac{1}{2} & \frac{1}{8} & 0 \\ \frac{1}{8} & \frac{1}{2} & \frac{3}{4} & \frac{1}{2} \\ 0 & 0 & \frac{1}{8} & \frac{1}{2} \end{pmatrix}.$$

And

$$e^r = \begin{pmatrix} 1/2 & 1/8 & 0 & 0 \\ 1/2 & 3/4 & 1/2 & 0 \\ 0 & 1/8 & 1/2 & 3/4 \\ 0 & 0 & 0 & 1/4 \\ 0 & 0 & 0 & 0 \end{pmatrix}, e^i = \begin{pmatrix} 1/8 & 0 & 0 & 0 & 0 \\ 3/4 & 1/2 & 0 & 0 & 0 \\ 1/8 & 1/2 & 1/4 & 0 & 0 \\ 0 & 0 & 3/4 & 3/4 & 1/4 \\ 0 & 0 & 0 & 1/4 & 3/4 \end{pmatrix}.$$

To show that there exists a tangent quarter-plane at the fixed points of $T^{IR}_{1,2}$ we need to show that the tangent to this curve at the fixed points of e^i exists, depends on the sub-dominant eigenvector and the corresponding eigenvalues is equal to the sub-dominant eigenvalues of the cubic B-spline subdivision that is 1/2.

So let us compute the Jordan form J of e^i and the corresponding Jordan basis matrix P:

$$J = \begin{pmatrix} 1 & 0 & 0 & 0 & 0 \\ 0 & \frac{1}{4} & 0 & 0 & 0 \\ 0 & 0 & \frac{1}{8} & 0 & 0 \\ 0 & 0 & 0 & \frac{1}{2} & 1 \\ 0 & 0 & 0 & 0 & \frac{1}{2} \end{pmatrix}, \; P = \begin{pmatrix} 0 & 0 & 1 & 0 & 0 \\ 0 & 0 & -2 & 0 & 1 \\ 0 & 1 & 7 & 0 & 2 \\ 1 & -2 & -10 & \frac{3}{4} & 0 \\ 1 & 1 & 4 & -\frac{3}{4} & -3 \end{pmatrix}.$$

The first ring R_0 around the fixed points of e^i is composed of a single B-spline whose control points are columns of e^r. So R_0 lies within the convex hull of these control points. Let us calculate their coordinates in the basis P:

$$P^{-1} \times e^r = \begin{pmatrix} \frac{1}{2} & \frac{1}{2} & \frac{1}{2} & \frac{1}{2} \\ -\frac{13}{2} & -\frac{11}{4} & -\frac{1}{2} & \frac{3}{4} \\ \frac{1}{2} & \frac{1}{8} & 0 & 0 \\ -\frac{34}{3} & -\frac{19}{3} & -2 & \frac{5}{3} \\ \frac{3}{2} & 1 & \frac{1}{2} & 0 \end{pmatrix}.$$

The fourth and fifth rows correspond to the chain of eigenvector corresponding to sub-dominant eigenvalue 1/2. The fifth row has non-negative components and only one zero component. However a positive component on the fourth row corresponds to this zero component. Since all the points inside the hull can be expressed as weighted sums of its

vertices with non-negative weights, no point inside can have a zero as its fourth and fifth coordinate. Therefore the tangent direction is given by the sub-dominant eigenvector of e^i.

So according to section 4.9.3 the tensor product has a quarter plane at the fixed points of $T^{IR}_{1,2}$. Also note that since the sub-dominant eigenvector of e^i depends only on the last two control points, the tangent plane in question depends only on the position of the control points for the intermediate curve.

Doo-Sabin side

Unfortunately the other side of the intermediate surface is not a tensor product of two curves. To study the differential behaviour at the fixed points of $T^{IL}_{1,2}$ we need to compute the corresponding eigenvectors and check the respected rings for points with zero components along the sub-dominant eigenvectors. From the subdivision matrices it can be established that the surface is symmetrical so we will only do the calculations for the fixed point of T^{IL}_1.

Let us calculate the Jordan form J and the corresponding Jordan basis of T^{IL}_1:

$$J = \left(\begin{array}{cccc|ccc|ccccccc}
1 & 0 & 0 & 0 & 0 & 0 & 0 & 0 & 0 & 0 & 0 & 0 & 0 & 0 \\
0 & 0 & 0 & 0 & 0 & 0 & 0 & 0 & 0 & 0 & 0 & 0 & 0 & 0 \\
0 & 0 & \frac{1}{16} & 0 & 0 & 0 & 0 & 0 & 0 & 0 & 0 & 0 & 0 & 0 \\
0 & 0 & 0 & \frac{1}{16} & 0 & 0 & 0 & 0 & 0 & 0 & 0 & 0 & 0 & 0 \\
0 & 0 & 0 & 0 & \frac{1}{2} & 1 & 0 & 0 & 0 & 0 & 0 & 0 & 0 & 0 \\
0 & 0 & 0 & 0 & 0 & \frac{1}{2} & 0 & 0 & 0 & 0 & 0 & 0 & 0 & 0 \\
0 & 0 & 0 & 0 & 0 & 0 & \frac{1}{2} & 0 & 0 & 0 & 0 & 0 & 0 & 0 \\
0 & 0 & 0 & 0 & 0 & 0 & 0 & \frac{1}{8} & 0 & 0 & 0 & 0 & 0 & 0 \\
0 & 0 & 0 & 0 & 0 & 0 & 0 & 0 & \frac{1}{8} & 0 & 0 & 0 & 0 & 0 \\
0 & 0 & 0 & 0 & 0 & 0 & 0 & 0 & 0 & \frac{1}{8} & 0 & 0 & 0 & 0 \\
0 & 0 & 0 & 0 & 0 & 0 & 0 & 0 & 0 & 0 & \frac{1}{4} & 1 & 0 & 0 \\
0 & 0 & 0 & 0 & 0 & 0 & 0 & 0 & 0 & 0 & 0 & \frac{1}{4} & 0 & 0 \\
0 & 0 & 0 & 0 & 0 & 0 & 0 & 0 & 0 & 0 & 0 & 0 & \frac{1}{4} & 1 \\
0 & 0 & 0 & 0 & 0 & 0 & 0 & 0 & 0 & 0 & 0 & 0 & 0 & \frac{1}{4}
\end{array}\right),$$

$$P = \left(\begin{array}{cccc|ccc|ccccccc}
0 & 0 & 1 & 0 & 0 & 0 & 0 & 1 & 0 & 0 & 0 & 1 & 0 & 0 \\
0 & 0 & -2 & 0 & 0 & 0 & 0 & -1 & 0 & 0 & 0 & 1 & 0 & 0 \\
0 & 0 & 1 & 0 & 0 & 0 & 0 & 0 & 0 & 0 & 0 & 0 & 0 & 0 \\
0 & 1 & 7 & 0 & 0 & 1 & 0 & 3 & 0 & 0 & 0 & 0 & 0 & 1 \\
0 & -1 & -6 & 0 & 0 & 1 & 0 & -3 & 0 & 0 & 0 & -3 & 0 & 0 \\
0 & 0 & -1 & 0 & 0 & 0 & 0 & 0 & 0 & 0 & 0 & -3 & 0 & -1 \\
1 & -\frac{3}{4} & 0 & 1 & \frac{1}{12} & 0 & 1 & 0 & 1 & 0 & \frac{1}{4} & 0 & \frac{1}{8} & 0 \\
4 & 0 & -20 & -3 & \frac{1}{3} & 0 & 0 & 0 & 0 & 1 & \frac{1}{4} & 0 & 0 & 0 \\
1 & \frac{3}{4} & \frac{80}{3} & 3 & \frac{1}{12} & \frac{5}{6} & -1 & -8 & -3 & -2 & -\frac{1}{2} & 8 & -\frac{1}{8} & 0 \\
0 & 0 & -\frac{20}{3} & -1 & 0 & 0 & 0 & 8 & 2 & 1 & 0 & 0 & 0 & 0 \\
1 & \frac{1}{4} & -4 & -1 & -\frac{1}{12} & -\frac{5}{6} & 1 & -18 & -5 & -2 & -\frac{1}{2} & 5 & -\frac{1}{8} & -1 \\
4 & 0 & 20 & 3 & -\frac{1}{3} & -2 & 0 & 48 & 12 & 5 & \frac{1}{4} & -12 & 0 & 0 \\
1 & -\frac{1}{4} & -\frac{68}{3} & -3 & -\frac{1}{12} & 0 & -1 & -38 & -9 & -4 & \frac{1}{4} & 3 & \frac{1}{8} & 1 \\
0 & 0 & \frac{20}{3} & 1 & 0 & 0 & 0 & 8 & 2 & 1 & 0 & 0 & 0 & 0
\end{array}\right).$$

Since the intermediate patch is subdivided into 4 patches, the outermost ring R_0 around

the fixed point of T_1^{IL} consists of three patches:

$$R_0 = T_1^L(\mathcal{A}^L) \cup T_2^L(\mathcal{A}^L) \cup T_2^{IL}(\mathcal{A}^{IL}).$$

All three patches lie within the convex hulls of their respective control points, since their corresponding subdivision matrices have non-negative components. We can calculate the coordinates of the respective control points in the basis P as follows by multiplying the corresponding matrix by P^{-1}. For two regular patches $= T_1^L(\mathcal{A}^L)$ and $T_2^L(\mathcal{A}^L)$ we obtain:

$$P^{-1} \times T_1^L = \begin{pmatrix}
1/12 & 1/12 & 1/12 & 1/12 & 1/12 & 1/12 & 1/12 & 1/12 & 1/12 \\
-1/2 & 1/2 & 1/2 & 0 & 0 & 0 & 0 & 0 & 0 \\
0 & 0 & 3/16 & 0 & 0 & 1/16 & 0 & 0 & 0 \\
0 & 0 & -5/4 & 0 & 0 & -5/12 & 0 & 0 & 0 \\
-109/12 & -109/12 & -109/12 & -17/4 & -17/4 & -17/4 & -5/12 & -5/12 & -5/12 \\
5/4 & 5/4 & 5/4 & 3/4 & 3/4 & 3/4 & 1/4 & 1/4 & 1/4 \\
7/12 & 11/24 & 1/3 & 3/8 & 1/4 & 1/8 & 1/6 & 1/24 & -1/12 \\
3/16 & -3/16 & -9/16 & 1/16 & -1/16 & -3/16 & 0 & 0 & 0 \\
-37/72 & 71/72 & 179/72 & -5/24 & 7/24 & 19/24 & -1/144 & -1/144 & -1/144 \\
-17/36 & -17/36 & -17/36 & -1/12 & -1/12 & -1/12 & 1/72 & 1/72 & 1/72 \\
38/3 & 38/3 & 38/3 & 14/3 & 14/3 & 14/3 & 1/6 & 1/6 & 1/6 \\
3/8 & 3/8 & 3/8 & 1/8 & 1/8 & 1/8 & 0 & 0 & 0 \\
-47/2 & -57/2 & -59/2 & -17/2 & -23/2 & -67/6 & 0 & -1 & 0 \\
-9/8 & -9/8 & -11/8 & -3/8 & -3/8 & -5/8 & 0 & 0 & -1/4
\end{pmatrix},$$

$$P^{-1} \times T_2^L = \begin{pmatrix}
1/12 & 1/12 & 1/12 & 1/12 & 1/12 & 1/12 & 1/12 & 1/12 & 1/12 \\
1/2 & 1/2 & -1/2 & 0 & 0 & 0 & 0 & 0 & 0 \\
0 & 3/16 & 9/16 & 0 & 1/16 & 3/16 & 0 & 0 & 0 \\
0 & -5/4 & -15/4 & 0 & -5/12 & -5/4 & 0 & 0 & -1/8 \\
-109/12 & -109/12 & -109/12 & -17/4 & -17/4 & -17/4 & -5/12 & -5/12 & -5/12 \\
5/4 & 5/4 & 5/4 & 3/4 & 3/4 & 3/4 & 1/4 & 1/4 & 1/4 \\
11/24 & 1/3 & 5/24 & 1/4 & 1/8 & 0 & 1/24 & -1/12 & -5/24 \\
-3/16 & -9/16 & -15/16 & -1/16 & -3/16 & -5/16 & 0 & 0 & 0 \\
71/72 & 179/72 & 287/72 & 7/24 & 19/24 & 31/24 & -1/144 & -1/144 & 17/144 \\
-17/36 & -17/36 & -17/36 & -1/12 & -1/12 & -1/12 & 1/72 & 1/72 & -1/9 \\
38/3 & 38/3 & 38/3 & 14/3 & 14/3 & 14/3 & 1/6 & 1/6 & -11/6 \\
3/8 & 3/8 & 3/8 & 1/8 & 1/8 & 1/8 & 0 & 0 & 0 \\
-57/2 & -59/2 & -53/2 & -23/2 & -67/6 & -15/2 & -1 & 0 & 5 \\
-9/8 & -11/8 & -15/8 & -3/8 & -5/8 & -9/8 & 0 & -1/4 & -1/4
\end{pmatrix}.$$

Here we have highlighted the rows corresponding to the sub-dominant eigenvectors. For both matrices one of the highlighted rows has strictly positive components. Therefore any point that is a weighted sum of the respective columns cannot have its coordinates corresponding to the sub-dominant eigenvectors simultaneously equal to zero. However should we calculate the coordinates of the control points for the third patch we would see that the convex hull includes the points with zeros at all three sub-dominant components simultaneously. So we need to compute a tighter hull. To achieve this we consider the next iteration. The third patch $T_2^{IL}(\mathcal{A}^{IL})$ consists of four smaller patches:

$$\mathcal{A}^{IL} = T_1^L(\mathcal{A}^{IL}) \cup T_2^L(\mathcal{A}^{IL}) \cup T_1^{IL}(\mathcal{A}^{IL}) \cup T_2^{IL}(\mathcal{A}^{IL}),$$

$$T_2^{IL}(\mathcal{A}^{IL}) = T_2^{IL}T_1^L(\mathcal{A}^{IL}) \cup T_2^{IL}T_2^L(\mathcal{A}^{IL}) \cup T_2^{IL}T_1^{IL}(\mathcal{A}^{IL}) \cup T_2^{IL}T_2^{IL}(\mathcal{A}^{IL}),.$$

Each of these patches lies within the convex hulls of its respective control points, and the patch $T_2^{IL}(\mathcal{A}^{IL})$ lies within the union of the four convex hulls. We calculate the coordinates of those control points in the basis P as

$$P^{-1} \times T_1^{IL} \times T_1^L(\mathcal{A}^L),$$

$$P^{-1} \times T_1^{IL} \times T_2^L(\mathcal{A}^L),$$

$$P^{-1} \times T_1^{IL} \times T_1^{IL}(\mathcal{A}^{IL}),$$

$$P^{-1} \times T_1^{IL} \times T_2^{IL}(\mathcal{A}^{IL}).$$

Here we provide only the rows that correspond to the sub-dominant eigenvectors. For the first two patches we get the following rows:

$$\begin{pmatrix} -79/24 & -79/24 & -79/24 & -11/8 & -11/8 & -11/8 & 1/24 & 1/24 & 1/24 \\ 5/8 & 5/8 & 5/8 & 3/8 & 3/8 & 3/8 & 1/8 & 1/8 & 1/8 \\ 1/6 & 5/48 & 1/24 & 1/16 & 0 & -1/16 & -1/24 & -5/48 & -1/6 \end{pmatrix},$$

$$\begin{pmatrix} -79/24 & -79/24 & -79/24 & -11/8 & -11/8 & -11/8 & 1/24 & 1/24 & 1/24 \\ 5/8 & 5/8 & 5/8 & 3/8 & 3/8 & 3/8 & 1/8 & 1/8 & 1/8 \\ 5/48 & 1/24 & -1/48 & 0 & -1/16 & -1/8 & -5/48 & -1/6 & -11/48 \end{pmatrix}.$$

For both patches there is a strictly positive row, so they do not contain any points with three zeros corresponding to the sub-dominant eigenvectors. For the last two patches we obtain the following rows:

$$\begin{pmatrix} -11/8 & -11/8 & -11/8 & 1/24 & 1/24 & 1/24 & 1/4 & 1/4 & 1/4 & 1/4 & -1/4 & -1/4 & -1/4 & -1/4 \\ 3/8 & 3/8 & 3/8 & 1/8 & 1/8 & 1/8 & 0 & 0 & 0 & 0 & 0 & 0 & 0 & 0 \\ 1/16 & 0 & -1/16 & -1/24 & -5/48 & -1/6 & -1/16 & -1/8 & -3/16 & -1/4 & -1/16 & -1/8 & -3/16 & -1/4 \end{pmatrix},$$

$$\begin{pmatrix} -11/8 & -11/8 & -11/8 & 1/24 & 1/24 & 1/24 & 1/4 & 1/4 & 1/4 & 1/4 & -1/4 & -1/4 & -1/4 & -1/4 \\ 3/8 & 3/8 & 3/8 & 1/8 & 1/8 & 1/8 & 0 & 0 & 0 & 0 & 0 & 0 & 0 & 0 \\ 0 & -1/16 & -1/8 & -5/48 & -1/6 & -11/48 & -1/8 & -3/16 & -1/4 & -5/16 & -1/8 & -3/16 & -1/4 & -5/16 \end{pmatrix}.$$

For both of them the components of the second row are non-negative. However each that has a 0 in a second component, also has a strictly negative component third component. So we conclude that no point inside the corresponding convex hull has all three sub-dominant components equal to 0 at the same time.

Final surface

The intermediate surface analysed above is presented in figure (see figure 5.26).

Our method can also be applied to fractal surfaces, and even spline patches can be connected to fractal surfaces (see figure 5.27).

5.3 Conclusion

In this chapter we studied the problem of connecting shapes defined by different iterative processes. Using the BCIFS formalism we defined an automaton that defines an intermediate curve. We also analysed the differential properties of that curve and modified the basic automaton to provide a more straightforward control over the shape of the intermediate curve. Then we applied a similar approach to building an intermediate surface. With the BCIFS formalism we described the topological subdivision of the intermediate surface and derived the continuity constraints. After that we analysed the differential proprieties of the constructed surface. We changed the basic automaton by introducing additional control points for the intermediate patch. Because we describe the intermediate surface as an attractor of a BCIFS and not as a subdivision scheme on a specific control mesh, we were able to connect different types of surfaces such as Doo-Sabin and Catmull-Clark surfaces as we demonstrated with our examples.

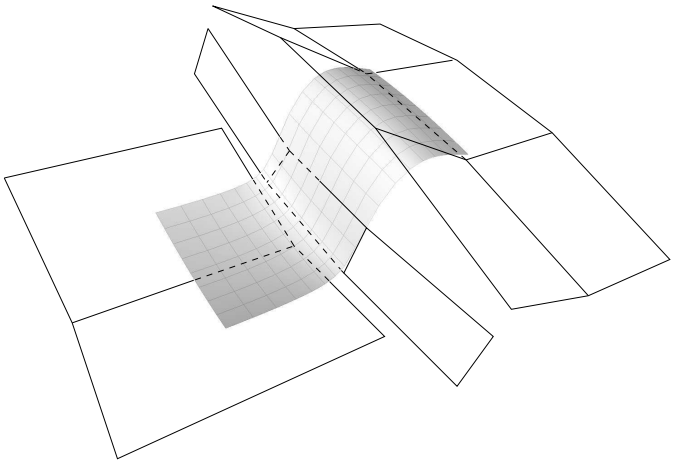

Figure 5.26: An intermediate surface between the Doo-Sabin and Catmull-Clark surfaces with control polygons for initial edges of initial surfaces and intermediate curve.

Figure 5.27: An intermediate surface between a fractal surface and a spline patch.

Chapter 6

Conclusion and perspectives

6.1 Conclusion

In this thesis we have studied the differential properties of self-similar sets. These sets are defined with Iterated Function Systems and its modification such as Controlled IFS and Boundary Controlled IFS. We have studied the wide range of differential behaviours that self-similar sets can exhibit and derived the necessary and sufficient conditions for differentiability for an everywhere dense set of points.

Previous works studied a limited set of shapes. [Ben09] studied the differential behaviour of curves in $\mathbb{R}^2$ and surfaces defined as the tensor product of curves. The studies of subdivision surfaces are limited to subdivision schemes with injective and regular characteristic maps. Our study deals with curves and surfaces in arbitrary dimensions and we utilise more general conditions than injectivity and regularity of the characteristic map.

We propose a more general definition of a tangent subspace than the classical tangent line or plane definitions. Our definition is based on the notion of the convergence of an angle between a secant and an affine subspace. This definition allows us to classify the multiple types of differential behaviour presented in attractors of the IFS such as "pinched" surface with only one tangent line at a point instead of a tangent plane or a rotating curve that touches the plane as well as classical cases of tangent line and a curve or a tangent plane and a surface. Then we use the properties of self-similarity to the necessary and sufficient conditions for existence of the tangent subspace.

The study of convergence is based on the notion of address. Each point of the IFS's attractor has an infinite string of symbols that identifies this point within the attractor. Based on this notion we have defined a nested set of neighbourhoods of the point. Studying the convergence of such nested sets allows us to study the differential behaviour of the attractor at the point in question. Using this notion we have studied the differential behaviour of a specific class of points. Namely points with periodic addresses. Such points form an everywhere dense set within the attractor.

We have shown that differential behaviour at the periodic points depends primarily on the eigenvalues and eigenvector of the transformation associated with the period found in its address. The existence of a tangent subspace depends on the sub-dominant eigenvalue(s). We have treated cases with different kinds of sub-dominant eigenvalue and its multiplicity.

We have also studied the behaviour produced by complex eigenvalues. Studying these different cases allowed us to derive the necessary and sufficient conditions.

Formulating these conditions enabled us to analyse the differential behaviour of various shapes. We studied the problem of joining shapes built by different iterative procedures. We suggested a method of constructing an intermediate curve between two curves and an intermediate surface between two surfaces. The initial shapes as well as the intermediate one is described as an attractor of BCIFS. Previously derived conditions allowed us to analyse the differential behaviour of the newly constructed shapes.

We also propose a way to construct an intermediate surface between two surfaces. We give a general topological subdivision of the intermediate surface between surfaces. Then we apply the general scheme to the problem of connecting Doo-Sabin (dual scheme) and Catmull-Clark (primal scheme) subdivision surfaces. Using the BCIFS formalism we derive the conditions on the subdivision matrices that guarantee the continuity of the intermediate surface. After that we use the necessary and sufficient conditions of the differentiability that we obtained previously to show when the intermediate surface has a tangent plane almost everywhere.

6.2 Perspectives and future work

Several problems are still open. First problem is the analysis of the differential behaviour of non-periodic points. The particular difficulty with such a set of points is that its position and immediate neighbourhood is dependent on the infinite non-periodic product of matrices. The notion of the joint spectral radius and Daubechies work on the infinite products of matrices [DL92] may be of interest for solving this problem.

Another unsolved problem is constructing shapes that belong to a certain continuity class with BCIFS. BCIFS formalism guarantees only C^0-continuity. The differential properties of the modelled shape depend on the eigenvector and eigenvalues of the subdivision matrices. Generally C^0-continuity constraints leave a certain number of degrees of freedom that allow to modify the differential behaviour of the shape. However these degrees of freedoms usually have a convoluted effect on the final shape. Hence a way to introduce higher degree continuity constraints to BCIFS model is needed.

We have also discussed the problem of controlling the differential behaviour and proposed some solutions for the particular cases in some of our examples (see chapter 5). However a more general approach that can be implemented in CAD systems in needed. This problem is closely related to the previous one. Solving these two problems will allow the development a CAD-system that will fully support the BCIFS model. Such a system will greatly facilitate the design and production process of complex shapes.

Appendix A

Appendix

A.1 Regular patches subdivision

Transformations that define the bi-quadratic patch subdivision:

$$L_1 = \begin{pmatrix} 9/16 & 3/16 & 0 & 3/16 & 1/16 & 0 & 0 & 0 & 0 \\ 3/16 & 9/16 & 9/16 & 1/16 & 3/16 & 3/16 & 0 & 0 & 0 \\ 0 & 0 & 3/16 & 0 & 0 & 1/16 & 0 & 0 & 0 \\ 3/16 & 1/16 & 0 & 9/16 & 3/16 & 0 & 9/16 & 3/16 & 0 \\ 1/16 & 3/16 & 3/16 & 3/16 & 9/16 & 9/16 & 3/16 & 9/16 & 9/16 \\ 0 & 0 & 1/16 & 0 & 0 & 3/16 & 0 & 0 & 3/16 \\ 0 & 0 & 0 & 0 & 0 & 0 & 3/16 & 1/16 & 0 \\ 0 & 0 & 0 & 0 & 0 & 0 & 1/16 & 3/16 & 3/16 \\ 0 & 0 & 0 & 0 & 0 & 0 & 0 & 0 & 1/16 \end{pmatrix}, \quad L_2 = \begin{pmatrix} 3/16 & 1/16 & 0 & 0 & 0 & 0 & 0 & 0 & 0 \\ 1/16 & 3/16 & 3/16 & 0 & 0 & 0 & 0 & 0 & 0 \\ 0 & 0 & 1/16 & 0 & 0 & 0 & 0 & 0 & 0 \\ 9/16 & 3/16 & 0 & 9/16 & 3/16 & 0 & 3/16 & 1/16 & 0 \\ 3/16 & 9/16 & 9/16 & 3/16 & 9/16 & 9/16 & 1/16 & 3/16 & 3/16 \\ 0 & 0 & 3/16 & 0 & 0 & 3/16 & 0 & 0 & 1/16 \\ 0 & 0 & 0 & 3/16 & 1/16 & 0 & 9/16 & 3/16 & 0 \\ 0 & 0 & 0 & 1/16 & 3/16 & 3/16 & 3/16 & 9/16 & 9/16 \\ 0 & 0 & 0 & 0 & 0 & 1/16 & 0 & 0 & 3/16 \end{pmatrix},$$

$$L_3 = \begin{pmatrix} 1/16 & 0 & 0 & 0 & 0 & 0 & 0 & 0 & 0 \\ 3/16 & 3/16 & 1/16 & 0 & 0 & 0 & 0 & 0 & 0 \\ 0 & 1/16 & 3/16 & 0 & 0 & 0 & 0 & 0 & 0 \\ 3/16 & 0 & 0 & 3/16 & 0 & 0 & 1/16 & 0 & 0 \\ 9/16 & 9/16 & 3/16 & 9/16 & 9/16 & 3/16 & 3/16 & 3/16 & 1/16 \\ 0 & 3/16 & 9/16 & 0 & 3/16 & 9/16 & 0 & 1/16 & 3/16 \\ 0 & 0 & 0 & 1/16 & 0 & 0 & 3/16 & 0 & 0 \\ 0 & 0 & 0 & 3/16 & 3/16 & 1/16 & 9/16 & 9/16 & 3/16 \\ 0 & 0 & 0 & 0 & 1/16 & 3/16 & 0 & 3/16 & 9/16 \end{pmatrix}, \quad L_4 = \begin{pmatrix} 3/16 & 0 & 0 & 1/16 & 0 & 0 & 0 & 0 & 0 \\ 9/16 & 9/16 & 3/16 & 3/16 & 3/16 & 1/16 & 0 & 0 & 0 \\ 0 & 3/16 & 9/16 & 0 & 1/16 & 3/16 & 0 & 0 & 0 \\ 1/16 & 0 & 0 & 3/16 & 0 & 0 & 3/16 & 0 & 0 \\ 3/16 & 3/16 & 1/16 & 9/16 & 9/16 & 3/16 & 9/16 & 9/16 & 3/16 \\ 0 & 1/16 & 3/16 & 0 & 3/16 & 9/16 & 0 & 3/16 & 9/16 \\ 0 & 0 & 0 & 0 & 0 & 0 & 1/16 & 0 & 0 \\ 0 & 0 & 0 & 0 & 0 & 0 & 3/16 & 3/16 & 1/16 \\ 0 & 0 & 0 & 0 & 0 & 0 & 0 & 1/16 & 3/16 \end{pmatrix}.$$

Transformations that define the bi-cubic patch subdivision:

$$R_1 = \begin{pmatrix} 1/16 & 1/64 & 0 & 0 & 0 & 0 & 0 & 0 & 0 & 0 & 0 & 0 & 0 & 0 & 0 & 0 \\ 1/16 & 3/32 & 1/16 & 1/64 & 0 & 0 & 0 & 0 & 0 & 0 & 0 & 0 & 0 & 0 & 0 & 0 \\ 0 & 1/64 & 1/16 & 3/32 & 0 & 0 & 0 & 0 & 0 & 0 & 0 & 0 & 0 & 0 & 0 & 0 \\ 0 & 0 & 0 & 1/64 & 0 & 0 & 0 & 0 & 0 & 0 & 0 & 0 & 0 & 0 & 0 & 0 \\ 3/8 & 3/32 & 0 & 0 & 1/4 & 1/16 & 0 & 0 & 1/16 & 1/64 & 0 & 0 & 0 & 0 & 0 & 0 \\ 3/8 & 9/16 & 3/8 & 3/32 & 1/4 & 3/8 & 1/4 & 1/16 & 1/16 & 3/32 & 1/16 & 1/64 & 0 & 0 & 0 & 0 \\ 0 & 3/32 & 3/8 & 9/16 & 0 & 1/16 & 1/4 & 3/8 & 0 & 1/64 & 1/16 & 3/32 & 0 & 0 & 0 & 0 \\ 0 & 0 & 0 & 3/32 & 0 & 0 & 0 & 1/16 & 0 & 0 & 0 & 1/64 & 0 & 0 & 0 & 0 \\ 1/16 & 1/64 & 0 & 0 & 1/4 & 1/16 & 0 & 0 & 3/8 & 3/32 & 0 & 0 & 1/4 & 1/16 & 0 & 0 \\ 1/16 & 3/32 & 1/16 & 1/64 & 1/4 & 3/8 & 1/4 & 1/16 & 3/8 & 9/16 & 3/8 & 3/32 & 1/4 & 3/8 & 1/4 & 1/16 \\ 0 & 1/64 & 1/16 & 3/32 & 0 & 1/16 & 1/4 & 3/8 & 0 & 3/32 & 3/8 & 9/16 & 0 & 1/16 & 1/4 & 3/8 \\ 0 & 0 & 0 & 1/64 & 0 & 0 & 0 & 1/16 & 0 & 0 & 0 & 3/32 & 0 & 0 & 0 & 1/16 \\ 0 & 0 & 0 & 0 & 0 & 0 & 0 & 0 & 1/16 & 1/64 & 0 & 0 & 1/4 & 1/16 & 0 & 0 \\ 0 & 0 & 0 & 0 & 0 & 0 & 0 & 0 & 1/16 & 3/32 & 1/16 & 1/64 & 1/4 & 3/8 & 1/4 & 1/16 \\ 0 & 0 & 0 & 0 & 0 & 0 & 0 & 0 & 0 & 1/64 & 1/16 & 3/32 & 0 & 1/16 & 1/4 & 3/8 \\ 0 & 0 & 0 & 0 & 0 & 0 & 0 & 0 & 0 & 0 & 0 & 1/64 & 0 & 0 & 0 & 1/16 \end{pmatrix},$$

$$R_2 = \begin{pmatrix} 1/16 & 1/64 & 0 & 0 & 0 & 0 & 0 & 0 & 0 & 0 & 0 & 0 & 0 & 0 & 0 & 0 \\ 1/16 & 3/32 & 1/16 & 1/64 & 0 & 0 & 0 & 0 & 0 & 0 & 0 & 0 & 0 & 0 & 0 & 0 \\ 0 & 1/64 & 1/16 & 3/32 & 0 & 0 & 0 & 0 & 0 & 0 & 0 & 0 & 0 & 0 & 0 & 0 \\ 0 & 0 & 0 & 1/64 & 0 & 0 & 0 & 0 & 0 & 0 & 0 & 0 & 0 & 0 & 0 & 0 \\ 3/8 & 3/32 & 0 & 0 & 1/4 & 1/16 & 0 & 0 & 1/16 & 1/64 & 0 & 0 & 0 & 0 & 0 & 0 \\ 3/8 & 9/16 & 3/8 & 3/32 & 1/4 & 3/8 & 1/4 & 1/16 & 1/16 & 3/32 & 1/16 & 1/64 & 0 & 0 & 0 & 0 \\ 0 & 3/32 & 3/8 & 9/16 & 0 & 1/16 & 1/4 & 3/8 & 0 & 1/64 & 1/16 & 3/32 & 0 & 0 & 0 & 0 \\ 0 & 0 & 0 & 3/32 & 0 & 0 & 0 & 1/16 & 0 & 0 & 0 & 1/64 & 0 & 0 & 0 & 0 \\ 1/16 & 1/64 & 0 & 0 & 1/4 & 1/16 & 0 & 0 & 3/8 & 3/32 & 0 & 0 & 1/4 & 1/16 & 0 & 0 \\ 1/16 & 3/32 & 1/16 & 1/64 & 1/4 & 3/8 & 1/4 & 1/16 & 3/8 & 9/16 & 3/8 & 3/32 & 1/4 & 3/8 & 1/4 & 1/16 \\ 0 & 1/64 & 1/16 & 3/32 & 0 & 1/16 & 1/4 & 3/8 & 0 & 3/32 & 3/8 & 9/16 & 0 & 1/16 & 1/4 & 3/8 \\ 0 & 0 & 0 & 1/64 & 0 & 0 & 0 & 1/16 & 0 & 0 & 0 & 3/32 & 0 & 0 & 0 & 1/16 \\ 0 & 0 & 0 & 0 & 0 & 0 & 0 & 0 & 1/16 & 1/64 & 0 & 0 & 1/4 & 1/16 & 0 & 0 \\ 0 & 0 & 0 & 0 & 0 & 0 & 0 & 0 & 1/16 & 3/32 & 1/16 & 1/64 & 1/4 & 3/8 & 1/4 & 1/16 \\ 0 & 0 & 0 & 0 & 0 & 0 & 0 & 0 & 0 & 1/64 & 1/16 & 3/32 & 0 & 1/16 & 1/4 & 3/8 \\ 0 & 0 & 0 & 0 & 0 & 0 & 0 & 0 & 0 & 0 & 0 & 1/64 & 0 & 0 & 0 & 1/16 \end{pmatrix},$$

$$R_3 = \begin{pmatrix}
1/64 & 0 & 0 & 0 & 0 & 0 & 0 & 0 & 0 & 0 & 0 & 0 & 0 & 0 & 0 & 0 \\
3/32 & 1/16 & 1/64 & 0 & 0 & 0 & 0 & 0 & 0 & 0 & 0 & 0 & 0 & 0 & 0 & 0 \\
1/64 & 1/16 & 3/32 & 1/16 & 0 & 0 & 0 & 0 & 0 & 0 & 0 & 0 & 0 & 0 & 0 & 0 \\
0 & 0 & 1/64 & 1/16 & 0 & 0 & 0 & 0 & 0 & 0 & 0 & 0 & 0 & 0 & 0 & 0 \\
3/32 & 0 & 0 & 0 & 1/16 & 0 & 0 & 0 & 1/64 & 0 & 0 & 0 & 0 & 0 & 0 & 0 \\
9/16 & 3/8 & 3/32 & 0 & 3/8 & 1/4 & 1/16 & 0 & 3/32 & 1/16 & 1/64 & 0 & 0 & 0 & 0 & 0 \\
3/32 & 3/8 & 9/16 & 3/8 & 1/16 & 1/4 & 3/8 & 1/4 & 1/64 & 1/16 & 3/32 & 1/16 & 0 & 0 & 0 & 0 \\
0 & 0 & 3/32 & 3/8 & 0 & 0 & 1/16 & 1/4 & 0 & 0 & 1/64 & 1/16 & 0 & 0 & 0 & 0 \\
1/64 & 0 & 0 & 0 & 1/16 & 0 & 0 & 0 & 3/32 & 0 & 0 & 0 & 1/16 & 0 & 0 & 0 \\
3/32 & 1/16 & 1/64 & 0 & 3/8 & 1/4 & 1/16 & 0 & 9/16 & 3/8 & 3/32 & 0 & 3/8 & 1/4 & 1/16 & 0 \\
1/64 & 1/16 & 3/32 & 1/16 & 1/16 & 1/4 & 3/8 & 1/4 & 3/32 & 3/8 & 9/16 & 3/8 & 1/16 & 1/4 & 3/8 & 1/4 \\
0 & 0 & 1/64 & 1/16 & 0 & 0 & 1/16 & 1/4 & 0 & 0 & 3/32 & 3/8 & 0 & 0 & 1/16 & 1/4 \\
0 & 0 & 0 & 0 & 0 & 0 & 0 & 0 & 1/64 & 0 & 0 & 0 & 1/16 & 0 & 0 & 0 \\
0 & 0 & 0 & 0 & 0 & 0 & 0 & 0 & 3/32 & 1/16 & 1/64 & 0 & 3/8 & 1/4 & 1/16 & 0 \\
0 & 0 & 0 & 0 & 0 & 0 & 0 & 0 & 1/64 & 1/16 & 3/32 & 1/16 & 1/16 & 1/4 & 3/8 & 1/4 \\
0 & 0 & 0 & 0 & 0 & 0 & 0 & 0 & 0 & 0 & 1/64 & 1/16 & 0 & 0 & 1/16 & 1/4
\end{pmatrix},$$

$$R_4 = \begin{pmatrix}
1/16 & 0 & 0 & 0 & 1/64 & 0 & 0 & 0 & 0 & 0 & 0 & 0 & 0 & 0 & 0 & 0 \\
3/8 & 1/4 & 1/16 & 0 & 3/32 & 1/16 & 1/64 & 0 & 0 & 0 & 0 & 0 & 0 & 0 & 0 & 0 \\
1/16 & 1/4 & 3/8 & 1/4 & 1/64 & 1/16 & 3/32 & 1/16 & 0 & 0 & 0 & 0 & 0 & 0 & 0 & 0 \\
0 & 0 & 1/16 & 1/4 & 0 & 0 & 1/64 & 1/16 & 0 & 0 & 0 & 0 & 0 & 0 & 0 & 0 \\
1/16 & 0 & 0 & 0 & 3/32 & 0 & 0 & 0 & 1/16 & 0 & 0 & 0 & 1/64 & 0 & 0 & 0 \\
3/8 & 1/4 & 1/16 & 0 & 9/16 & 3/8 & 3/32 & 0 & 3/8 & 1/4 & 1/16 & 0 & 3/32 & 1/16 & 1/64 & 0 \\
1/16 & 1/4 & 3/8 & 1/4 & 3/32 & 3/8 & 9/16 & 3/8 & 1/16 & 1/4 & 3/8 & 1/4 & 1/64 & 1/16 & 3/32 & 1/16 \\
0 & 0 & 1/16 & 1/4 & 0 & 0 & 3/32 & 3/8 & 0 & 0 & 1/16 & 1/4 & 0 & 0 & 1/64 & 1/16 \\
0 & 0 & 0 & 0 & 1/64 & 0 & 0 & 0 & 1/16 & 0 & 0 & 0 & 3/32 & 0 & 0 & 0 \\
0 & 0 & 0 & 0 & 3/32 & 1/16 & 1/64 & 0 & 3/8 & 1/4 & 1/16 & 0 & 9/16 & 3/8 & 3/32 & 0 \\
0 & 0 & 0 & 0 & 1/64 & 1/16 & 3/32 & 1/16 & 1/16 & 1/4 & 3/8 & 1/4 & 3/32 & 3/8 & 9/16 & 3/8 \\
0 & 0 & 0 & 0 & 0 & 0 & 1/64 & 1/16 & 0 & 0 & 1/16 & 1/4 & 0 & 0 & 3/32 & 3/8 \\
0 & 0 & 0 & 0 & 0 & 0 & 0 & 0 & 0 & 0 & 0 & 0 & 1/64 & 0 & 0 & 0 \\
0 & 0 & 0 & 0 & 0 & 0 & 0 & 0 & 0 & 0 & 0 & 0 & 3/32 & 1/16 & 1/64 & 0 \\
0 & 0 & 0 & 0 & 0 & 0 & 0 & 0 & 0 & 0 & 0 & 0 & 1/64 & 1/16 & 3/32 & 1/16 \\
0 & 0 & 0 & 0 & 0 & 0 & 0 & 0 & 0 & 0 & 0 & 0 & 0 & 0 & 1/64 & 1/16
\end{pmatrix}.$$

A.2 Intermediate patches subdivision

Subdivision matrices for the Doo-Sabin side of intermediate surface.

$$T_1^L = \begin{pmatrix}
9/16 & 3/16 & 0 & 3/16 & 1/16 & 0 & a & b & 0 \\
3/16 & 9/16 & 9/16 & 1/16 & 3/16 & 3/16 & b & a & a \\
0 & 0 & 3/16 & 0 & 0 & 1/16 & 0 & 0 & b \\
3/16 & 1/16 & 0 & 9/16 & 3/16 & 0 & d & e & 0 \\
1/16 & 3/16 & 3/16 & 3/16 & 9/16 & 9/16 & e & d & d \\
0 & 0 & 1/16 & 0 & 0 & 3/16 & 0 & 0 & e \\
0 & 0 & 0 & 0 & 0 & 0 & g & i & 0 \\
0 & 0 & 0 & 0 & 0 & 0 & h & h & g \\
0 & 0 & 0 & 0 & 0 & 0 & i & g & h \\
0 & 0 & 0 & 0 & 0 & 0 & 0 & 0 & i \\
0 & 0 & 0 & 0 & 0 & 0 & k & m & 0 \\
0 & 0 & 0 & 0 & 0 & 0 & l & l & k \\
0 & 0 & 0 & 0 & 0 & 0 & m & k & l \\
0 & 0 & 0 & 0 & 0 & 0 & 0 & 0 & m
\end{pmatrix}, \quad T_2^L = \begin{pmatrix}
3/16 & 0 & 0 & 1/16 & 0 & 0 & b & 0 & 0 \\
9/16 & 9/16 & 3/16 & 3/16 & 3/16 & 1/16 & a & a & b \\
0 & 3/16 & 9/16 & 0 & 1/16 & 3/16 & 0 & b & a \\
1/16 & 0 & 0 & 3/16 & 0 & 0 & e & 0 & 0 \\
3/16 & 3/16 & 1/16 & 9/16 & 9/16 & 3/16 & d & d & e \\
0 & 1/16 & 3/16 & 0 & 3/16 & 9/16 & 0 & e & d \\
0 & 0 & 0 & 0 & 0 & 0 & i & 0 & 0 \\
0 & 0 & 0 & 0 & 0 & 0 & h & g & i \\
0 & 0 & 0 & 0 & 0 & 0 & g & h & h \\
0 & 0 & 0 & 0 & 0 & 0 & 0 & i & g \\
0 & 0 & 0 & 0 & 0 & 0 & m & 0 & 0 \\
0 & 0 & 0 & 0 & 0 & 0 & l & k & m \\
0 & 0 & 0 & 0 & 0 & 0 & k & l & l \\
0 & 0 & 0 & 0 & 0 & 0 & 0 & m & k
\end{pmatrix},$$

$$T_1^{IL} = \begin{pmatrix}
3/16 & 1/16 & 0 & a & b & 0 & 0 & 0 & 0 & 0 & 0 & 0 & 0 & 0 \\
1/16 & 3/16 & 3/16 & b & a & a & 0 & 0 & 0 & 0 & 0 & 0 & 0 & 0 \\
0 & 0 & 1/16 & 0 & 0 & b & 0 & 0 & 0 & 0 & 0 & 0 & 0 & 0 \\
9/16 & 3/16 & 0 & d & e & 0 & 0 & 0 & 0 & 0 & 0 & 0 & 0 & 0 \\
3/16 & 9/16 & 9/16 & e & d & d & 0 & 0 & 0 & 0 & 0 & 0 & 0 & 0 \\
0 & 0 & 3/16 & 0 & 0 & e & 0 & 0 & 0 & 0 & 0 & 0 & 0 & 0 \\
0 & 0 & 0 & g & i & 0 & 3/8 & 3/32 & 0 & 0 & 1/8 & 1/32 & 0 & 0 \\
0 & 0 & 0 & h & h & g & 3/8 & 9/16 & 3/8 & 3/32 & 1/8 & 3/16 & 1/8 & 1/32 \\
0 & 0 & 0 & i & g & h & 0 & 3/32 & 3/8 & 9/16 & 0 & 1/32 & 1/8 & 3/16 \\
0 & 0 & 0 & 0 & 0 & i & 0 & 0 & 0 & 3/32 & 0 & 0 & 0 & 1/32 \\
0 & 0 & 0 & k & m & 0 & 1/8 & 1/32 & 0 & 0 & 3/8 & 3/32 & 0 & 0 \\
0 & 0 & 0 & l & l & k & 1/8 & 3/16 & 1/8 & 1/32 & 3/8 & 9/16 & 3/8 & 3/32 \\
0 & 0 & 0 & m & k & l & 0 & 1/32 & 1/8 & 3/16 & 0 & 3/32 & 3/8 & 9/16 \\
0 & 0 & 0 & 0 & 0 & m & 0 & 0 & 0 & 1/32 & 0 & 0 & 0 & 3/32
\end{pmatrix},$$

$$T_2^{IL} = \begin{pmatrix}
1/16 & 0 & 0 & b & 0 & 0 & 0 & 0 & 0 & 0 & 0 & 0 & 0 & 0 \\
3/16 & 3/16 & 1/16 & a & a & b & 0 & 0 & 0 & 0 & 0 & 0 & 0 & 0 \\
0 & 1/16 & 3/16 & 0 & b & a & 0 & 0 & 0 & 0 & 0 & 0 & 0 & 0 \\
3/16 & 0 & 0 & e & 0 & 0 & 0 & 0 & 0 & 0 & 0 & 0 & 0 & 0 \\
9/16 & 9/16 & 3/16 & d & d & e & 0 & 0 & 0 & 0 & 0 & 0 & 0 & 0 \\
0 & 3/16 & 9/16 & 0 & e & d & 0 & 0 & 0 & 0 & 0 & 0 & 0 & 0 \\
0 & 0 & 0 & i & 0 & 0 & 3/32 & 0 & 0 & 0 & 1/32 & 0 & 0 & 0 \\
0 & 0 & 0 & h & g & i & 9/16 & 3/8 & 3/32 & 0 & 3/16 & 1/8 & 1/32 & 0 \\
0 & 0 & 0 & g & h & h & 3/32 & 3/8 & 9/16 & 3/8 & 1/32 & 1/8 & 3/16 & 1/8 \\
0 & 0 & 0 & 0 & i & g & 0 & 0 & 3/32 & 3/8 & 0 & 0 & 1/32 & 1/8 \\
0 & 0 & 0 & m & 0 & 0 & 1/32 & 0 & 0 & 0 & 3/32 & 0 & 0 & 0 \\
0 & 0 & 0 & l & k & m & 3/16 & 1/8 & 1/32 & 0 & 9/16 & 3/8 & 3/32 & 0 \\
0 & 0 & 0 & k & l & l & 1/32 & 1/8 & 3/16 & 1/8 & 3/32 & 3/8 & 9/16 & 3/8 \\
0 & 0 & 0 & 0 & m & k & 0 & 0 & 1/32 & 1/8 & 0 & 0 & 3/32 & 3/8
\end{pmatrix}.$$

Subdivision matrices for the Catmull Clark side of intermediate surface.

$$T_1^R = \begin{pmatrix}
1/4 & 1/16 & 0 & 0 & 1/16 & 1/64 & 0 & 0 & 0 & 0 & 0 & 0 & ma & na & 0 & 0 \\
1/4 & 3/8 & 1/4 & 1/16 & 1/16 & 3/32 & 1/16 & 1/64 & 0 & 0 & 0 & 0 & mb & nb & ma & na \\
0 & 1/16 & 1/4 & 3/8 & 0 & 1/64 & 1/16 & 3/32 & 0 & 0 & 0 & 0 & 0 & nc & mb & nb \\
0 & 0 & 0 & 1/16 & 0 & 0 & 0 & 1/64 & 0 & 0 & 0 & 0 & 0 & 0 & 0 & nc \\
1/4 & 1/16 & 0 & 0 & 3/8 & 3/32 & 0 & 0 & 1/4 & 1/16 & 0 & 0 & me & ne & 0 & 0 \\
1/4 & 3/8 & 1/4 & 1/16 & 3/8 & 9/16 & 3/8 & 3/32 & 1/4 & 3/8 & 1/4 & 1/16 & mf & nf & me & ne \\
0 & 1/16 & 1/4 & 3/8 & 0 & 3/32 & 3/8 & 9/16 & 0 & 1/16 & 1/4 & 3/8 & 0 & ng & mf & nf \\
0 & 0 & 0 & 1/16 & 0 & 0 & 0 & 3/32 & 0 & 0 & 0 & 1/16 & 0 & 0 & 0 & ng \\
0 & 0 & 0 & 0 & 1/16 & 1/64 & 0 & 0 & 1/4 & 1/16 & 0 & 0 & mi & ni & 0 & 0 \\
0 & 0 & 0 & 0 & 1/16 & 3/32 & 1/16 & 1/64 & 1/4 & 3/8 & 1/4 & 1/16 & mj & nj & mi & ni \\
0 & 0 & 0 & 0 & 0 & 1/64 & 1/16 & 3/32 & 0 & 1/16 & 1/4 & 3/8 & 0 & nk & mj & nj \\
0 & 0 & 0 & 0 & 0 & 0 & 0 & 1/64 & 0 & 0 & 0 & 1/16 & 0 & 0 & 0 & nk \\
0 & 0 & 0 & 0 & 0 & 0 & 0 & 0 & 0 & 0 & 0 & 0 & mm & nm & 0 & 0 \\
0 & 0 & 0 & 0 & 0 & 0 & 0 & 0 & 0 & 0 & 0 & 0 & mn & nn & mm & nm \\
0 & 0 & 0 & 0 & 0 & 0 & 0 & 0 & 0 & 0 & 0 & 0 & 0 & no & mn & nn \\
0 & 0 & 0 & 0 & 0 & 0 & 0 & 0 & 0 & 0 & 0 & 0 & 0 & 0 & 0 & no \\
0 & 0 & 0 & 0 & 0 & 0 & 0 & 0 & 0 & 0 & 0 & 0 & mq & nq & 0 & 0 \\
0 & 0 & 0 & 0 & 0 & 0 & 0 & 0 & 0 & 0 & 0 & 0 & mr & nr & mq & nq \\
0 & 0 & 0 & 0 & 0 & 0 & 0 & 0 & 0 & 0 & 0 & 0 & 0 & ns & mr & nr \\
0 & 0 & 0 & 0 & 0 & 0 & 0 & 0 & 0 & 0 & 0 & 0 & 0 & 0 & 0 & ns
\end{pmatrix},$$

$$T_2^R = \begin{pmatrix}
1/16 & 0 & 0 & 0 & 1/64 & 0 & 0 & 0 & 0 & 0 & 0 & 0 & na & 0 & 0 & 0 \\
3/8 & 1/4 & 1/16 & 0 & 3/32 & 1/16 & 1/64 & 0 & 0 & 0 & 0 & 0 & nb & ma & na & 0 \\
1/16 & 1/4 & 3/8 & 1/4 & 1/64 & 1/16 & 3/32 & 1/16 & 0 & 0 & 0 & 0 & nc & mb & nb & ma \\
0 & 0 & 1/16 & 1/4 & 0 & 0 & 1/64 & 1/16 & 0 & 0 & 0 & 0 & 0 & 0 & nc & mb \\
1/16 & 0 & 0 & 0 & 3/32 & 0 & 0 & 0 & 1/16 & 0 & 0 & 0 & ne & 0 & 0 & 0 \\
3/8 & 1/4 & 1/16 & 0 & 9/16 & 3/8 & 3/32 & 0 & 3/8 & 1/4 & 1/16 & 0 & nf & me & ne & 0 \\
1/16 & 1/4 & 3/8 & 1/4 & 3/32 & 3/8 & 9/16 & 3/8 & 1/16 & 1/4 & 3/8 & 1/4 & ng & mf & nf & me \\
0 & 0 & 1/16 & 1/4 & 0 & 0 & 3/32 & 3/8 & 0 & 0 & 1/16 & 1/4 & 0 & 0 & ng & mf \\
0 & 0 & 0 & 0 & 1/64 & 0 & 0 & 0 & 1/16 & 0 & 0 & 0 & ni & 0 & 0 & 0 \\
0 & 0 & 0 & 0 & 3/32 & 1/16 & 1/64 & 0 & 3/8 & 1/4 & 1/16 & 0 & nj & mi & ni & 0 \\
0 & 0 & 0 & 0 & 1/64 & 1/16 & 3/32 & 1/16 & 1/16 & 1/4 & 3/8 & 1/4 & nk & mj & nj & mi \\
0 & 0 & 0 & 0 & 0 & 0 & 1/64 & 1/16 & 0 & 0 & 1/16 & 1/4 & 0 & 0 & nk & mj \\
0 & 0 & 0 & 0 & 0 & 0 & 0 & 0 & 0 & 0 & 0 & 0 & nm & 0 & 0 & 0 \\
0 & 0 & 0 & 0 & 0 & 0 & 0 & 0 & 0 & 0 & 0 & 0 & nn & mm & nm & 0 \\
0 & 0 & 0 & 0 & 0 & 0 & 0 & 0 & 0 & 0 & 0 & 0 & no & mn & nn & mm \\
0 & 0 & 0 & 0 & 0 & 0 & 0 & 0 & 0 & 0 & 0 & 0 & 0 & 0 & no & mn \\
0 & 0 & 0 & 0 & 0 & 0 & 0 & 0 & 0 & 0 & 0 & 0 & nq & 0 & 0 & 0 \\
0 & 0 & 0 & 0 & 0 & 0 & 0 & 0 & 0 & 0 & 0 & 0 & nr & mq & nq & 0 \\
0 & 0 & 0 & 0 & 0 & 0 & 0 & 0 & 0 & 0 & 0 & 0 & ns & mr & nr & mq \\
0 & 0 & 0 & 0 & 0 & 0 & 0 & 0 & 0 & 0 & 0 & 0 & 0 & 0 & ns & mr
\end{pmatrix},$$

$$T_1^{IR} = \begin{pmatrix}
1/16 & 1/64 & 0 & 0 & 0 & 0 & 0 & 0 & ma & na & 0 & 0 & 0 & 0 & 0 & 0 & 0 & 0 & 0 & 0 \\
1/16 & 3/32 & 1/16 & 1/64 & 0 & 0 & 0 & 0 & mb & nb & ma & na & 0 & 0 & 0 & 0 & 0 & 0 & 0 & 0 \\
0 & 1/64 & 1/16 & 3/32 & 0 & 0 & 0 & 0 & 0 & nc & mb & nb & 0 & 0 & 0 & 0 & 0 & 0 & 0 & 0 \\
0 & 0 & 0 & 1/64 & 0 & 0 & 0 & 0 & 0 & 0 & 0 & nc & 0 & 0 & 0 & 0 & 0 & 0 & 0 & 0 \\
3/8 & 3/32 & 0 & 0 & 1/4 & 1/16 & 0 & 0 & me & ne & 0 & 0 & 0 & 0 & 0 & 0 & 0 & 0 & 0 & 0 \\
3/8 & 9/16 & 3/8 & 3/32 & 1/4 & 3/8 & 1/4 & 1/16 & mf & nf & me & ne & 0 & 0 & 0 & 0 & 0 & 0 & 0 & 0 \\
0 & 3/32 & 3/8 & 9/16 & 0 & 1/16 & 1/4 & 3/8 & 0 & ng & mf & nf & 0 & 0 & 0 & 0 & 0 & 0 & 0 & 0 \\
0 & 0 & 0 & 3/32 & 0 & 0 & 0 & 1/16 & 0 & 0 & 0 & ng & 0 & 0 & 0 & 0 & 0 & 0 & 0 & 0 \\
1/16 & 1/64 & 0 & 0 & 1/4 & 1/16 & 0 & 0 & mi & ni & 0 & 0 & 0 & 0 & 0 & 0 & 0 & 0 & 0 & 0 \\
1/16 & 3/32 & 1/16 & 1/64 & 1/4 & 3/8 & 1/4 & 1/16 & mj & nj & mi & ni & 0 & 0 & 0 & 0 & 0 & 0 & 0 & 0 \\
0 & 1/64 & 1/16 & 3/32 & 0 & 1/16 & 1/4 & 3/8 & 0 & nk & mj & nj & 0 & 0 & 0 & 0 & 0 & 0 & 0 & 0 \\
0 & 0 & 0 & 1/64 & 0 & 0 & 0 & 1/16 & 0 & 0 & 0 & nk & 0 & 0 & 0 & 0 & 0 & 0 & 0 & 0 \\
0 & 0 & 0 & 0 & 0 & 0 & 0 & 0 & mm & nm & 0 & 0 & 3/8 & 3/32 & 0 & 0 & 1/8 & 1/32 & 0 & 0 \\
0 & 0 & 0 & 0 & 0 & 0 & 0 & 0 & mn & nn & mm & nm & 3/8 & 9/16 & 3/8 & 3/32 & 1/8 & 3/16 & 1/8 & 1/32 \\
0 & 0 & 0 & 0 & 0 & 0 & 0 & 0 & 0 & no & mn & nn & 0 & 3/32 & 3/8 & 9/16 & 0 & 1/32 & 1/8 & 3/16 \\
0 & 0 & 0 & 0 & 0 & 0 & 0 & 0 & 0 & 0 & 0 & no & 0 & 0 & 0 & 3/32 & 0 & 0 & 0 & 1/32 \\
0 & 0 & 0 & 0 & 0 & 0 & 0 & 0 & mq & nq & 0 & 0 & 1/8 & 1/32 & 0 & 0 & 3/8 & 3/32 & 0 & 0 \\
0 & 0 & 0 & 0 & 0 & 0 & 0 & 0 & mr & nr & mq & nq & 1/8 & 3/16 & 1/8 & 1/32 & 3/8 & 9/16 & 3/8 & 3/32 \\
0 & 0 & 0 & 0 & 0 & 0 & 0 & 0 & 0 & ns & mr & nr & 0 & 1/32 & 1/8 & 3/16 & 0 & 3/32 & 3/8 & 9/16 \\
0 & 0 & 0 & 0 & 0 & 0 & 0 & 0 & 0 & 0 & 0 & ns & 0 & 0 & 0 & 1/32 & 0 & 0 & 0 & 3/32
\end{pmatrix},$$

$$T_2^{IR} = \begin{pmatrix}
1/64 & 0 & 0 & 0 & 0 & 0 & 0 & 0 & na & 0 & 0 & 0 & 0 & 0 & 0 & 0 & 0 & 0 & 0 & 0 \\
3/32 & 1/16 & 1/64 & 0 & 0 & 0 & 0 & 0 & nb & ma & na & 0 & 0 & 0 & 0 & 0 & 0 & 0 & 0 & 0 \\
1/64 & 1/16 & 3/32 & 1/16 & 0 & 0 & 0 & 0 & nc & mb & nb & ma & 0 & 0 & 0 & 0 & 0 & 0 & 0 & 0 \\
0 & 0 & 1/64 & 1/16 & 0 & 0 & 0 & 0 & 0 & 0 & nc & mb & 0 & 0 & 0 & 0 & 0 & 0 & 0 & 0 \\
3/32 & 0 & 0 & 0 & 1/16 & 0 & 0 & 0 & ne & 0 & 0 & 0 & 0 & 0 & 0 & 0 & 0 & 0 & 0 & 0 \\
9/16 & 3/8 & 3/32 & 0 & 3/8 & 1/4 & 1/16 & 0 & nf & me & ne & 0 & 0 & 0 & 0 & 0 & 0 & 0 & 0 & 0 \\
3/32 & 3/8 & 9/16 & 3/8 & 1/16 & 1/4 & 3/8 & 1/4 & ng & mf & nf & me & 0 & 0 & 0 & 0 & 0 & 0 & 0 & 0 \\
0 & 0 & 3/32 & 3/8 & 0 & 0 & 1/16 & 1/4 & 0 & 0 & ng & mf & 0 & 0 & 0 & 0 & 0 & 0 & 0 & 0 \\
1/64 & 0 & 0 & 0 & 1/16 & 0 & 0 & 0 & ni & 0 & 0 & 0 & 0 & 0 & 0 & 0 & 0 & 0 & 0 & 0 \\
3/32 & 1/16 & 1/64 & 0 & 3/8 & 1/4 & 1/16 & 0 & nj & mi & ni & 0 & 0 & 0 & 0 & 0 & 0 & 0 & 0 & 0 \\
1/64 & 1/16 & 3/32 & 1/16 & 1/16 & 1/4 & 3/8 & 1/4 & nk & mj & nj & mi & 0 & 0 & 0 & 0 & 0 & 0 & 0 & 0 \\
0 & 0 & 1/64 & 1/16 & 0 & 0 & 1/16 & 1/4 & 0 & 0 & nk & mj & 0 & 0 & 0 & 0 & 0 & 0 & 0 & 0 \\
0 & 0 & 0 & 0 & 0 & 0 & 0 & 0 & nm & 0 & 0 & 0 & 3/32 & 0 & 0 & 0 & 1/32 & 0 & 0 & 0 \\
0 & 0 & 0 & 0 & 0 & 0 & 0 & 0 & nn & mm & nm & 0 & 9/16 & 3/8 & 3/32 & 0 & 3/16 & 1/8 & 1/32 & 0 \\
0 & 0 & 0 & 0 & 0 & 0 & 0 & 0 & no & mn & nn & mm & 3/32 & 3/8 & 9/16 & 3/8 & 1/32 & 1/8 & 3/16 & 1/8 \\
0 & 0 & 0 & 0 & 0 & 0 & 0 & 0 & 0 & 0 & no & mn & 0 & 0 & 3/32 & 3/8 & 0 & 0 & 1/32 & 1/8 \\
0 & 0 & 0 & 0 & 0 & 0 & 0 & 0 & nq & 0 & 0 & 0 & 1/32 & 0 & 0 & 0 & 3/32 & 0 & 0 & 0 \\
0 & 0 & 0 & 0 & 0 & 0 & 0 & 0 & nr & mq & nq & 0 & 3/16 & 1/8 & 1/32 & 0 & 9/16 & 3/8 & 3/32 & 0 \\
0 & 0 & 0 & 0 & 0 & 0 & 0 & 0 & ns & mr & nr & mq & 1/32 & 1/8 & 3/16 & 1/8 & 3/32 & 3/8 & 9/16 & 3/8 \\
0 & 0 & 0 & 0 & 0 & 0 & 0 & 0 & 0 & 0 & ns & mr & 0 & 0 & 1/32 & 1/8 & 0 & 0 & 3/32 & 3/8
\end{pmatrix}.$$

The following values of parameters were used in the example presented in section 5.2.5. $a = 0$, $b = 0$, $d = 1/4$, $e = 1/4$, $g = 1/4$, $h = 1/4$, $i = 0$, $k = 0$, $l = 0$, $m = 0.$, $ma = 0$, $mb = 0$, $me = 0$, $mf = 0$, $mi = 1/8$, $mj = 1/8$, $mm = 3/8$, $mn = 3/8$,

$mq = 0$, $mr = 0$, $na = 0$, $nb = 0$, $nc = 0$, $ne = 0$, $nf = 0$, $ng = 0$, $ni = 1/32$, $nj = 3/16$, $nk = 1/32$, $nm = 3/32$, $nn = 9/16$, $no = 3/32$, $nq = 0$, $nr = 0$, $ns = 0$.

List of Figures

2.1 A curve with half-tangent at the endpoints and a non-injective characteristic map. 6
2.2 Graph of the characteristic map as a projection from $\mathbb{R}^2$. 7

3.1 Sierpiński triangle. 15
3.2 A sequence of compact sets approximating the Sierpiński triangle. 15
3.3 Simple IFS as a CIFS automaton. 17
3.4 A projective IFS as a CIFS automaton. 18
3.5 A BCIFS representation of a vertex. 19
3.6 A BCIFS representation of an edge with two subdivision operators. 19
3.7 An automaton representing a curve with two edge subdivisions $T^e_{0,1}$ and two different vertex subdivisions T^{v^l}, T^{v^r}. 20
3.8 Vertex spaces are embedded into the higher dimension curve space. 20
3.9 The first level of the edge subdivision. 20
3.10 The first and second levels of subdivision. 20
3.11 Unfolding of the automaton after applying the adjacency and incidence constraints. 21
3.12 General structure of the subdivision matrices for a curve with n control points, whose vertices are controlled by p control points. 21
3.13 Left: a cubic spline with 4 control points. Right: a fractal curve with 3 control points. 22
3.14 An automaton for the surface with four edges. 23
3.15 Incidence and adjacency constraints for quadrangular surface subdivision. Each subdivided face has to be connected with neighbouring faces by sharing respective edges (represented by solid-line ellipses), while edge subdivision must be an edge for one of the subdivided faces (dotted-line ellipses). 24
3.16 Control mesh for a cubic B-spline patch. 25
3.17 Left: An automaton for the irregular patch. Right: a schematic subdivision of the irregular patch. 26
3.18 Left: a control mesh for a bi-quadratic spline patch with one irregular vertex. Green mesh represents the first step of the subdivision. Right: a control mesh for three irregular bi-quadratic patches that share their irregular vertex and the limit surface. 26

4.1 Left: the curve is tangent to the plane Oxy. Right: the surface is tangent to the z axis. 32
4.2 An angle between a secant and an affine subspace. 32
4.3 An illustration of example 5. 34
4.4 Left: one set of rings around the unique address point $(0, 0)$. Right: two sets of rings around the double address point $(1/2, 0)$. 36
4.5 Angular deviation is the biggest possible angle between pq and E such that $q \in \mathcal{A}$. 37
4.6 The maximum possible angular deviation is $\frac{\pi}{2}$. 38
4.7 Two examples of lines s_i for rings R_i. 49
4.8 Study of the differential behaviour of a quadatic B-spline curve: the standard basis of BI^3 is shown in gray; the eigenbasis of T_1 in black. The yellow line is the sub-space of BI^3 with coordinates $(\cdot, 0, \cdot)$ in the eigenbasis. Ring R_0 of the point v_0 is shown in red and the hatched blue polygon is the convex set that contains ring R_0. 51
4.9 A curve with two different half-tangent at the double address point. 54
4.10 Left-hand image shows the Doo-Sabin subdivision scheme applied on the control mesh shown in black, the green mesh is obtained by one iteration and the red curve is the limit curve. Right-hand image shows the subdivision with modified weights. 54
4.11 A projective IFS as a CIFS automaton. 54
4.12 Left-hand image: Doo-Sabin subdivision scheme applied on the suitcase corner mesh; right-hand image: the subdivision with modified weights, the studied curves (patch borders) are highlighted. 57
4.13 Left: attractor of the IFS $\{T_1, T_2\}$; right: attractor of $\{T_1, T_2'\}$. Even if both IFS share the transformation T_1, the tangents are different at the origin. . . . 57
4.14 The Takagi curve is an attractor of an IFS without a complete set of eigenvectors. 59
4.15 One step of the pyramidal subdivision. One patch with 5 control points is subdivided into 4 patches. Each pair of new patches share 2 edge control points. 60
4.16 Three different iterations of pyramidal surface. 61
4.17 Tensor product of Takagi curves defined in the barycentric space BI^{16}. 63
4.18 The tensor product of Takagi curves projected into the cube gives the same surface as the product of two classical 2D curves. Note that the surface does not have tangent planes but tangent lines at the corners. 63
4.19 A schematic representation of a ring on a tensor product of curves. 65

5.1 Top: initial BCIFS. Each branch of the automaton corresponds to an initial curve. Bottom: Possible attractor of that BCIFS: two B-splines of different degrees. 68
5.2 Top: modified BCIFS, with an intermediate state i and additional transitions leading to and from it. Bottom: The attractor of this BCIFS: two initial curves and their two copies. 69
5.3 Unfolding of the automaton from figure 5.2. 70

5.4 Possible attractor of the automaton from figure 5.2 with adjacency and incidence constraints in place. Two initial curves and two segment of the new intermediate curve are connected pairwise. 70
5.5 Final BCIFS with an intermediate state and all required transitions. 71
5.6 Unfolding of the automaton from figure 5.5. 71
5.7 Control points for two splines that compose R_0. 73
5.8 A connection between a cubic and a quadratic spline. Positive sub-dominant eigenvalue yields G_1-continuity. $a = 0.131$, $b = 0.2$, $c = 0.38$, $d = 0.289$, $k = 0.11$, $l = 0.12$, $m = 0.1$, $n = 0.12$, sub-dominant eigenvalues $\lambda_1 \approx 0.696$. . 74
5.9 Top: new control points. Bottom: old control points. The control points reposition used to obtain tighter convex hulls. 75
5.10 A connection between a cubic and a quadratic spline. The sub-dominant eigenvalue is complex and both parts of the curve are spiralling towards the fixed point. $a = 0.065$, $b = 0.115$, $c = 0.115$, $d = 0.675$, $k = 0.6$, $l = 0.35$, $m = 0$, $n = 0.09$, sub-dominant eigenvalues $\lambda_{3,4} \approx 0.082 \pm 0.602i$. 77
5.11 Refined BCIFS with two intermediate states. 77
5.12 Two intermediate curves between the fractal curve and B-spline. Three control point are used to control the shape of the curve. 80
5.13 Intermediate curve between the fractal curve and B-spline. Such configuration of control points defines different half-tangents. 81
5.14 Initial BCIFS. Each branch of the automaton corresponds to an initial surface. 82
5.15 Top: Automaton describing the subdivision of the intermediate patch. Note that edge and vertex states are omitted to conserve space. Bottom: Schematic representation of the same subdivision. 82
5.16 The automaton depicting top and bottom edges subdivision of the intermediate patch. 83
5.17 Part of the graph representing one iteration of the automaton. 83
5.18 Part of the graph representing one step of the subdivision. This part shows two R patches and the common edge between them. 84
5.19 Part of the graph representing one step of the subdivision. This part shows the top row of three patches and the edges between them. 85
5.20 Continuous approximation of the limit surface. 86
5.21 A schematic representation of several subdivision steps of the intermediate surface. Red and blue squares present the regular patches, green ones represent the irregular patches. 87
5.22 Top: Refined BCIFS with two intermediate states. Bottom: Corresponding subdivision scheme. 87
5.23 Control meshes for two intermediate patches. Left: Doo-Sabin side. Right: Catmull-Clark Side. Colored meshes represent different parts of the first step of the subdivision. Please note that since the two intermediate patches are independent we treat them separately, thus the mesh for the intermediate curve is presented twice. 89
5.24 Catmull-Clark intermediate patch as tensor product of its edges. 90
5.25 An automaton representing the subdivision of the irregular edge. 91
5.26 An intermediate surface between the Doo-Sabin and Catmull-Clark surfaces with control polygons for initial edges of initial surfaces and intermediate curve. 95

5.27 An intermediate surface between a fractal surface and a spline patch. 95

Bibliography

[Bar86] Michael F. Barnsley. Fractal functions and interpolation. *Constructive Approximation*, 2(1):303–329, 1986.

[Bar88] Michael Barnsley. *Fractals everywhere*. Academic Press Professional, Inc., San Diego, CA, USA, 1988.

[Ben09] Hicham Bensoudane. *Etude differentielle des formes fractales*. PhD thesis, Université de Bourgogne, 2009.

[BGN09] Hicham Bensoudane, Christian Gentil, and Marc Neveu. Fractional half-tangent of a curve described by iterated function system. *Journal Of Applied Functional Analysis*, 4(2):311–326, April 2009.

[BH89] Michael F. Barnsley and Andrew N. Harrington. The calculus of fractal interpolation functions. *Journal of Approximation Theory*, 57(1):14 – 34, 1989.

[BMZ04] Ioana Boier-Martin and Denis Zorin. Differentiable parameterization of catmull-clark subdivision surfaces. In *Proceedings of the 2004 Eurographics/ACM SIGGRAPH symposium on Geometry processing*, SGP '04, pages 155–164, New York, NY, USA, 2004. ACM.

[CC78] E. Catmull and J. Clark. Recursively generated b-spline surfaces on arbitrary topological meshes. *Computer-Aided Design*, 10(6):350 – 355, 1978.

[CE98] ZAIR Chems Eddine. *Formes fractales a pôles basées sur une généralisation des IFS*. PhD thesis, Université Claude Bernard Lyon 1, 1998.

[CLH01] Wayne O. Cochran, Robert R. Lewis, and John C. Hart. The normal of a fractal surface. *The Visual Computer*, 17(4):209–218, 2001.

[DL92] Ingrid Daubechies and Jeffrey C Lagarias. Sets of matrices all infinite products of which converge. *Linear algebra and its applications*, 161:227–263, 1992.

[DS78] D. Doo and M. Sabin. Behaviour of recursive division surfaces near extraordinary points. *Computer-Aided Design*, 10(6):356 – 360, 1978.

[Gou10] Gilles Gouaty. *Modélisation géométrique itérative sous contraintes*. PhD thesis, école Polytechnique Fédération de Lausanne, 2010.

[Hut81] John Hutchinson. Fractals and self-similarity. *Indiana University Journal of Mathematics*, 30(5):713–747, 1981.

[KSD12] J. Kosinka, M. Sabin, and N. Dodgson. Cubic subdivision schemes with double knots. *Computer Aided Geometric Design*, 2012.

[LL03] A. Levin and D. Levin. Analysis of quasi uniform subdivision. *Applied and Computational Harmonic Analysis*, 15(1):18–32, 2003.

[Loo87] C. Loop. Smooth subdivision surfaces based on triangles. Master's thesis, University of Utah, 1987.

[Man82] Benoit B. Mandelbrot. *The Fractal Geometry of Nature*. W. H. Freeman, August 1982.

[Mas91] Peter R Massopust. Vector—valued fractal interpolation functions and their box dimension. *aequationes mathematicae*, 42(1):1–22, 1991.

[MG01] Géraldine Morin and Ron Goldman. On the smooth convergence of subdivision and degree elevation for bézier curves. *Computer Aided Geometric Design*, 18(7):657 – 666, 2001.

[PGSL13a] Sergey Podkorytov, Christian Gentil, Dmitry Sokolov, and Sandrine Lanquetin. Geometry control of the junction between two fractal curves. *Computer-Aided Design*, 45(2):424 – 431, 2013. Solid and Physical Modeling 2012.

[PGSL13b] Sergey Podkorytov, Christian Gentil, Dmitry Sokolov, and Sandrine Lanquetin. Joining primal/dual subdivision surfaces. *Lecture Notes in Computer Science*, 2013. To appear in procedings to Mathematical Methods for Curves and Surfaces 2012.

[Pra98] Hartmut Prautzsch. Smoothness of subdivision surfaces at extraordinary points. *Advances in Computational Mathematics*, 9:377–389, 1998. 10.1023/A:1018945708536.

[Rei95] Ulrich Reif. A unified approach to subdivision algorithms near extraordinary vertices. *Computer Aided Geometric Design*, 12(2):153 – 174, 1995.

[SGB12] Dmitry Sokolov, Christian Gentil, and Hicham Bensoudane. Differential behaviour of iteratively generated curves. In *Curves and Surfaces*, volume 6920 of *Lecture Notes in Computer Science*, pages 663–680. Springer Berlin / Heidelberg, 2012.

[SL03] Jos Stam and Charles Loop. Quad/triangle subdivision. *Computer Graphics Forum*, 22(1):79–85, 2003.

[SLG05] Scott Schaefer, David Levin, and Ron Goldman. Subdivision schemes and attractors. In *Symposium on Geometry Processing*, pages 171–180. Citeseer, 2005.

[SW05] Scott Schaefer and Joe Warren. On c2 triangle/quad subdivision. *ACM Trans. Graph.*, 24(1):28–36, January 2005.

[Zor00] Denis Zorin. A method for analysis of c 1-continuity of subdivision surfaces. *SIAM Journal on Numerical Analysis*, 37(5):1677–1708, 2000.

[ZT96] Chems Eddine Zair and Eric Tosan. Fractal modeling using free form techniques. *Comput. Graph. Forum*, 15(3):269–278, 1996.

[ZT97] Chems Eddine Zair and Eric Tosan. Unified ifs-based model to generate smooth or fractal forms. *Surface Fitting and Multiresolution Methods*, pages 335–344, 1997.

Résumé :

Nous nous intéressons à la modélisation de formes complexes de type structures arborescences, formes lacunaires ou surfaces rugueuses. Ces formes sont intéressantes de par leurs propriétés physiques particulières : objets légers, économie de matière, résistance mécanique, absorption acoustique importante. Les modèles basés sur le concept de la géométrie fractale permettent de générer de telles formes et notamment les formes auto-similaires. A partir des travaux de Barnsley sur les systèmes itérés de fonctions, Tosan et al, ont proposé une extension, Boundary Controled Iterated Funcions Systems (BCIFS) pour contrôler plus facilement les formes et faciliter leur description. Nous nous intéressons aux propriétés différentielles des formes décrites par BCIFS.
Nous proposons une définition plus générale d'espace tangent qui permet de caractériser le comportement de cas non-classiquement différentiables. Nous montrons que l'étude du comportement différentiel peut alors se faire simplement par analyse des valeurs propres et vecteurs propres généralisés des opérateurs de subdivision. Il devient alors possible de contrôler ces propriétés différentielles.
Nous présentons une application de nos résultats, en proposant une méthode pour construire des raccords entre deux structures définies par des processus de subdivision différents. Cette méthode est appliquée pour la construction d'un raccord entre une surface de subdivision de Doo-Sabin (schéma dual) et une surface de subdivision de Catmull-Clark (schéma primal).

Mots-clés : courbe fractale, surface fractale, IFS, espace tangent, subdivision

Abstract:

We are interested in modelling complex shapes such as tree-like structures, porous structures and rough surfaces. Such structures possess particular physical properties: weight-to-volume ratio, mechanical resistance, acoustical absorption, etc. Fractal geometry is a relatively new branch of mathematics that allows modelling such objects. Based on Barnsley's work on Iterative Functions Systems (IFS), Tosan et al proposed a model called Boundary Controlled IFS (BCIFS) that allows us to easily describe and control such objects. In this thesis we focus on the differential properties of the shapes described with BCIFS.
We propose a generalisation to the tangent space that allows us to characterise various cases of differential behaviour, some of which are considered non-differentiable in classical sense. We derive the necessary and sufficient conditions for existence of a tangent space based on the analysis of the eigenvalues and generalised eigenvectors of the subdivision operators. We also show that it is possible to control the differential behaviour.
As an application of our results, we propose a method of constructing the junction between different structures. This method is applied to construct a junction between Doo-Sabin subdivision (dual scheme) and Catull-Clark subdivision (primal scheme).

SPIM

■ École doctorale SPIM - Université de Bourgogne/UFR ST BP 47870 F - 21078 Dijon cedex
■ tél. +33 (0)3 80 39 59 10 ■ ed-spim@univ-fcomte.fr ■ www.ed-spim.univ-fcomte.fr

UNIVERSITÉ DE BOURGOGNE